

Institut für Ernährungs- und Lebensmittelwissenschaften

**Sensor platform for rapid detection and  
quantification of indicator and pathogenic  
bacteria on food contact surfaces**

**Dissertation**

zur Erlangung des Grades

Doktor der Ingenieurwissenschaften (Dr.-Ing.)

der Landwirtschaftlichen Fakultät

der Rheinischen Friedrich-Wilhelms-Universität Bonn

von

***Grigori Badalyan***

aus

*der Eriwan, Armenien*

Bonn 2021

Referent: *Prof. Dr. André Lipski*

Korreferent:

*Prof. Dr. Mark Büking*

*Prof. Dr. Rainer Stamminger*

Tag der mündlichen Prüfung: 08/12/2020

Angefertigt mit Genehmigung der Landwirtschaftlichen  
Fakultät der Universität Bonn

## Table of Contents

List of abbreviations .....	6
Graphical Abstract .....	8
Summary.....	11
1 Introduction.....	15
1.1 Microbiological safety of food products.....	15
1.2 Indicator bacteria ( <i>E. coli</i> / Coliforms).....	17
1.3 Pathogenic bacteria ( <i>Staphylococcus aureus</i> ).....	19
1.4 Cross contamination and survival of bacteria on food contact surfaces.....	20
1.5 Detection of bacteria on food contact surfaces .....	24
1.6 Colorimetric sensors .....	26
1.7 Fluorometric sensors .....	28
1.8 Electrochemical sensors .....	29
1.9 Cyclic Voltammetry.....	30
1.10 Screen-printed electrodes .....	31
1.11 Electrochemical detection of bacteria.....	32
2 Objective.....	35
2.1 Specific goals .....	35
3 Proposed platform.....	36
4 Experimental work.....	37
4.1 Electrochemical detection of the target analytes .....	39
4.2 Preparation of graphene solution .....	40
4.3 Modification of carbon SPEs.....	41

4.4	Bacteria cultivation and enumeration.....	41
4.5	Testing of bacterial attachment to gels.....	42
4.6	Optimization of pH and optical characteristics of the gel	43
4.7	Testing inducers and accelerator reagents .....	44
4.8	Preparation of gel-modified electrodes .....	46
4.9	Bacterial attachment and enumeration on stainless steel surfaces.....	47
4.10	Voltammetric detection of bacterial cultures .....	48
4.11	Voltammetric detection of bacteria on stainless steel surfaces.....	49
4.12	Statistical analyses .....	50
5	Results .....	51
5.1	Electrochemical detection of target analytes.....	51
5.2	Detection of target analytes on graphene modified carbon electrodes .....	60
5.3	Development of Gel-electrode system.....	62
5.3.1	Gel characteristics.....	62
5.3.2	Electrochemical characteristics of gel–electrode system .....	66
5.4	Detection of bacteria using developed GR/PAAGC electrode system in culture .....	73
5.5	Detection of other bacteria with GR/PAAGC sensor platform in culture.....	87
5.6	Detection of bacteria on stainless steel surfaces .....	88
5.7	Colorimetric properties of the gel system.....	100

6	Discussion .....	112
6.1	Electrochemical detection of target analytes.....	112
6.2	Detection of target analytes on graphene modified carbon electrodes .....	119
6.3	Development of Gel-electrode system.....	121
6.3.1	Gel characteristics.....	121
6.3.2	Electrochemical characteristics of gel–electrode system.....	124
6.4	Detection of bacteria using developed GR/PAAGC electrode system in culture .....	128
6.5	Detection of other bacteria with GR/PAAGC sensor platform in culture.....	139
6.6	Detection of bacteria on stainless steel surfaces .....	141
6.7	Colorimetric properties of the gel system.....	146
7	Conclusion and outlook .....	151
8	Bibliography.....	155
9	Appendix.....	173
	Appendix 1 Growth of <i>E. coli</i> on commercial chromogenic media .....	173
	Appendix 2 Calibration of plate count and Optical density (OD) values.....	176
	Appendix 3 Results on growth of <i>E. coli</i> on stainless steel surfaces .....	182

## List of abbreviations

4-MU	7-Hydroxy-4-methylcoumarin
4-MUG	4-Methylumbelliferyl- $\beta$ -D-glucopyranosiduronic acid
4-NP	4-nitrophenol
4-NL	4-nitroaniline
4-NPP	4-nitrophenylphosphocholine
4-NLD	L-Alanyl-p-nitroanilide
5,4-BCIGP	5-Bromo-4-chloro-3-indoly- $\beta$ -D-glucuronide
5,4-DDI	5,5 -Dibromo-4,4 -dichloroindigo
6-CIGP	6-Chloro-3-indoxyl- $\beta$ -D-galactopyranoside
6-DI	6,6' -Dichloro-Indigo
ABS	Absorbance
B-PER	Bacterial Protein Extraction Reagent
CCP	Critical Control Points
CM	Cultural method
DDM	<i>n-Dodecyl--D-Maltoside</i>
EPS	Extracellular Polymeric Substance
GR/PAAGC	Graphene modified polyacrylamide gel carbon electrode
HACCP	Hazard Analysis and Critical Control Point
IPTG	Isopropyl- $\beta$ -D-thiogalactopyranoside
OBG	<i>n-Octyl-<math>\beta</math>-D-Glucuropyranoside</i>

<b>OBDG</b>	<b>Methyl-B-D-Glucuronide</b>
<b>ODTG</b>	<b>n-Octyl-β-D-thiogalactopyranoside</b>
<b>PAA</b>	<b>Polyacrylamide gel</b>
<b>PBS</b>	<b>Phosphate-buffered <i>saline</i></b>
<b>RFU</b>	<b>Relative fluorescence unit</b>
<b>RTE</b>	<b>Ready to Eat</b>
<b>SDS</b>	<b>Sodium dodecyl sulfate</b>
<b>Sens</b>	<b>Sensor</b>
<b>Soil</b>	<b>Food residues on food contact surfaces</b>
<b>SPE</b>	<b>Screen-Printed Electrodes</b>
<b>StSt</b>	<b>Stainless Steel</b>
<b>Tryton X-100</b>	<b>4-(1,1,3,3-Tetramethylbutyl)phenyl- polyethylene glycol</b>
<b><math>I_{pa}/I_{pc}</math></b>	<b>Anodic/cathodic peak currents</b>
<b><math>E_{pa}/E_{pc}/ \Delta E</math></b>	<b>Anodic/cathodic potentials/potential difference</b>





## Zusammenfassung

Die durch Lebensmittel übertragenen pathogenen Bakterien stellen ein globales Problem für das allgemeine Gesundheitswesen dar. Beispielsweise zeigen *E. coli* und Coliforme den hygienischen Status für Lebensmittel im Allgemeinen aber auch innerhalb der verschiedenen Verarbeitungsschritte auf.

Hierbei sind Kontaktoberflächen eine Hauptquelle der Kontamination bzw. der Kreuzkontamination. Daher kann ein Frühwarnsystem in der Lebensmittelproduktion ein wichtiges Werkzeug für diese Art der Kontamination sein.

Die Entwicklung eines solchen Frühwarnsystems mittels eines neuartigen Ansatzes ist Inhalt dieser Doktorarbeit.

Die Kombination einer elektrochemischen und einer optischen Sensorplattform (GR/PAAGC Sensor), basiert auf einer Kohlenstoffelektrode, die durch ein Graphen modifiziertes Polyacrylamidgel (PAA) gekennzeichnet ist.

Die optimierte Formel von PAA und Agar-Agar erhöhte die Hafteigenschaften des Gels, was für die Bakterienrückgewinnung entscheidend ist und dafür sorgt, dass es an der Kontaktfläche haftet. Die vorliegende Arbeit beschreibt sowohl die Entwicklung des Systems als auch die Entwicklung des Aufbaus.

Implementiert wurde dieser Ansatz für die Untersuchung von Coliformen, *E. coli* und *St. aureus* auf den Kontaktoberflächen der Lebensmittelproduktion.

Neue elektrochemische Reporter der enzymatischen Aktivität für ausgewählte Bakterien wurden getestet (6-CIGP, 5,4-BCIGP, 4-

MUG, 4-NPP und 4-NL). Die Reaktionsprodukte,  $\beta$ -D-Galaktosidase,  $\beta$ -D-Glukuronidase und Phospholipase wurden durch den GR/PAAGC Sensor nachgewiesen.

In einem Optimierungsschritt konnte durch die Verwendung von IPTG, ODTG, OBG und OBDG im Gel eine Reduktion der Untersuchungszeit erreicht werden. Weiterhin konnte durch den Zusatz von Graphen das voltmetrische Signal erhöht werden bzw. wurde die Leitfähigkeit des Polyacrylamidgels verbessert.

Die anodischen und kathodischen Signale des freigesetzten Produkts waren in guter Korrelation zur Konzentration der Coliformen, *E. coli* und *St. aureus*. Hierbei wurden bakterielle Zellkonzentration untersucht, die sich von  $1.8 \log_{10}\text{CFU/ml}$  bis  $8 \log_{10}\text{CFU/ml}$  erstreckten, die für eine Messung benötigte Zeit betrug drei Stunden.

Nach einer Optimierungsphase war sowohl die Empfindlichkeit für *E. coli* ( $0.6 \log_{10}\text{CFU/cm}^2$  bis  $7 \log_{10}\text{CFU/cm}^2$ ) als auch für *St. aureus* ( $1.6 \log_{10}\text{CFU/cm}^2$  bis  $6 \log_{10}\text{CFU/cm}^2$ ) signifikant erhöht.

Zusätzlich konnte auf Edelstahloberflächen die Messzeit auf 30 Minuten reduziert werden.

Die in dieser Arbeit entwickelte schnelle, empfindliche reproduzierbare und spezifische Sensorplattform kann nun für Industrieapplikationen weiterentwickelt werden. Dabei kann diese on-line / at-line Applikation sowohl als single-use Option als auch real-time Monitoring eingesetzt werden.

## Summary

Foodborne pathogenic bacteria represent a global problem for public health. *Escherichia coli* and Coliforms indicates the possible contamination of food, water and food processing environments. In food processing environment contact surfaces act as harbor for bacteria and can be one of the main sources of contamination and cross contamination of food at different production stages. For any food processing factory, it is essential to count with an early warning sampling and detecting method for food pathogenic and indicator bacteria. The lack of early warning system as well as the disadvantageous (e.g. long detection time, sample preparation and different dilution steps for the enumeration) of the existing methods served as a base for conducting this doctoral work. A novel combined colorimetric and voltammetric sensor platform based on screen printed carbon electrode coated by graphene modified polyacrylamide gel (GR/PAAGC) was developed. The developed platform that contains new electrochemical substrates and construction materials was implemented for efficient sampling, sensitive detection and enumeration of Coliforms, *E. coli* and *Staphylococcus aureus* on food contact surfaces. In this work the whole development process of the sensor is presented and each construction steps are described in details. The optimized formula of polyacrylamide (PAA) and agar-agar increased the adhesive properties of the gel, being crucial for the bacterial recovery, attached to food contact surfaces. The 6-Chloro-3-indoxyl- $\beta$ -D-galactopyranoside (6-CIGP), 5-Bromo-4-chloro-3-indolyl- $\beta$ -D-glucuronide (5,4-BCIGP), 4-Methylumbelliferyl- $\beta$ -D-

glucopyranosiduronic acid (4-MUG), 4-nitrophenylphosphocholine (4-NPP) and L-Alanyl-p-nitroanilide (4-NLD) were used as new electrochemical reporters for  $\beta$ -D-Galactosidase,  $\beta$ -D-Glucuronidase and Phospholipase C activity. The released 6,6'-Dichloro-Indigo (6-DI), 5,5'-Dibromo-4,4'-dichloroindigo (5,4-DDI), 7-Hydroxy-4-methylcoumarin (4-MU), 4-nitrophenol (4-NP) and 4-nitroaniline (4-NL) were directly detected by GR/ PAAGC platform. The presence of Isopropyl- $\beta$ -D-thiogalactopyranoside (IPTG), n-Octyl- $\beta$ -D-thiogalactopyranoside (ODTG), n-Octyl- $\beta$ -D-Glucopyranoside (OBG) and Methyl-B-D-Glucuronide (OBDG) in the gel contributed to reduction of the detection time. The addition of graphene enhanced the voltammetric signal and increased the conductivity of PAA gel. The later increased the adhesive properties of the sensor platform. The optical signals produced by mentioned products could be detected both visually or spectrophotometrically. However, the electrochemical detection was more sensitive comparing to the optical one. The anodic and cathodic peaks of the released products were directly proportional to the concentration of Coliforms, *E. coli* and *St. aureus*. Bacterial cell concentration ranging from 1.8  $\log_{10}$ CFU/mL to 8  $\log_{10}$ CFU/mL were detected. Well-shaped, sharp voltammetric curves were generated within 3 h. Redox peaks exhibited good sensitivity. After series of optimization experiments, Coliforms and *E. coli* ranging from 0.4  $\log_{10}$ CFU/cm<sup>2</sup> to 7  $\log_{10}$ CFU/cm<sup>2</sup> as well as *St. aureus* ranging from 1.6  $\log_{10}$ CFU/cm<sup>2</sup> to 6  $\log_{10}$ CFU/cm<sup>2</sup> on stainless steel surfaces were detected within 30 min. The optimization of optical characteristics of PAA gel system allowed production of rapid visible signals (within 30 min) in case of the presence of target bacteria. The developed GR/PAA-gel carbon

sensor platform can be used for rapid (30 min) single detection of Coliform bacteria, as well as for the real-time monitoring of growth of Coliform bacteria on stainless steel surfaces during processing shift. The designed sensor platform was successfully applied for detection of Coliforms in real processing conditions typical for food processing factories. The GR/PAA-gel carbon sensor platform (i) could detect the specific electrochemical signal produced by Coliforms on surfaces in the presence of complex molecules of the food soil, (ii) it detected Coliforms on clean stainless steel surfaces (absence of any soil and organic matter) after 4 h drying at low temperatures ~15 °C as well as survived Coliform cells in 15 minutes after disinfection with industrial sanitizer and finally (iii) it was successfully applied for the real time monitoring Coliform bacteria on stainless steel surfaces during work shift (8 h). This validates the practical feasibility of the proposed sensor platform. The designed technique does not require sample preparation steps and can be used in food industry by none qualified (microbiology food laboratory) personal. The developed sensor platform possessed high reproducibility and robustness.

Inclusion of the second enzyme (L-Alanine-Aminopeptidase, produced by Gram-negative bacteria) in the system increased the specificity and robustness of the developed method for Coliforms and *E. coli*. Novel rapid sensor for detection of total Gram-negative bacteria could be developed in the future and the already developed platform could serve as a base for this. The rapid detection of *St. aureus* based on Phospholipase C activity could be a base for development of novel sensor for rapid electrochemical detection of group of pathogens possessing based Phospholipase C activity using already optimized sensor as a starting point. Although, the

developed technique was successfully applied to stainless steel surfaces, it can be easily adapted to (i) other surface types (plastic, wood), (ii) food processing environment and (iii) food samples (from raw material to ready to eat food).

Beside, rapidity and sensitivity the proposed sensor can be used for detecting and distinguishing the target bacteria both in heavy soiled, contaminated as well as cleaned and disinfected environments.

# 1 Introduction

## 1.1 Microbiological safety of food products

Foodborne pathogens represent a global problem for public health. Thousands of people in the world acquire foodborne illnesses every year due to growth and survival of pathogenic bacteria in the food chain (Adell et al. 2018, Rivera et al. 2018). More than 320 000 human illness cases are reported annually in the European Union. In 2017, European Food Safety Authority reported more than 350000 confirmed cases (~11700 outbreak related cases) occurred due to food and waterborne zoonoses (EU, European Food Safety Authority report 2018). In Europe there was a large outbreak caused by *Escherichia coli* in 2011. Mentioned outbreak was caused by an unusual strain that was similar to enteroaggregative *E. coli* (EAEC) of serotype O104:H4. This outbreak caused almost 50 deaths, 800 cases of hemolytic-uremic syndrome, and 3000 cases of acute gastroenteritis (Navarro-Garcia 2014).

Control of foodborne pathogenic bacteria remains the main step that protects consumers from foodborne diseases. Control of foodborne pathogens is usually done using food safety management systems such Hazard Analysis & Critical Control Point (HACCP). HACCP is a preventive food safety management system. HACCP is a scientific and effective approach to identify, evaluate and control hazards that are significant for food safety (Blackburn 2007, Yang et al. 2019). For example, the implementation of HACCP system decreased the number of total aerobic bacteria and Coliforms in ice cream samples (Allata et al. 2017). Highly positive effect was observed during

implementation of HACCP in meat processing companies. At least 1log reduction of hygiene indicator organisms on food contact surfaces was observed. The implementation of HACCP also reduced the number of *Enterobacteriaceae* and *Staphylococcus* positive samples (Tomasevic et al. 2016). The microbial testing acquired high significance for the correct implementation of HACCP system. Microbiological testing is an important mechanism used for establishment of prerequisite programs, conducting hazard analysis, monitoring critical control points, performing corrective actions, validating and verifying the HACCP plan (Kvenberg et al. 2000).

For example, detection of *St. aureus* during establishment of critical control points (CCPs) in processing of cold-smoked trout improved the effectiveness of implemented HACCP system and facilitated development of control strategy of mentioned microorganism. In fish processing plant the microbial testing showed that liquid salt was the main source of contamination of ready to eat salmon products (Grigoryan et al. 2010). Another example is the meat processing plant, where the microbial testing showed that raw materials had significant role in contamination of ground beef.

Microbiological risk assessment is another method to control of foodborne hazards and to develop more effective HACCP plans (Ding et al. 2016). However, during performing the risk assessment procedures of pathogenic microorganisms in food and food processing plants the following features of microorganisms should be considered. The number of microorganisms can increase during processing and storage of food. They often can enter into inactivated (but not totally killed) stage. They can be transferred from



contaminated objects to uncontaminated ones due to cross-contamination (Barlow et al. 2015).

In general, microbiological testing during processing of food products, will allow to (i) understand the overall picture of hazards in the processing, (ii) will assist the development of effective reproducible control and preventive strategies and (iii) will increase the efficiencies of food safety management programs and (iv) will reduce the cross contamination at every stage of processing.

## **1.2 Indicator bacteria (*E. coli* / Coliforms)**

*E. coli* and Coliforms usually serve as primary indicators of contamination of food, water and food processing environments (Jay 1995, Odonkor 2013, Martin et al. 2016). For the first time *E. coli* was used as an index of fecal pollution by the end of 19<sup>th</sup> century because it could be isolated and identified more readily than individual waterborne pathogens. In 1895, *E. coli* was tested as a measure of drinking water potability. Since then, the Coliforms were used as indicators of pathogens in water and later on in foods (Schardinger 1892, Smith 1895). Usually, it is an importance for rapid, easy and robust detection of food safety indicator microorganisms. They should also be distinguishable from other bacteria as well as always be present when the pathogen of concern is present (Jay 2005). The most typical strains of *E. coli* are motile, produce acid and gas from lactose at 44 °C and below, form indole at both 37 °C and 44 °C, and fail to utilize citrate. They produce positive reaction in the methyl red and negative in the Voges–Proskauer tests (Mead 2007). However, there are also pathogenic

strains of *E. coli* such as enteropathogenic *E. coli* (EPEC), enterotoxigenic *E. coli* (ETEC), enteroinvasive *E. coli* (EIEC), enterohaemorrhagic *E. coli* (EHEC) and enteroaggregative *E. coli* (EAEC) (Nataro et al. 1998).

$\beta$ -D-Glucuronidase is specific enzyme for *E. coli*, being present in 94-97 % of tested strains (Heery et al. 2016). The gene encoding  $\beta$ -D-Glucuronidase, *gus A* (formerly *uidA*), was originally isolated from *E. coli* (Jefferson et al. 1986). Together with *gus A* other genes involved in glucuronide metabolism at the same region of *E. coli* chromosome, thus forming the GUS operon (Fig 1). Glucuronide substrates are taken up by *E. coli* via a specific transporter, the glucuronide permease, cleaved by  $\beta$ -D-Glucuronidase, and the formed glucuronic acid residue is used as a carbon source.

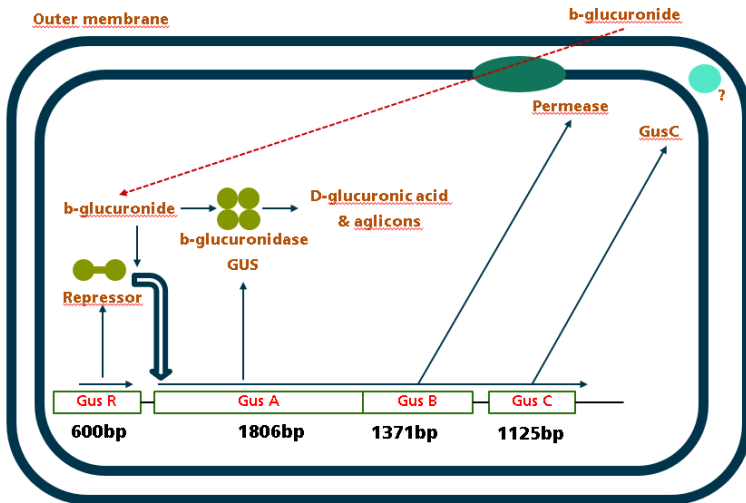


Figure 1 The GUS operon in *E. coli* (adapted from (Wilson, Hughes, & Jefferson, 1992))

Currently, the Coliform bacteria are located in several families which constitute the recently described order *Enterobacterales* (Adeolu et al. 2016). Among the *Enterobacteriaceae*, those strains that ferment lactose, usually with acid and gas production, are together termed 'coliforms' and include species of *Citrobacter*, *Enterobacter*, *Escherichia* and *Klebsiella*. With the introduction of enzyme-based tests, the definition includes bacteria within the family *Enterobacteriaceae* that possess the  $\beta$ -D-galactosidase enzyme (Zhang et al. 2015). Possession of the gene *lacZ*, is the most prominent feature of the Coliforms (Molina et al. 2015). In Coliforms, the *lacZ* gene product  $\beta$ -D-Galactosidase is responsible for cleavage of lactose into glucose and galactose.  $\beta$ -D-Galactosidase-positive reaction has been included also in to the definition of Coliform bacteria by APHA standard (APHA 2005). B-D-Galactosidase, can be easily detectable using different chromogenic and fluorogenic indoxyl, coumarin and phenol based substrates.

### **1.3 Pathogenic bacteria (*Staphylococcus aureus*)**

Phospholipase C plays important roles in the pathogenesis of disease. The toxic Phospholipase C can interact with eukaryotic cell membranes and hydrolyze phosphatidylcholine and sphingomyelin, leading to cell lysis. A variety of pathogenic bacteria produces Phospholipase C (Titball 1993). Among them is the well known as well as widespread commensal bacterium and pathogen *Staphylococcus aureus*. *St. aureus* causes many types of human infections and syndromes (Kobayashi et al. 2015). *St. aureus* is a non-motile, catalase, positive, facultative anaerobic Gram-

positive bacteria. It is a mesophilic bacteria, grows optimally around 37°C. It generally survives well under severe conditions and is resistant to high salt content, drying and freezing (Adams 2009). Staphylococcal food poisoning is one of the most common food-borne diseases in the world. Mentioned disease is caused by ingestion of staphylococcal toxins following the ingestion of enterotoxins that are produced by coagulase-positive staphylococci, mainly *St. aureus* (De Buyser et al. 2012). Methicillin-resistant *St. aureus* is the most commonly identified antimicrobial-resistant pathogen in many parts of the world (Taylor 2013). As it was mentioned above, the *St. aureus* causes illness due to production of specific toxins, superantigens, and exoenzymes. *St. aureus* produces two types of exoproteins: Phospholipase C (including phosphatidylinositol (PI)-specific Phospholipase C (PI-PLC)) and sphingomyelinase (beta-haemolysin, beta-toxin), which are surface associated a heterogeneous group of esterases (Daugherty et al. 1993, Schmiel et al. 1999, White et al. 2014). Phospholipases are lipolytic esterases which cleave glycerol-phospholipids, the major structural lipids in eukaryotic membranes (Flores-Díaz et al. 2016). Phospholipase C (including PI-PLC) are produced by several Gram-positive pathogens, including *Bacillus spp.*, *Listeria monocytogenes*, *St. aureus* and *Clostridium spp.* (Titball 1993).

#### **1.4 Cross contamination and survival of bacteria on food contact surfaces**

An important feature of any food safety and hygiene program is the prevention of cross-contamination. Cross-

contamination is the contamination of final product with any biological, physical or chemical hazards coming from raw materials, intermediate products and prevalence in food processing environment (Huss et al. 2003). The cross contamination scheme is shown in Fig. 2. From the microbiological point of view, the cross-contamination means the transfer of microorganisms from contaminated matrix to uncontaminated matrix, both directly or indirectly. In food processing environment contact surfaces act as harbor for bacteria and can be one of the main sources of contamination and cross contamination of food at different production stages (Gkana et al. 2017). The microorganisms usually attach to working surfaces of food processing equipment, tables, cutting boards, utensils, conveyor belts, knives, cutting boards which are mainly made of stainless steel and plastic materials (Keeratipibul et al. 2017). Several food contact surfaces in meat processing are shown in Fig 3. Different bacterial species may survive the stressful conditions on open surfaces. Cleaning and disinfection can provide stress to cells, but not necessarily kill them.

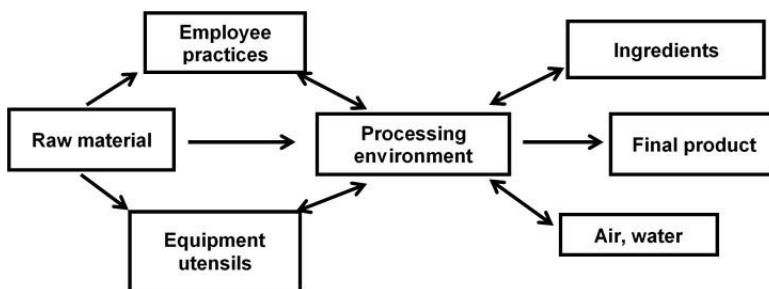


**Figure 2 Routes of contamination in a food processing plant. Adapted from (Huss et al., 2003).**

Foodborne pathogenic bacteria such *Salmonella enteritidis*, *Staphylococcus aureus* and *Campylobacter jejuni* could survive on dry stainless steel surfaces within 96h, 24h and 4h respectively, in case of moderate level of initial contamination (Kusumaningrum et al. 2003). Another important aspect of attachment of microorganisms to stainless steel surfaces is the formation of biofilm. The formation of biofilm is shown in Fig. 4. The first and important stage of the biofilm formation is the attachment of bacteria to surface (Abdallah et al. 2014). After adaptation and growth the different layers of bacterial colonies are formed, which follows by the formation of extracellular polymeric matrix. The matrix consists of microbial cells, the substratum (biotic or abiotic), and the surrounding medium (food residues, soil, water etc.) (Velmourougane et al. 2017). In the biofilm, bacteria are protected from stresses such lack of nutrient, presence of disinfectants, pH changes and etc. Additionally, microorganisms are able to release from biofilm, causing cross-contamination of products and already cleaned surfaces during food processing (Szczepanski et al. 2014, Buzón-Durán et al. 2017, Lin et al. 2017). Several indicator and pathogenic bacteria are able to form biofilm on food contact surfaces (Adator et al. 2018) determined the ability of *E. coli* to form biofilm on stainless steel plates.

Several authors detected *St. aureus* from the biofilm formed on stainless steel surfaces (Lee et al. 2015, Vazquez-Sanchez et al. 2018). Thus, formation of biofilm significantly increases the probability of cross-contamination and drastically complicates the control of pathogenic bacteria at food processing facilities. Therefore, it is crucial to detect bacteria on food contact surfaces before

formation of biofilm as well as to detect target bacteria in complex biofilm.

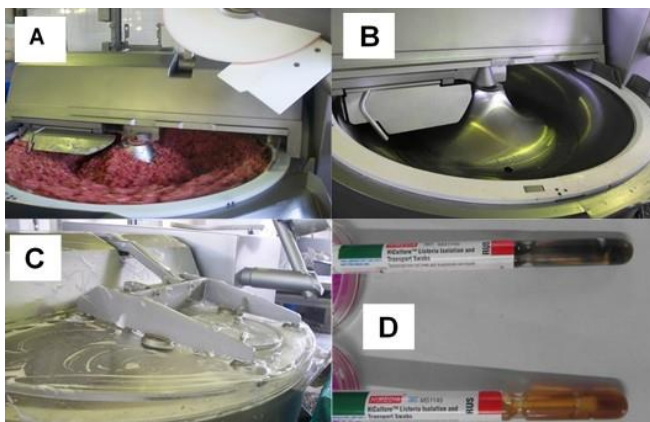


Figure 3 Different food contact surfaces in meat processing factory. A) Meat cutter during processing. B) Meat cutter during cleaning. C) Disinfected meat cutter surface. D) Transport swabs for *Listeria monocytogenes* taken from meat cutter surface in a) 30 minutes and b) 3h after disinfection.

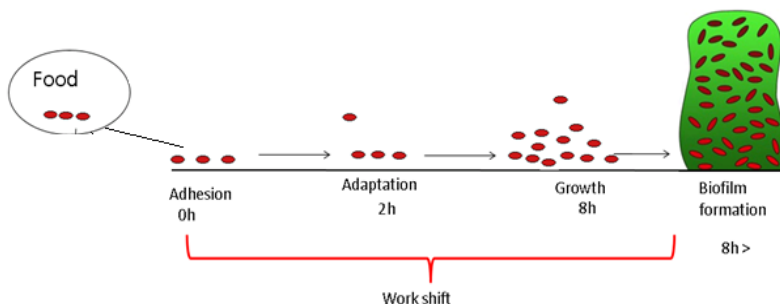


Figure 4 Schematic representation of bacterial attachment and growth on food contact surfaces during work shift, before formation of biofilm



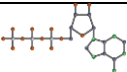

## **1.5 Detection of bacteria on food contact surfaces**

For any food processing factory, it is essential to count with an early warning sampling method: for real time monitoring of contamination of food contact surfaces, in time prevention of cross contamination and in place assessment of efficiency of cleaning and disinfecting procedures. Such solution will give an opportunity for significant reduction of consumers protection, economical loses and for feasible management of microbiological risks in certain food processing plants. There are two principal commercially available methodologies for sampling, detection and enumeration of microorganisms on food contact surfaces and both use mechanism of adhesive force. The first one represents rubbing the target surface with sponge or swab. In this case, bacteria attach to the swab or sponge surface and then is transferred to the agar plate. The second technique consists in pressing the solid agar contact plate on to target surface. The bacteria imprint on the surface of agar and become visible after incubation. General or specific media can be used to detect total either aerobic or anaerobic microorganisms, indicator organisms or pathogens. Both of these conventional methods are time consuming (results can be obtained only in 24 h up to 7 days after sampling), but on the other hand have low cost. The advantages and disadvantages of existing methods are presented in Table 1. The relatively modern immunology-based methods as well as molecular methods could be used in combination with swabbing technique for detection of bacteria on food contact surfaces in shorter periods. However, high cell numbers are necessary in case of immunological methods. Therefore, pre-enrichment procedures



are required. Thus, the qualified personal as well as labor-intensive procedures are essential for the appropriate detection and identification of target bacteria food contact surfaces with the above mentioned method. Molecular techniques have explicit advantages in comparison with cultural and immunological methods. The main features of molecular methods are high specificity, sensitivity and accuracy. However, they require skilled laboratory personal, expensive materials and equipment as well as several experimental steps. Therefore, the mentioned relatively rapid techniques cannot be used for detection of indicator and pathogenic bacteria during work shift period by food factory personal. Thus, the new, cheap tools with one-step operation, which allow to get reliable and robust results in very short time periods will be the perfect solution for controlling and preventing the microbial hazards coming from food processing environment. Sensors or biosensors could give such solution. Biosensors offer a rapid and cost-effective method of bacterial detection, which can be performed at the point of care without the need for a specialist user (Ahmed et al. 2014).

**Table 1 Methods/techniques of detection and quantification of bacteria on food contact surfaces, currently available in food industry.**

Method	Advantages	Disadvantages	Picture	Reference
Swabbing method	Detection and enumeration Applicable for crevices	Time (24 h-7 days) medium recovery efficiency		<a href="http://www.pixabay.com">www.pixabay.com</a>
Agar touching	Detection and enumeration High recovery efficiency	Time (24 h-7 days) Not applicable for narrow areas		<a href="http://www.pexels.com">www.pexels.com</a>
ATP swab	Rapid results (2 min.)	Applicable for assessment of general cleanness Impossible to differentiate bacteria from other substances		<a href="http://www.pixabay.com">www.pixabay.com</a>
PCR	Sensitive, robust, specific	Long sample preparation, multiple steps, expensive kits, qualified personal		<a href="http://www.pixabay.com">www.pixabay.com</a>

## 1.6 Colorimetric sensors

The colorimetric sensor is an instrument, which compares amount of light getting through unknown solution and amount of light getting through pure solvent. It determines the difference in intensity of initial light and transmitted light. The source light is passed through filter and concentrated using lens. Then this light is targeted on a sample. The light transmits through the sample

and the transmitted light is measured by detector (Bjelkhagen 2004) (Fig.5). An ideal sensor should have the following characteristics: selectivity, sensitivity, robustness, accuracy, precision, minimal error, reproducibility, linearity etc. Selectivity of a sensor is the ability to detect the target analyte among other compounds and substances. The sensitivity refers to detection of the target analyte at very low concentrations (Piriya V.S et al. 2017).

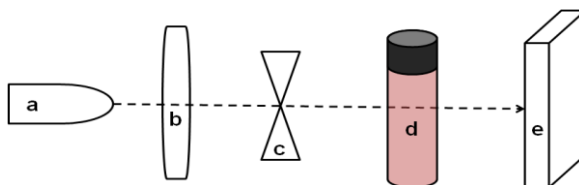


**Figure 5 Working principle of simple colorimeter. The light generated from the light source (a) passes through the lens (b), filter and sample (d) and the transmitted light is measured by the detector(e).**

Detection of bacteria by colorimetric techniques is widely used in practice. Usually simple colorimetric tools such colorimeter or spectrophotometer are used to detect change of color caused by presence of target bacteria (Cho et al. 2017). In recent years several types of new generation colorimetric sensors were developed. One of examples is colorimetric paper based analytical device, miniaturized analytical platform used for portable sensing applications. Change of the color occurs due to chemical reaction between an enzyme produced by target bacteria and colorimetric substrate. The color change can be detected by the naked eye or digital camera (Yakoh et al. 2018). Other type of colorimetric sensors are designed using gels or hydrogels. Hydrogels are three-

dimensional flexible networks of water-soluble polymers (Bhattacharya et al. 2017). The novel and useful property of the hydrogel in biosensor applications is the ability of the hydrogel to preserve the activity of sensing materials and also embed large number of substrates in high density (Miyata et al. 1999). The colorimetric sensor based on combination of portable optical sensor with a chitosan based hydrogel was applied for detection of *E. coli* cells (Sadat Ebrahimi et al. 2015). Chromogenic substrate 5,4-DDI -  $\beta$ -d-glucuronide was embedded into chitosan gel. 5,4-DDI was realized into the hydrogel upon reaction of mentioned substrate with the enzyme  $\beta$ -glucuronidase. The intense blue color produced by 5,4-DDI was detected by bare eye in hydrogel films. The novel colorimetric hydrogel based porous matrix was developed for detection of *E. coli* in water samples using specific enzyme activity (Gunda et al. 2016).

## 1.7 Fluorometric sensors

A fuorometer measures the fluorescence emitted by a fluorophore after being excited at lower wavelengths. The intensity of that emission depends on the concentration of the target analyte (De Acha et al. 2019). In order to construct fluorescent sensor two main components are required. The first is fluorophore and the second is receptor or recognition element. Fluorophore serve as signal transducer that transfer information into optical signal (Duke et al. 2010). Fluorogenic substrates have a used also in microbiology (Orenga et al. 2009). Most of them are coumarin-based substrates. The detection method of target bacteria is based on fluorometric

signal produced by fluorescent coumarin formed due to reaction of bacterial enzyme with substrate. Many of the fluorogenic substrates based on 4-MU or 7,4-MU are included into media or kits for rapid detection and identification of microorganisms (Manafi 1996). However, in recent years rapid, specific and more sensitive assays comparing to classical fluorogenic media and kits, for the detection of bacteria were developed. 4-MU- $\beta$ -d-glucuronide was used as a substrate for development of the rapid method for detection of *E. coli* in drinking water (Hesari et al. 2016).

## **1.8 Electrochemical sensors**

Electrochemical sensors possess high sensitivity, selectivity and robustness at low cost (Dhahi et al. 2010). All these characteristics are used for development of novel platforms with improved sensitivity to detect food-borne pathogenic bacteria. Electrochemical detection is based on a chemical or physical change on the electrode surface or near it. The change occurred due to interaction of target analyte with the electrode. As a result, the change of potential or current takes place, which generates the electrical signal. Target analyte is detected by registration of the generated signal and depending on signal type its detection system is termed potentiometry, amperometry and voltammetry, respectively (Stradiotto et al. 2003).

## 1.9 Cyclic Voltammetry

Electrode reaction mechanisms are studied mainly by voltammetry (Scholz 2015). Voltammogram represents a plot of potential versus current. In voltammetry usually the current signal is recorded at the chosen potential (Ozkan et al. 2015). Cyclic voltammetry (CV) is the most common voltammetry technique. According to (Ozkan et al. 2015) The important parameters in CV are the magnitudes of the peak currents:  $I_{p,a}$  (anodic) and  $I_{p,c}$  (cathodic), and the potentials at which peaks occur:  $E_{p,a}$  (anodic) and  $E_{p,c}$  (cathodic). The most difficult procedure in analyzing the cyclic voltammogram is the measuring the exact values of peak currents. The value of  $E_{p,a,c}$  is useful in characterizing compounds and can be used for identification (Espinoza et al. 2019). In case of reversible CV reaction the difference between anodic and cathodic potentials ( $\Delta E_p$ ) are equal to  $57/n$  mV and the relation of anodic and cathodic peak currents is equal to 1 (Pleskov 2007). One of the most important parameter of cyclic voltammetry analyses is the scan rate. The scan rate of the experiment controls how fast the applied potential is scanned. Faster scan rates result in higher currents due to a decrease in the size of the diffusion layer. If  $\Delta E_p$  is greater than  $57/n$  mV then the reaction is not fully reversible. For a quasi-reversible system the anodic peak is shifted to more positive potentials and the cathodic peak to more negative potentials (Ciobanu et al. 2007). In case of quasi-reversible system the potential peak depends on scan rate, the difference of anodic and cathodic potentials increases with the scan rate, the anodic and

cathodic peak currents depend on square root of scan rate in a non-linear way, and linearly depend on concentration of the analyte (Elgrishi et al. 2018). In case of irreversible CV systems, the decrease of current peaks height is occurred. The increase of the separation of cathodic and anodic potentials is occurred. In this case the dependence of peak potential on the scan rate is observed. The positive and negative shift of the anodic and cathodic potentials respectively is inherent for irreversible system. In case of irreversible CV system the potential depends on the scan rate, peak current is proportional to square root of the scan rate, and peak current is linearly proportional to concentration (Elgrishi et al. 2018).

## **1.10 Screen-printed electrodes**

Disposable screen-printed electrodes (SPEs) became popular in recent years for developing new generation of electrochemical sensor platforms. They have number of advantages comparing to classical electrodes and systems. One of the advantages is the low cost. Second, are the wide variety materials of working electrodes to choose, such as gold, platinum, silver, carbon, graphene and etc. Beside this, the already chosen surface of working electrode can be easily modified and improved depends on the purpose of use. Very low sample volumes (up to microliters), comparing to classical systems, made them indispensable from practical point of view. In addition, miniaturized size of screen-printed electrodes allows construction of portable devices and on-site detection of the target analyte. Finally, previous issues occurred with classical electrodes (e.g. memory effect and cleaning processes) can

be avoided using SPEs (Taleat et al. 2014). The main components of screen-printed electrodes are shown in Fig. 6. Screen-printed electrodes are produced with screen-printing machine using ink of different conductive materials. Usually, the commercial screen printed electrodes produced on the ceramic support. SPEs provide excellent platforms for the rapid detection of bacteria.

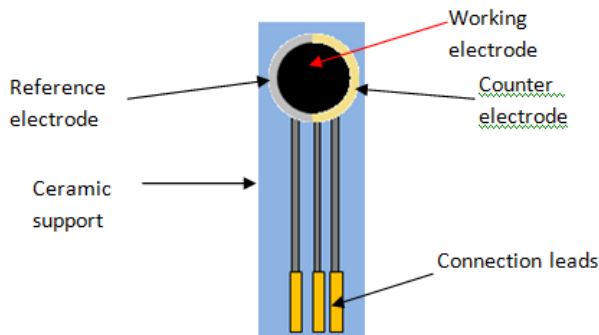


**Figure 6 Schematic representation of screen-printed electrode**

## 1.11 Electrochemical detection of bacteria

Electrochemical techniques are used for the detection of whole bacteria, bacterial metabolites and enzymes (Ivnitski et al. 2000). Detection of specific electrochemical signals inherent for different biological targets could be done without highly specialized material or instrumentation (Kuss et al. 2018).

Several authors have described electrochemical approaches for detection of bacterial enzyme and detection of specific bacterial groups based on their enzymatic activity. Tschirhart et al. (Tschirhart et al. 2016) reported electrochemical detection of  $\beta$ -D-Galactosidase of the whole and lysed cells using 4-aminophenyl  $\beta$ -D-



Galactopyranoside substrate. The detection of acyl homoserine lactones (inducers of quorum sensing) by indirectly measurement of  $\beta$ -D-Galactosidase activity on gold microelectrode arrays, using the mentioned 4-aminophenyl- $\beta$ -D-galactopyranoside substrate, was performed by Baldrich et al. (Baldrich et al. 2011). The mentioned method represents electrochemical (cyclic voltammetry) detection of PAPG consumption and PAP production due to  $\beta$ -D-Galactosidase activity, produced by studied bacteria, which was generated in response to the presence of quorum sensing autoinducers such acyl homoserine lactones. The  $\beta$ -D-Galactosidase based amperometric detection of *E. coli* using PAPG substrate was demonstrated by Mittelman et al. and Cheng et al. (Mittelman et al. 2002, Cheng et al. 2008) on disposable screen printed carbon electrodes and nanotubes modified glassy carbon electrodes respectively.

Most of the developed electrochemical techniques have been designed for detection of target bacteria in water samples with relatively easy filtration method (where the filtration used as immobilization of bacteria on substrate) comparing to challenging sampling of bacteria from food contact surfaces. To our knowledge, there is no commercially available, low-cost, single-step electrochemical platform designed for real time monitoring of growth, detection and quantification of Coliforms on food contact surfaces in food processing industry during production shift. To date, the chromogenic indoxyl, phenol as well as fluorogenic coumarin based substrates were used only for colorimetric and fluorometric detection and quantification of Coliforms, *E. coli* and pathogenic bacteria on conventional chromogenic agars or by improved colorimetric devices. The electrochemical detection of these bacteria using

above-mentioned substrates has never been reported. Detection and quantification of *St. aureus* using optical signal generated due to reaction Phospholipase C with specific substrate activity also has never been reported previously and mentioned reaction has never been used in chromogenic agars specific for *St. aureus*. The modification of screen printed electrodes with the gel containing polyacrylamide and agar-agar for detection of bacteria has never been performed. The combination of optical and electrochemical signals for the simultaneous detection of foodborne bacteria on food contact surfaces has never been performed previously. Thus, in present work we described the construction, optimization and testing of the platform for novel electrochemically and optically active gel modified sensor for the specific and rapid detection and quantification of Coliforms, *E. coli* and *St. aureus* on food contact surfaces.

## 2 Objective

Design a combined electrochemical and optical device/sensor platform for rapid and selective detection and enumeration of Coliforms, *E. coli* and *St. aureus* on food contact surfaces.

### 2.1 Specific goals

- Develop a gel system for the rapid and efficient attachment of bacteria from food contact surfaces.
- Develop an electrochemical (voltammetric) sensing system (gel-electrode system) for rapid detection of target bacteria.
- Modify the developed gel-electrode system to increase the detection efficiency and specificity.
- Develop an optical (colorimetric/fluorometric) sensing system for rapid detection of target bacteria.
- Combine and incorporate the developed two systems into the previously developed gel system.
- Apply developed platform for detection of target bacteria in culture media.
- Apply developed platform for the detection, quantification and monitoring of target bacteria on stainless steel surface.
- Validate the obtained results with the classical microbiological methods (according to standards).

### 3 Proposed platform

The schematic illustration of the proposed platform is shown in Fig. 7. The planned platform should possess the following features:

- Optimal design to allow easy, on site sampling of food contact surfaces.
- Detect and differentiate the above-mentioned bacteria from the other microflora in food processing environment.
- Monitor bacteria on food contact surfaces in real time.
- One-step operation principle (no enrichment, or other extra preparation steps).

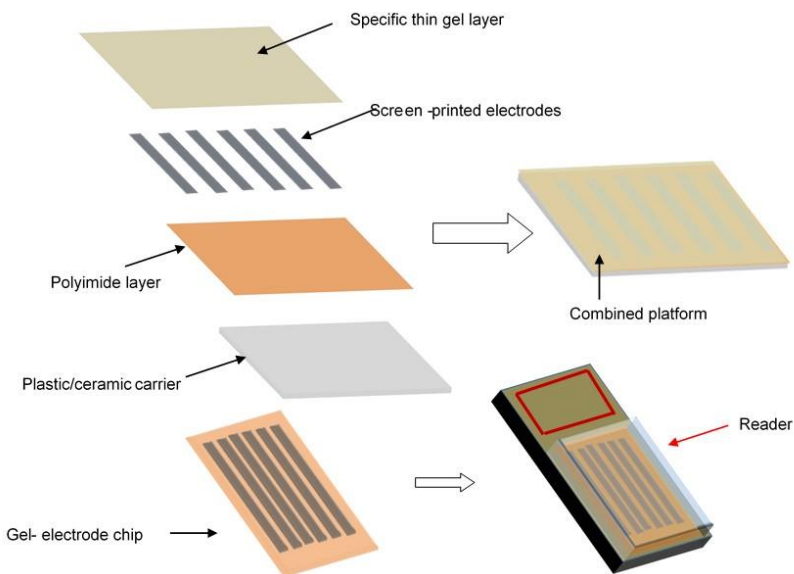
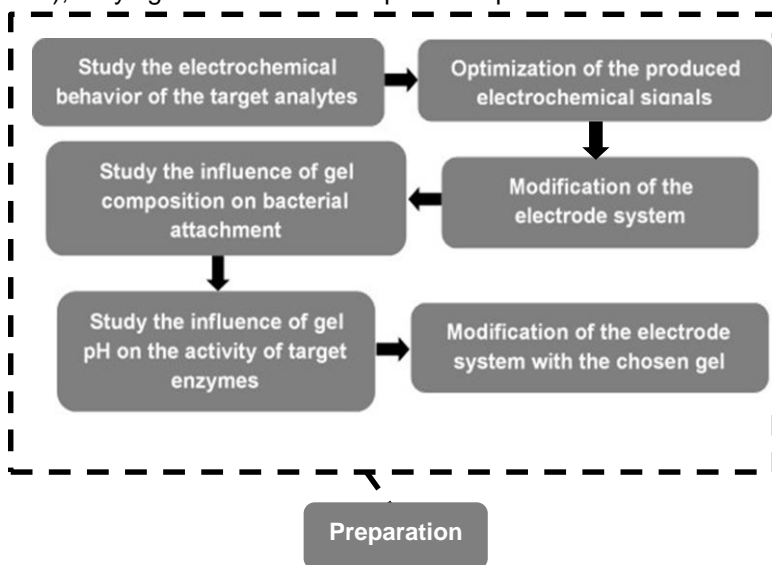


**Figure 7 Schematic illustration of proposed sensor platform.**

The thin layer of gel consists of substrate for electrochemical and optical reaction, accelerator reagents and inducer. The electrode system is made by imprinting the carbon ink on the bottom surface of the gel. Ready gel-electrode system is attached to the plastic or ceramic carrier by adhesive. The ready, combined gel-electrode platform on cheap is applied to the tested surface by pressing it on the target surface for 4 minutes. Then the chip is placed in to the reader, equipped with colorimeter and potentiostat.

## 4 Experimental work

The present PhD work is comprised of several different stages, which results should provide the necessary information to be used as base for the construction of the proposed sensor platform. The experimental scheme (Fig. 8) is a general scheme which will be executed for the 3 selected bacteria (*E. coli*, total Coliforms and *St. aureus*), varying in each case the specific experimental conditions.



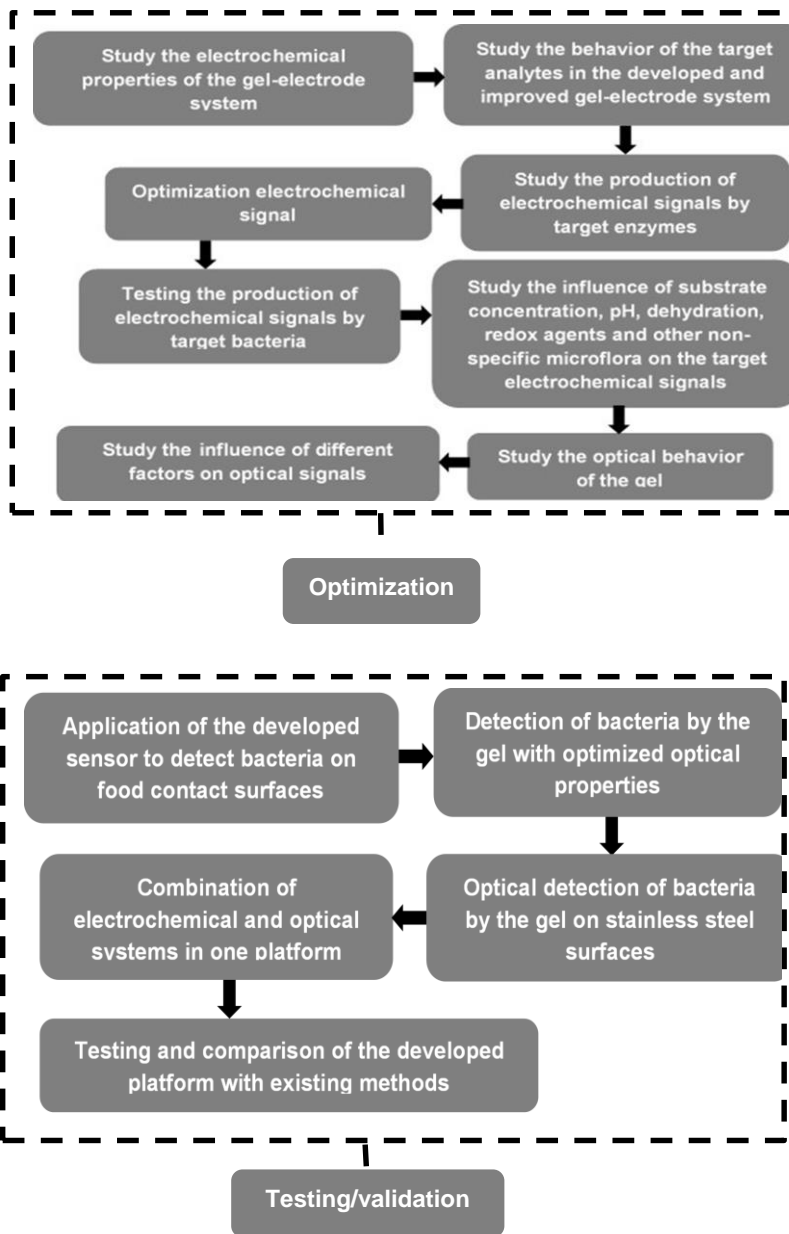
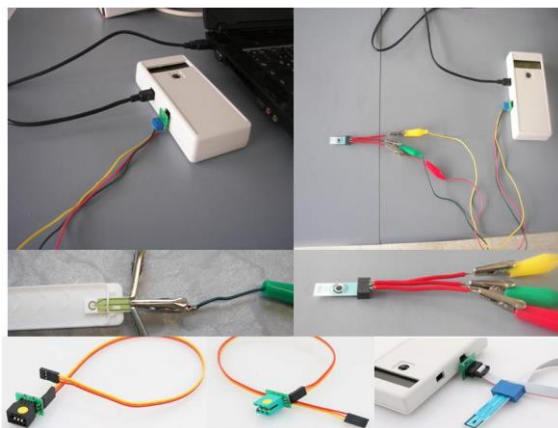


Figure 8 The main experimental steps of the present work.

## 4.1 Electrochemical detection of the target analytes

Cyclic voltammetry was used for all types of electrochemical analyses performed in this work. CV experiments were performed using CheapStat potentiostat (Fig.9) (IO Rodeo Inc, USA) equipped with commercial connector for SPEs and interfaced in computer with CheapStat user interface. Electrochemical measurements were conducted at room temperature. Each measurement was done with a new disposable screen-printed electrode. Disposable screen-printed carbon and gold electrodes (Ref. 110, C220AT DropSens, Metrohm, Germany) were used in this study. Carbon and gold SPEs consisted of three-electrode system. Carbon electrode includes 4mm diameter working (carbon) electrode, auxiliary (carbon) and reference (silver/silver chloride) electrodes. Gold electrode includes 4mm diameter working (gold) electrode, auxiliary (gold) and reference (silver/silver chloride) electrodes.



**Figure 9 CheapStat potentiostat with different adapters for SPEs**

Preparation of stock solutions of the target analytes (5,5' – dibromo-4,4'-dichloro-indigo /6,6'-Dichloro-Indigo, 4-methylumbelliferone, and 4-nitrophenol) was done as follows: 0.03 g of 5,5 – dibromo-4,4-dichloro-indigo/6,6-Dichloro-Indigo, 0.017 g of 4-MU and 0.014 g of 4-NP was diluted into 1ml mixture of DMSO (Dimethyl sulfoxide, CHEMSOLUTE, Germany) and distilled water (1:1). Then the appropriate dilutions in phosphate buffer saline PBS (1x, pH=7.4) from each solution were made. Fifty microliters of each target analyte solution were transferred on to surface of carbon or gold SPEs in order to measure the voltammetric signals. The blank solutions (i.e. substrate in PBS) for each analyte were prepared by dissolving the 1 mg of 5-4-BCIG, 4-MUG and 4- NPP in 1 ml of PBS and heating (by shaking) at 99 °C for 3 minutes in Eppendorf Thermomixer. Fifty microliters from each blank solution were transferred on to surface of carbon or gold SPEs in order to measure the voltammetric signals.

## **4.2 Preparation of graphene solution**

Hundred microgram of hydrophilic graphene nanoplatelets (GNPs) (Sigma-Aldrich, Germany) were dispersed in 10 mL of 1:1 mixture of DMF (N,N-Dimethylformamid, CHEMSOLUTE, Germany) and distilled water (DW). The mixture was sonicated in a sonication water bath (Sonorex, Bandelin, Germany) at room temperature, at 150 W, 50 Hz, for 1 h. Then the ready dispersion was stored in plastic tube in dry and dark place for the future use.



### 4.3 Modification of carbon SPEs

Four microliters of previously prepared graphene dispersion was transferred on the working surface of carbon SPEs. Then, the electrodes (in open Petri dishes) were dried at room temperature until the full evaporation of the liquid. Thereafter, the drying continued at the 65 °C for 18 hours in incubator. Then cyclic voltammetry of ready modified bare electrodes were performed at 50 mV/S scan rate, at the potential ranging from -800 mV to 1200 mV. Then ready electrodes were stored at dry and dark place for the future use.

### 4.4 Bacteria cultivation and enumeration

Freeze-dried cultures of *E. coli* DSM 498, *E. coli* DSM 301, *Hafnia alvei* DSM 30163<sup>T</sup>, *Klebsiella pneumonia* DSM 30104, *Bacillus pumilus* DSM 27<sup>T</sup>, *Pseudomonas fluorescence* DSM 50090<sup>T</sup> and *Lactobacillus acidophilus* DSM 20079 were obtained from Leibniz Institute DSMZ-German Culture Collection. Each strain was revived by adding 0.5 mL of liquid media (Nutrient broth, Sigma Aldrich®, Germany) to the dry pellet. Suspended cultures were transferred to Nutrient broth and Nutrient agar plates (Sigma Aldrich®, Germany) and were incubated at 37 °C (*E. coli* DSM 498, *E. coli* DSM 301, *Klebsiella pneumonia* DSM 30104) and at 30 °C (*H. alvei* DSM 30163<sup>T</sup>, *B. pumilus* DSM 27<sup>T</sup>, *P. fluorescence* DSM 50090<sup>T</sup> and *Lactobacillus acidophilus* DSM 20079) for 24h. The Coliform strains *E. coli* DSM 498, *E. coli* DSM 301, *H. alvei* DSM 30163<sup>T</sup>, and *K. pneumonia* DSM 30104 were cultured on HiCrome™

Coliform agar (Sigma Aldrich, Germany) in order to confirm their  $\beta$ -D-Galactosidase activity and to increase strain selectivity. *E. coli* DSM 301 was cultured on HiCrome™ *E. coli* and Endo agars. *St. aureus* DSM 799 was cultured on Mannitol Salt and Baird Parker agars. *Lactobacillus acidophilus* DSM 20079 was cultured on MRS agar.

A mixture of Coliform bacteria was prepared by transferring of each Coliform strain (half of 3 mm loop) to 200 mL nutrient broth. The viable concentrations of the mixed Coliforms, *E. coli* DSM 301 and *St. aureus* DSM 799 cultures were determined by monitoring of the growth by optical density (OD<sub>600</sub>) and plate count method during 24 hour by shaking at 37 °C. For each new experiment, the same inoculation conditions were used. The working suspension with the inoculation level of 8.6 log<sub>10</sub>CFU/mL (4x10<sup>8</sup>CFU/mL) was centrifuged at 7000 rpm/min for 20 minutes, washed twice with phosphate buffer saline (PBS, pH 7.4) and re-suspended in physiological saline solution. Suspended cultures were serially diluted and enumerated to verify the initial concentration. Bacterial cultures were further diluted to reach concentrations ranging from 0.6 log<sub>10</sub>CFU/mL to 8.6 log<sub>10</sub>CFU/mL to use them in the following experiments.

#### **4.5 Testing of bacterial attachment to gels**

Four types of gels containing 5 g/L Peptone, 5 g/L NaCl, 2 g/l KH<sub>2</sub>PO<sub>4</sub>, 2 g/L K<sub>2</sub>HPO<sub>4</sub>, 10 g/L agar-agar, 1 g/L polyacrylamide and 3 g/L meat extract (Carl Roth, Germany) in different combinations have been tested (Table 2). After sterilizing at 120 °C for 15 min., 20 mL of each gel was uniformly poured into plastic Petri dishes and stored at 4 °C for 18 h. Stainless steel

coupons were inoculated at different concentrations (0.6 log<sub>10</sub>CFU/mL to 3.6 log<sub>10</sub>CFU/mL) of Coliform bacteria (*E. coli* DSM 498, *E. coli* DSM 301, *Hafnia alvei* DSM 30163<sup>T</sup>, *Klebsiella pneumonia* DSM 30104) and *St. aureus* DSM 799 by the above-described method. After drying, the stainless steel coupons were attached, by contact, to the surfaces of four different gels for 5min. To ensure an equal pressure and attachment conditions for every sample, 300 g weights were placed on top of each coupon. After incubation at 37 °C for 24 h, the attached colony form units were counted.

**Table 2 Compositions of four types of gels used for the sensor platform**

Concentration	Name			
	Gel-1	Gel-2	Gel-3	Gel-4
5 g/L	Peptone	Peptone	Peptone	Peptone
2 g/L	KH <sub>2</sub> PO <sub>4</sub>	KH <sub>2</sub> PO <sub>4</sub>	KH <sub>2</sub> PO <sub>4</sub>	KH <sub>2</sub> PO <sub>4</sub>
2 g/L	K <sub>2</sub> HPO <sub>4</sub>	K <sub>2</sub> HPO <sub>4</sub>	K <sub>2</sub> HPO <sub>4</sub>	K <sub>2</sub> HPO <sub>4</sub>
5 g/L	NaCl	NaCl	NaCl	NaCl
10 g/L	Agar	Agar	Agar	Agar
1 g/L		Polyacrylamide		Polyacrylamide
3 g/L			Meat extract	Meat extract

#### 4.6 Optimization of pH and optical characteristics of the gel

The gel, with the highest attachment efficiency, was used for testing the influence of pH on β-D- Galactosidase, β-D-

Glucuronidase and Phospholipase C activity. The gels with pH values ranging from 6.0 to 8.0 were prepared by addition of 1 M HCL or 0.1 M NaOH, respectively. After sterilization, the gels were cooled down to 50 °C following with addition of 0.5 g/L 6-CIGP and 0.2 g/L IPTG (Carl Roth, Germany) as well as 0.5 g/L 4-NPP (VWR, Germany) to the gel intended for the Phospholipase C activity. After appropriate mixing, the gels were poured into 6-well polystyrene plates (VWR, Germany) and dried for 2 h. Then, 0.01 mg/mL  $\beta$ -D-Galactosidase and Phospholipase C (Sigma-Aldrich, Germany) diluted in PBS were injected to all gels, except the blanks. Thereafter, half of the plates were placed in to microplate reader (Synergy MX, Biotech, Germany) for detection of optical signal and the other part were placed in the incubator for visual control of color formation. The part of plates were incubated at 42 °C and another part at 37 °C for 2 h for period. Absorbance was measured at 530 nm and 420 nm wavelengths. The color and fluorescence formation due to  $\beta$ -D- Galactosidase and  $\beta$ -D- Glucuronidase in the gel system was studied by the following method: the 0.1 mg/mL of the mentioned enzymes were injected in to the gel system containing 0.5 mg/mL of 6-CIGP,5,4-BCIGP and 4-MU respectively. Then the gels were incubated at 37°C for 3h. The color formation was monitored visually and spectrophotometrically every 10 minutes. The fluorescence was monitored in the fuorometer and UV chamber.

#### **4.7 Testing inducers and accelerator reagents**

The next step was the optimization of the enzyme inducers and membrane permeabilization reagents for each target

bacteria. The IPTG and OBDG were used as inducers of  $\beta$ -D-Galactosidase and  $\beta$ -D-glucuronidase for Coliforms and *E. coli* respectively. The suspensions with different concentrations of IPTG and OBDG (varying from 0.1 mg/ml to 0.8 mg/ml) were prepared by dissolving them in to PBS (varying from 0.1 mg/ml to 0.8 mg/ml). Different cell permeabilization reagents (accelerators) namely SDS (Sodium dodecyl sulfate), TrytonX-100(4-(1,1,3,3-Tetramethylbutyl) phenyl-polyethylene glycol), B-PER (Bacterial Protein Extraction Reagent), DDM (n-Dodecyl-D-Maltoside), ODTG and OBG were used. The 0.005mg/mL PBS suspensions were prepared for each reagent. Hundred microliters of bacterial suspension were added to microplate well containing 100  $\mu$ L of specific broth (the same composition as the Gel-2, but without agar and acrylamide) with 0.5 mg/mL of specific substrate. Then 50  $\mu$ L from each inducer plus 25  $\mu$ L from each accelerator were added to the same well. Then the microplate was incubated at 37 °C for 3 h and the parallel plates were placed in the microplate reader for the same time. Two hundred microliters of each bacterial suspension were added to the Eppendorf tube containing 200  $\mu$ L of above-mentioned specific broth (with 0.5mg/mL substrate) and then the 100  $\mu$ L of each inducer and 50  $\mu$ L of each accelerator were added to the tube. The Eppendorf tubes were incubated in Thermomixer at 37°C. Selected inducers and accelerators gels with the optimized concentrations (0.2 mg/mL for inducers and 0.2 mg/mL for accelerators) were incorporated in to the gel by adding them to the melted gel (40 °C) before pouring the gel in to 6-well pates or covering the screen-printed electrode.

## 4.8 Preparation of gel-modified electrodes

The gels with the optimized composition and pH values were chosen for the future experiments. All gel components with appropriate concentrations (Table 2) components were mixed and stirred on magnetic stirrer for 30 minutes. After adjustment of pH the substrate, accelerating reagent and the inducer with the appropriate concentrations (0.2 mg/mL inducer and 0.005 mg/mL accelerator) were added and the solutions were transferred to Eppendorf tubes. The gel mixtures undergone thermal treatment in thermomixer (Eppendorf, Germany) at 98 °C for 2 minutes. Gels were prepared weekly using ultrapure water obtained from CHEMSOLUTE® (Germany).

The coating of SPEs by gel was performed by drop-casting and electrochemical deposition methods (Carrington et al. 2006, Pérez-Ràfols et al. 2017). For this, 0.1 mL of the gel was dropped on the screen-printed electrode surface. Gel drop was carefully spread to cover whole electrode surface. Drop-casting was done with high accuracy to obtain uniform, thin-layer gel films. Each of the covered electrode was placed in separate plastic Petri dishes and stored in dark and dry place for 1 h. Electrochemical deposition of casted gel films were performed by cyclic voltammetry at a scan rate of 20 mV, at potential range from -700 to 800 mV. For the graphene-gel modified carbon screen-printed electrodes A volume of 200 µL and 500 µL of the previously prepared graphene dispersion was transferred to 800 µl and 1800 µl of gel (which was cooled down to 50 °C) and then deposition on screen printed electrodes took place.

Screen-printed electrodes covered with thin gel layer were used for the future experiments (Fig. 10).

#### 4.9 Bacterial attachment and enumeration on stainless steel surfaces

Stainless steel coupons (5cmx5cm, Type 304, 2b finish) were cleaned using acetone and alkaline detergent, prior its use. The cleaned coupons were boiled in DW for 15 minutes, dried for 24 h, and autoclaved at 121 °C for 15 minutes as described by Son et al. (Son et al. 2016).

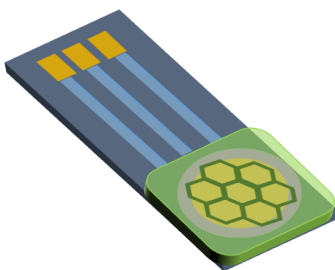


**Figure 10 Schematic representation of gel-modified screen-printed electrode.**

After this period, the center of each 25 cm<sup>2</sup> coupon was inoculated with 1 mL of suspension containing Coliforms (*E. coli* DSM 498, *E. coli* DSM 301, *Hafnia alvei* DSM 30163<sup>T</sup>, *Klebsiella pneumonia* DSM 30104), *E. coli* DSM 301 and *St. aureus* DSM 799 cultures with concentrations ranging from 0.6 log<sub>10</sub>CFU/mL to 8.6 log<sub>10</sub>CFU/mL. To simulate working /soiled conditions, meat juice was used as soiling agent. Meat juice was prepared by homogenization of fresh minced meat and further filtration with paper filter. Filtered juice was

sterilized by syringe using 0.2 µm, sterile, PTFE membrane filters (Millipore, Germany). Sterile meat juice was stored at -20°C for future experiments. The meat juice was transferred, spread and dried (for 30 min) on the surface before inoculation with the Coliform bacteria (*E. coli* DSM 498, *E. coli* DSM 301, *Hafnia alvei* DSM 30163<sup>T</sup>, *Klebsiella pneumonia* DSM 30104). The stainless steel surfaces were incubated in the presence of Coliform bacteria (*E. coli* DSM 498, *E. coli* DSM 301, *Hafnia alvei* DSM 30163<sup>T</sup>, *Klebsiella pneumonia* DSM 30104), meat juice and nutrient broth during 48 hours at 37 °C. The cleaned and sanitized stainless steel surfaces were inoculated with the 8 log<sub>10</sub>CFU/mL suspension of Coliforms (*E. coli* DSM 498, *E. coli* DSM 301, *Hafnia alvei* DSM 30163<sup>T</sup>, *Klebsiella pneumonia* DSM 30104) and incubated at 15 °C for 4 h. The sampling of stainless steel surfaces contaminated with Coliforms (*E. coli* DSM 498, *E. coli* DSM 301, *Hafnia alvei* DSM 30163<sup>T</sup>, *Klebsiella pneumonia* DSM 30104) and meat juice was done at every 1 h with designed sensor. Verification of final concentration of the attached Coliform bacteria on the clean (sterile DW) and soiled (meat juice) stainless steel surfaces was done by wet-swabbing and agar touching methods according to (ISO18593 2004) and (FNES4 2017) standards.

#### **4.10 Voltammetric detection of bacterial cultures**

Coliform bacteria (*E. coli* DSM 498, *E. coli* DSM 301, *Hafnia alvei* DSM 30163<sup>T</sup>, *Klebsiella pneumonia* DSM 30104), *E. coli* DSM 301 and *St. aureus* DSM 799 cultures were prepared by previously described method (see 4.4) to get concentrations ranging



from 0.6 log<sub>10</sub>CFU/mL to 7.6 log<sub>10</sub>CFU/mL. Hundred microliters aliquots of each bacterial suspension were transferred to the gel-electrode system. The same volume of *B. pumilus* DSM 27<sup>T</sup> and *P. fluorescens* DSM 50090<sup>T</sup> culture suspensions (7.6 log<sub>10</sub>CFU/mL) as well as 6.6 log<sub>10</sub>CFU/mL *L. acidophilus* DSM 20079 were also injected to separate gel-electrode systems as negative controls. The gel-electrode systems were incubated at 37 °C at 42 °C – 44 °C (negative controls were incubated at 35 °C because higher temperatures may inhibit metabolic activity of these strains) for 3 h. Cyclic voltammetric measurements of each concentration were conducted every 20 min. CV experiments were performed using CheapStat potentiostat (IO Rodeo Inc, USA) equipped with commercial connector for screen-printed electrodes (SPEs) and interfaced in computer with CheapStat user interface. Electrochemical measurements (scan rate of 50 mV/s) were conducted at room temperature. Each measurement was done with a new disposable screen-printed sensor. Control CV measurements of the gel system, without substrate or injected bacterial suspension were also performed.

#### **4.11 Voltammetric detection of bacteria on stainless steel surfaces**

Attachment experiments to stainless steel surfaces (25 cm<sup>2</sup>) were done by the above-described method (see 4.10). Stainless steel coupons inoculated with bacterial suspensions ranging from 0.6 log<sub>10</sub>CFU/mL to 7.6 log<sub>10</sub>CFU/mL were prepared. Both clean (covered with sterile DW) and soiled (covered with sterile meat juice) surfaces were used. Gel-electrode systems were

attached to coupons in twenty randomly chosen contact points. Sterile 20 g weights were applied to each gel-electrode system. The total attachment time was 8 minutes. After touching and removing of the coupons from the electrodes, the gel-electrodes systems were incubated at 37 °C and 42 °C – 44 °C (for Coliforms) for 3 h. In parallel prepared coupons were examined by wet swabbing and agar touching methods.

#### 4.12 Statistical analyses

All measurements and tests were performed in triplicate. Data shown represent the average from at least three measurements (using different electrodes in case of electrochemical tests). All CFU values were log<sub>10</sub>-transformed. The Student' t-test (Microsoft® office excel® 2016) was used to compare the means of attachment efficiencies of different gels. The limit of detection (LOD) was calculated according following formula:  $LOD = (k \times sb)/m$ . Where **k** coefficient equal to 2 or 3 at confident levels of 92.1 % and 98.3 % respectively; **sb** is the standard deviation of the blank and **m** is the calibration sensitivity that is slope of the linear plot between concentration and current. The data from electrochemical experiments were analyzed in open sources freeware package “eL-Chem Viewer” (Hrbac et al. 2014).

## 5 Results

### 5.1 Electrochemical detection of target analytes

The electrochemical detection and properties of the target analytes are discussed in this section. The voltammetric signals produced by 5,4-DDI on gold SPEs are shown in Fig. 11.

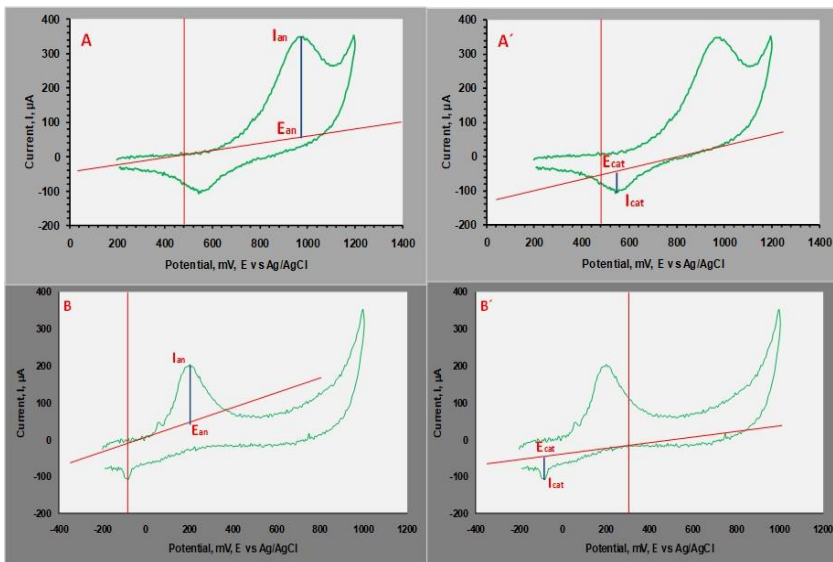


**Figure 11** Electrochemical behavior of 5,4-DDI on screen printed gold electrode. **A, A')** The CV curves produced by 5,4-DDI at potential range: 50 mV to 1200 mV;  $V_{scan} = 50$  mV/s;  $E_{pa} \sim 970$  mV,  $E_{pc} \sim 560$  mV;  $I_{pa} \sim 350$   $\mu$ A,  $I_{pc} \sim -100$   $\mu$ A. **B, B')** The CV curves produced by 5,4-DDI at potential range: -200 mV to 1200 mV;  $V_{scan} = 50$  mV/s;  $E_{pa} \sim 200$  mV,  $E_{pc} \sim -80$  mV;  $I_{pa} \sim 200$   $\mu$ A,  $I_{pc} \sim -100$   $\mu$ A. Analyses of the electrochemical data and CV curve parameters was done using el-Che mViewer package.

As shown in Fig. 11A, the voltammogram of 5,4-DDI had both anodic and cathodic peaks however irreversibility of CV curve was observed. The ratio of cathodic and anodic peak currents ( $I_{p}^{red}/I_{p}^{ox}$ ) value was equal to 0.2. The CV voltammograms of 5,4-DDI on the

gold screen-printed electrode at the potential ranging from -200 mV to 1200 mV are shown in Fig. 11B. The anodic potential decreased from 970 mV to 200 mV and the cathodic increased from -560 mV to -90 mV. The voltammetric peaks produced by 5,4-DDI on gold SPEs at the potential range varying from -200 mV to 300 mV are shown in Fig. 12A. In this case, the potential difference decreased up to ~ 120 mV and the ratio of cathodic and anodic currents increased from 0.1 to 0.5. The CV curve produced due to redox reaction of 5, 4-DDI on carbon electrodes in the similar potential range (-200 mV to 300 mV) is shown in Fig. 12B. The quasi-reversible curve ( $i_{cat}/i_{an} = 1$ ,  $\Delta E_p = 180$  mV) showed negative potential shift. The electrochemical behavior of different concentrations of 5,4-DDI on gold and carbon electrodes is shown in Fig. 13.

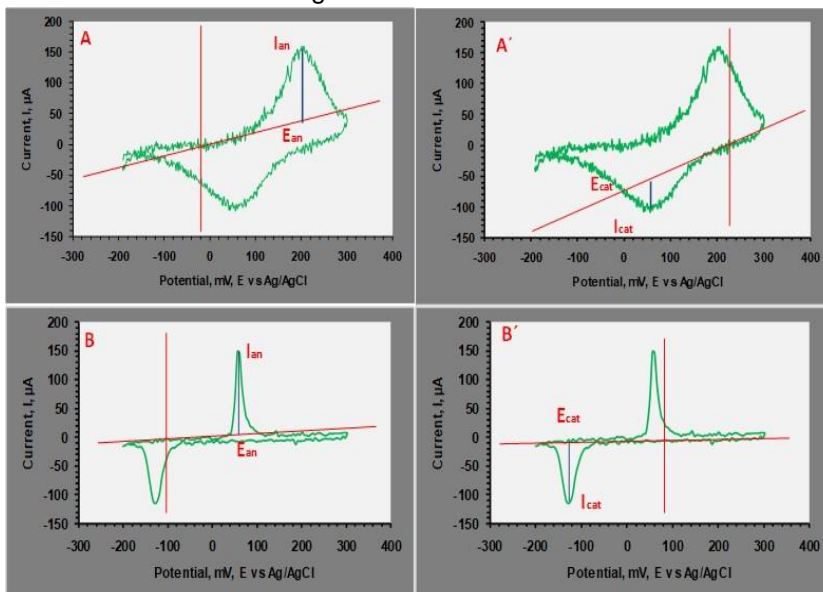


**Figure 12** Electrochemical behavior of 5, 4-DDI on screen printed gold and carbon electrodes. A, A') The CV curves produced by 5-4-DDI on gold electrode at potential range: -200 mV to 300 mV;  $V_{scan} = 50$  mV/s;

$E_{pa} \sim 200$  mV,  $E_{pc} \sim 56$  mV;  $I_{pa} \sim 122$   $\mu$ A,  $I_{pc} \sim 60$   $\mu$ A. B, B') The CV curves produced by 5-4-DDI on carbon electrode at potential range: -200 mV to 300 mV;  $V_{scan} = 50$  mV/s;  $E_{pa} \sim 60$  mV,  $E_{pc} \sim -127$  mV;  $I_{pa} \sim 83$   $\mu$ A,  $I_{pc} \sim 82$   $\mu$ A. Analyses of the electrochemical data and CV curve parameters was done using el-Che mViewer package.

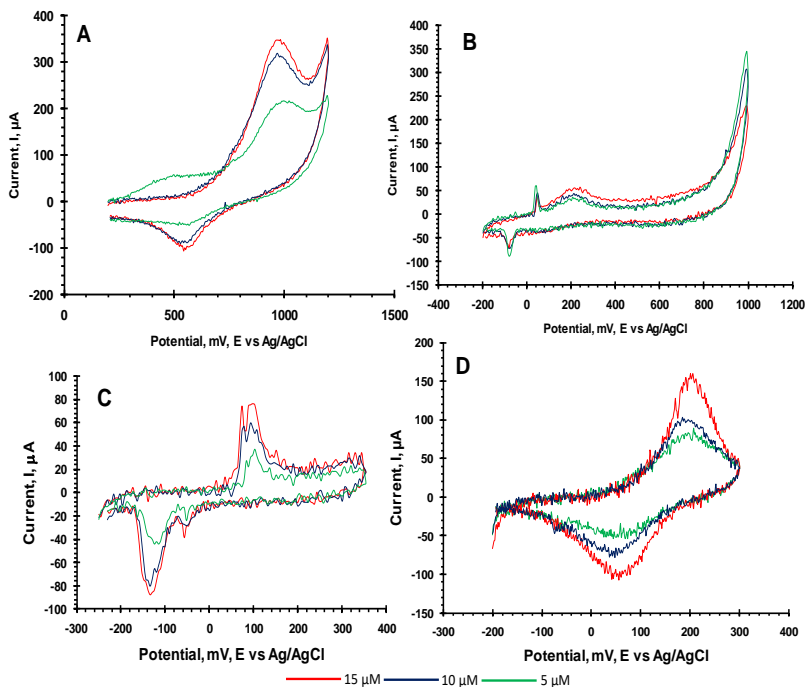


**Figure 13** CV curves produced by different concentrations (Green-5  $\mu$ M; Dark blue – 10  $\mu$ M; Red - 15  $\mu$ M) of 5-4-DDI on gold and carbon electrodes. A) The CV curves produced by 5-4-DDI on gold electrode at potential range: 50 mV to 1200 mV;  $V_{scan} = 50$  mV/s. B) The CV curves produced by 5-4-DDI on gold electrode at potential range: -200 mV to 1200 mV;  $V_{scan} = 50$  mV/s. C) The CV curves produced by 5-4-DDI on carbon electrode at potential range: -200 mV to 300 mV;  $V_{scan} = 50$  mV/s. D) The CV curves produced by 5-4-DDI on gold electrode at potential range: -200 mV to 300 mV;  $V_{scan} = 50$  mV/s.

All peak currents increased by increasing concentration of 5-4-DDI. The shapes and peaks of all voltammograms obtained in 4 different

scanning ranges were correspond to initial CV curves of 5,4-DDI. The CV curves produced by 5,4-BCIG in all potential ranges on gold and carbon electrodes are shown in Fig. 14. Conducted CV measurements have shown that blank solution (1 mg/ml substrate in PBS) produced well-shaped redox signals in all previously tested potential ranges on gold electrodes. On carbon electrodes the substrate produced small cathodic current ( $-20\mu\text{A}$ ) and did not produced any signal at the  $E_{\text{an}}=100\text{ mV}$  where the  $5\text{ }\mu\text{M}$  of target analyte showed sharp CV peak. The small anodic current was detected at negatively shifted potential ( $E_{\text{an}}=70\text{ mV}$ ,  $I_{\text{an}} = 15\text{ }\mu\text{A}$ ). The redox behavior of 5,4-DDI on carbon electrode at negative potential ranges is shown in Fig.15A. The CV curve formed during scan from  $-600\text{ mV}$  to  $400\text{ mV}$  potential at  $50\text{ mV/s}$  scan rate had a 2 anodic peaks at  $-240\text{ mV}$  and  $130\text{ mV}$  respectively and one cathodic peak at  $-305\text{ mV}$ . The results of CV measurements of 5,4-BCIG substrate at the selected potential range are shown in Fig. 15B. The blank solution (5,4-BCIG in PBS,  $\text{pH}=7.4$ ) did not produce any CV peak at the tested potentials. The redox behavior of different concentrations of 5,4-DDI varied from  $5$  to  $25\text{ }\mu\text{M}$  on carbon electrodes (Fig. 16A). A good linear relationship ( $R^2=0.98$  for anodic and  $R^2=0.97$  for cathodic) was found between anodic and cathodic peak currents and tested concentrations (Fig 16B). The influence of different scan rates on CV curves produced by 5,4-DDI is shown in Fig. 17A. The linear-log and linear relationship was found between square roots of applied scan rates and anodic and cathodic currents ( $R^2=0.98$ ) (Fig. 17B, C). A good linear relationship ( $R^2=0.97$ ) between increasing  $\Delta E$  values and scan rates was obtained. The electrochemical behavior of 4-MU on carbon SPEs is shown in Fig.

18. The 4-MU produced irreversible CV peak at  $E_{an} = \sim 665$  mV at the potential range varying from 0 to 1000 mV. There was no detection of redox peaks at lower and negative potential ranges.

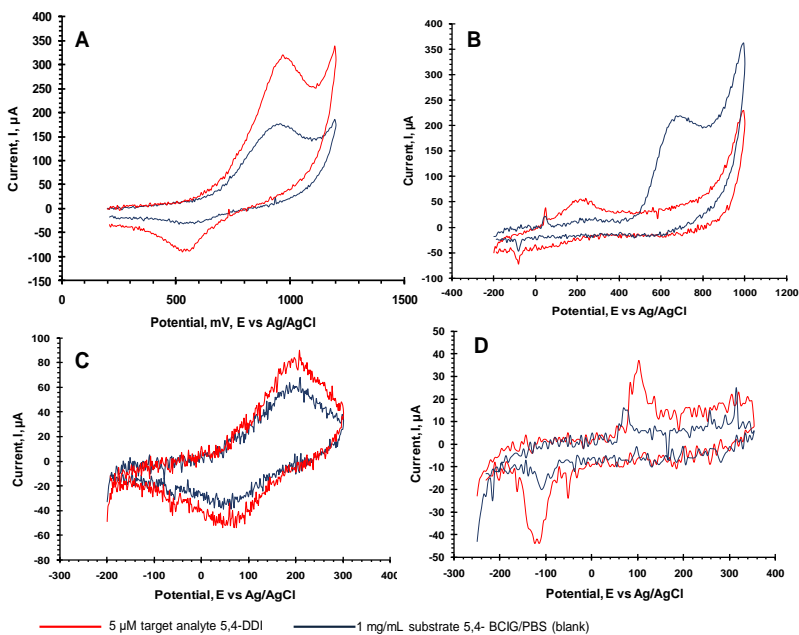


**Figure 14 Comparison of the CV curves produced by the blank (5-4-BCIG in PBS, pH=7,4) (Dark blue) and target analyte (5-4-DDI) (Red) on gold and carbon electrodes.  $V_{scan} = 50$  mV/s. A) Gold electrode, 50 mV to 1200 mV; B) Gold electrode, -200 mV to 1000 mV; C) Gold electrode, -200 mV to 300 mV; D) Carbon electrode, -200 mV to 300 mV.**

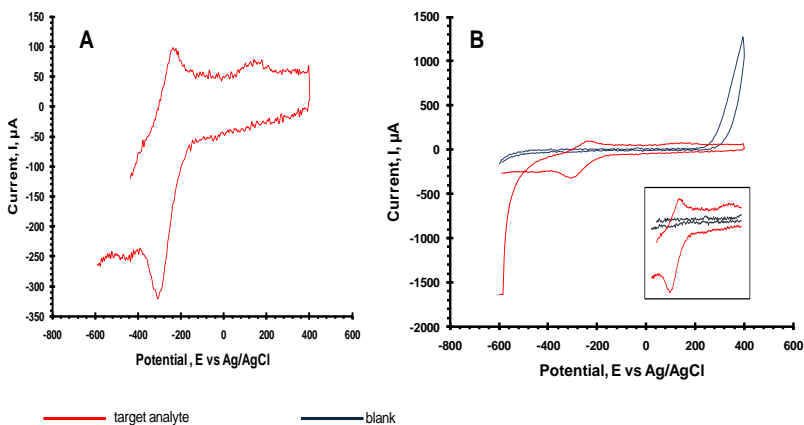


**Figure 15 A) CV curve produced by 5,4-DDI (red) on carbon electrodes at optimized potential range: -600 mV to 400 mV;  $V_{scan} = 50$  mV/s. B) CV curved produced by 5,4-BCIG (dark blue) and 5,4-DDI (red) on carbon electrodes at optimized potential range: -600 mV to 400 mV;  $V_{scan} = 50$  mV/s.  $I_{an} = 95 \mu\text{A}$  for 5,4-DDI;  $I_{an} = 10 \mu\text{A}$  for 5,4-BCIG.  $I_{cat} = -320 \mu\text{A}$  for 5,4-DDI;  $I_{cat} = -15 \mu\text{A}$  for 5,4-BCIG.**

The electrochemical activity of different concentrations of 4-MU on carbon screen printed electrodes is shown in Fig. 19A. The linear relationship ( $R^2=0.99$ ) was found between increasing concentrations of 4-MU and anodic peak currents (Fig. 19B). The electrochemical behavior of the blank solution (1mg/ml of 4-MUGLUC in PBS, pH=7.4) on carbon electrodes is shown in Fig 19C. No any redox peaks were detected in the potential ranging from 0 to 800 mV, at scan rate 50 mV/s. The electrochemical behavior of 4-NP on carbon electrode is shown in Fig. 20. 4-Np produced irreversible anodic peak at potential  $E_{an} = \sim 890$  mV. The CV peaks produced by different concentrations of 4-NP ranging from 1  $\mu\text{M}$  to 15  $\mu\text{M}$  in the selected potential range, at 50 mV scan rate are shown in Fig 21A.



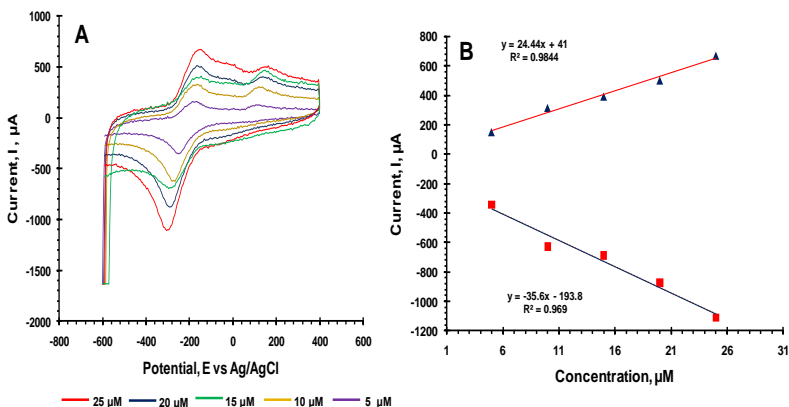


**Figure 16 A) CV curves produced by different concentrations of 5,4-DDI on carbon electrodes in optimized potential range. B) Correlation between anodic and cathodic peak currents and concentrations of 5,4-DDI.**

The linear relationship ( $R^2=0.98$ ) was found between increasing concentrations and anodic peak currents (Fig. 21B). The electrochemical behavior of blank solution (1 mg/ml 4-NPP in PBS, pH = 7.4) in the potential range varying from -400 mV to 1000 mV, at 50 mV/s scan rate is shown in Fig 21C. The blank solution did not produce any significant electrochemical signal ( $I_{an}=2 \mu\text{A}$ ).

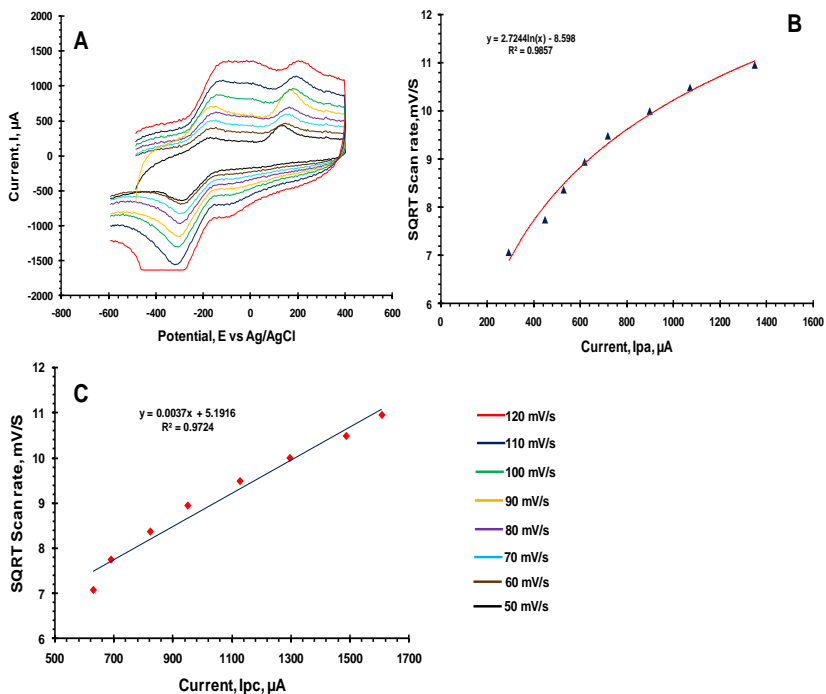


Figure 17 A) CV curves produced by 5-4-DDI at different scan rates on carbon electrodes. B) Linear-log relationship between square roots of scan rates and anodic peak currents. C) Linear relationship between square roots of scan rates and cathodic peak currents.

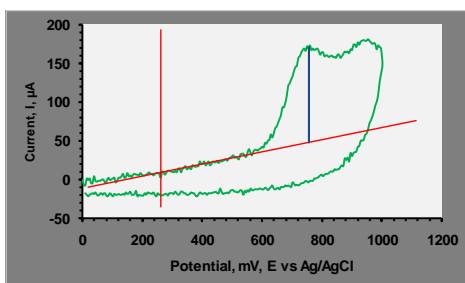
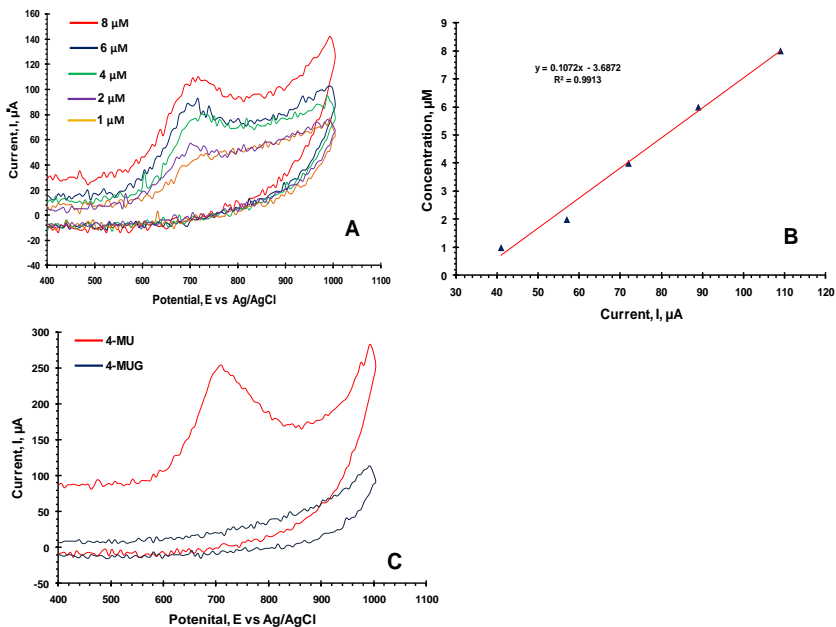
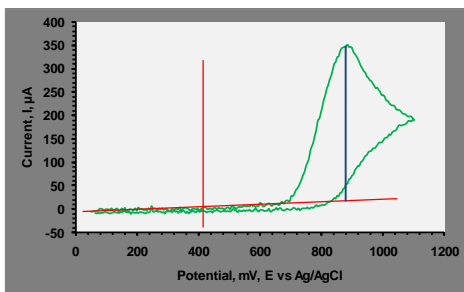


Figure 18 CV curve produced due to oxidation of 4-MU on carbon screen printed electrode



**Figure 19** A) Voltammetric signals produced by different concentrations of 4-MU on carbon electrode. The potential range is 0 mV to 1000 mV,  $V_{\text{scan}} = 50$  mV/s. B) Correlation between increasing concentration of 4-MU and anodic peak currents. C) Electrochemical behavior of 4-MU and 4-MUG on carbon electrode. Potential range is 0 mV to 1000 mV,  $V_{\text{scan}} = 50$  mV/s.  $i_{\text{an}} = 250$   $\mu\text{A}$  for 20  $\mu\text{M}$  4-MU,  $i_{\text{an}} = 15$   $\mu\text{A}$  for 1mg/mL 4-MUG.



**Figure 20** Cyclic voltammetry signal produced by 4-NP on carbon screen-printed electrode.

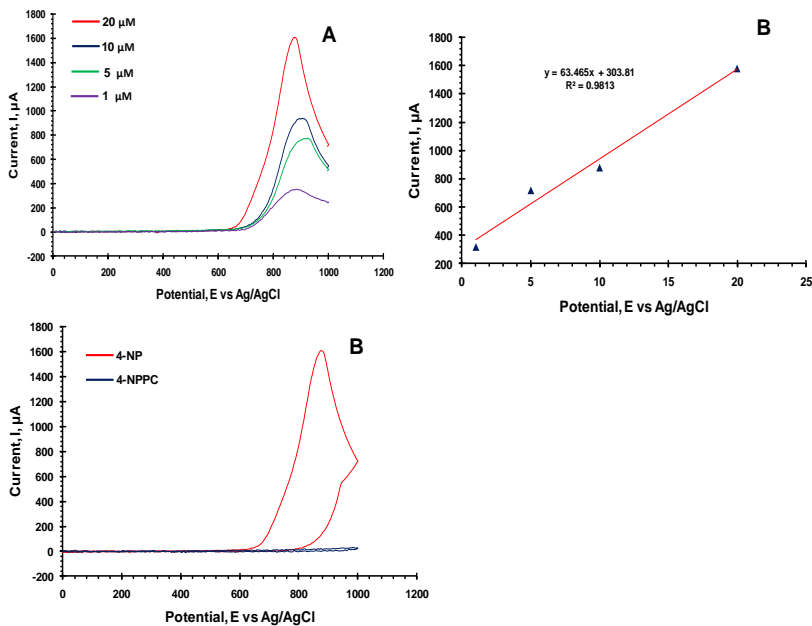


**Figure 21** A) CV curves produced by different concentrations of 4-NP on carbon screen printed electrodes. B) Correlation curve of electrochemical signals and different concentrations of 4-NP. C) Electrochemical behavior of 4-NP and 4NPP.  $i_{an} = 1600 \mu\text{A}$  for 4-NP;  $i_{an} = 2 \mu\text{A}$  for 4-NPP.

## 5.2 Detection of target analytes on graphene modified carbon electrodes

The electrochemical behavior of 5,4-DDI, 4-MU and 4-NP on GNPs modified SPEs is shown in Fig 22. On GNPs modified electrodes, all three substances produced CV peaks at the previously defined potential ranges. In case of 5,4-DDI, the positive shift from -251 mV to -174 mV and from -290 mV to -266 mV was noticed for anodic and cathodic potential peaks respectively. In

comparison with bare carbon electrode the increase of intensities of anodic and cathodic peak currents from 135  $\mu\text{A}$  to 314  $\mu\text{A}$ , 70  $\mu\text{A}$  to 294  $\mu\text{A}$  and from 296  $\mu\text{A}$  to 629  $\mu\text{A}$  was noticed for two anodic and on cathodic peak currents respectively on GNPs modified carbon electrode. On GNPs modified electrode 4-MU produced irreversible anodic peak at  $\sim 712$  mV potential instead of  $\sim 665$  mV on bare carbon electrode.

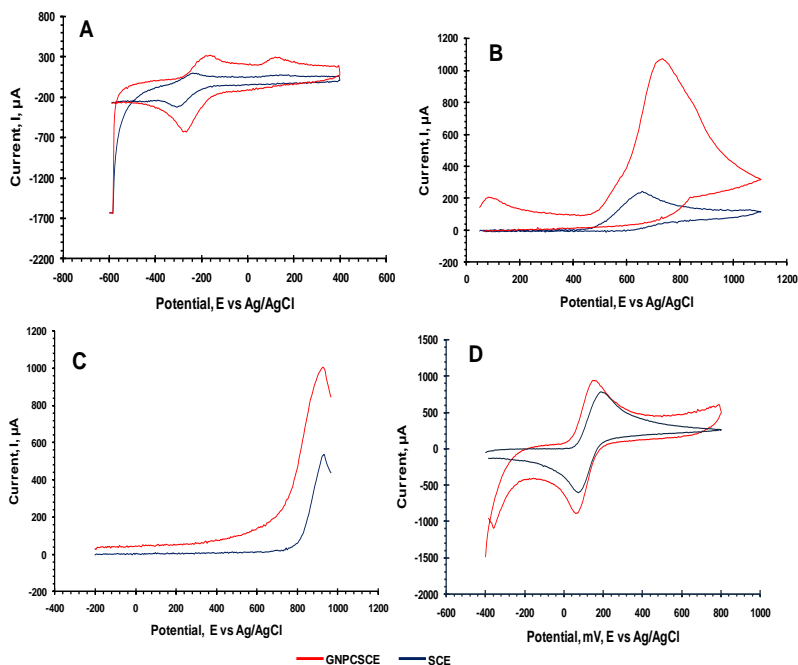


**Figure 22** CV curves produced by A) 5,4-DDI; B) 4-MU; C) 4-NP and D) 4-AP on graphene modified (red) and unmodified (dark blue) carbon electrodes.

The anodic peak current on GNPs modified electrode increased from 235  $\mu\text{A}$  to 1070  $\mu\text{A}$  (Fig. 22 B). The significant increase of anodic potential current from 330  $\mu\text{A}$  to 1330  $\mu\text{A}$  also was noticed in case of

4-NP, however the negative shift (from 870 mV to 800 mV) of anodic potential occurred (Fig. 22 C). The electrochemical behavior of 4-AP on both electrodes is shown in Fig. 22D. On the bare carbon electrode the 4-AP produced quasi-reversible ( $I_{pc}/I_{pan}=0.76$ ;  $\Delta E_p=100$ ) duck shaped CV curve in the potential range varying from -400 mV to 800 mV. The improvement of reversibility parameters ( $I_{pc}/I_{pan}=0.95$ ;  $\Delta E_p=70$ ) of CV curve produced by 4-AP on GNPs carbon electrode was noticed. The increase of current intensities from 780  $\mu$ A to 930  $\mu$ A and from 600  $\mu$ A to 880  $\mu$ A was noticed for anodic and cathodic peak currents respectively.

## 5.3 Development of Gel-electrode system

### 5.3.1 Gel characteristics

The attachment efficiency of mixed suspension of *E. coli* DSM 498, *E. coli* DSM 301, *Hafnia alvei* DSM 30163<sup>T</sup>, *Klebsiella pneumonia* DSM 30104 to each agar-gels are presented in Fig 23. The Gel-2 (see 4.5) showed the highest attachment efficiency (96%) among all tested compositions. The attachment efficiency of *St. aureus* to different gel compositions is shown in Fig. 24. There was no significant difference ( $P=0.07$ ) between attachment efficiencies of different concentrations of Coliforms and *St. aureus* DSM 799 cells to the Gel -2.

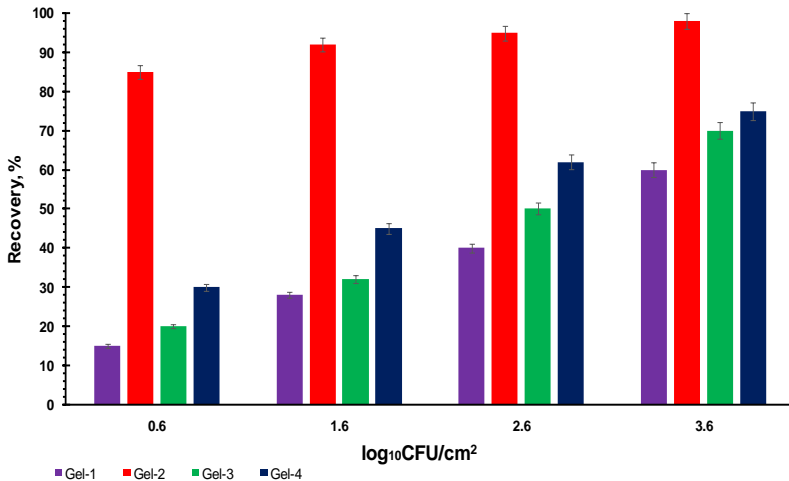


**Figure 23 Percentage of recovery of mixed Coliforms culture (*.coli* DSM 498, *E.coli* DSM 301, *Hafnia alvei* DSM 30163<sup>T</sup>, *Klebsiella pneumonia* DSM 30104) from stainless steel surfaces. The mean values of attachment efficiencies of four types of gels are presented. Gel compositions: Gel-1 (5 g/L peptone + 2 g/L KH<sub>2</sub>PO<sub>4</sub> + 2 g/L K<sub>2</sub>HPO<sub>4</sub> + 5 g/L NaCl + 10 g/L agar ); Gel-2 (5 g/L peptone + 2 g/L KH<sub>2</sub>PO<sub>4</sub> + 2 g/L K<sub>2</sub>HPO<sub>4</sub> + 5 g/L NaCl + 10 g/L agar + 1 g/L polyacrylamide); Gel-3 (5 g/L peptone + 2 g/L KH<sub>2</sub>PO<sub>4</sub> + 2 g/L K<sub>2</sub>HPO<sub>4</sub> + 5 g/L NaCl + 10 g/L agar + 3 g/L meat extract); Gel-4 (5 g/L peptone + 2 g/L KH<sub>2</sub>PO<sub>4</sub> + 2 g/L K<sub>2</sub>HPO<sub>4</sub> + 5 g/L NaCl + 10 g/L Agar + 1 g/L polyacrylamide + 2 g/L meat extract). The Gel-2 and Gel-4 contain polyacrylamide. Gel-1 and Gel-3 contain agar-agar. Gel-2 showed >80% efficiency for all concentrations of Coliforms in comparison with Gel-1 (max= 60%).**

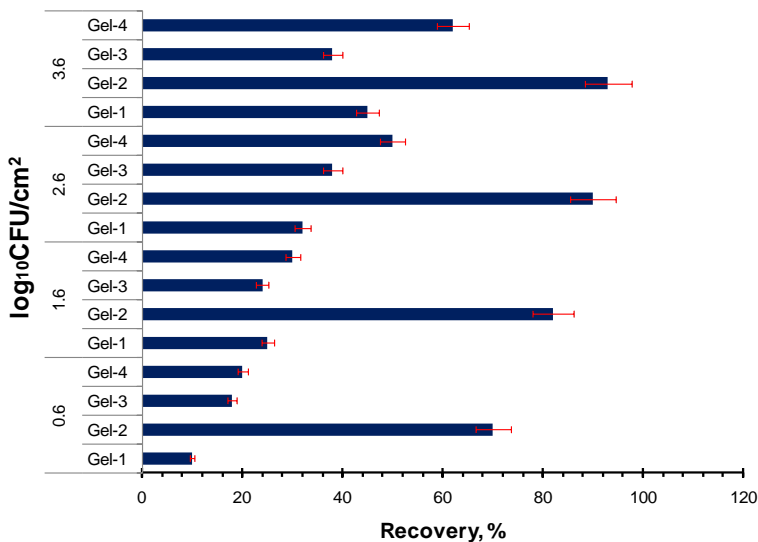


**Figure 24 Percentage of recovery of *St. aureus* DSM 799 from stainless steel surfaces.**

The influence of pH on  $\beta$ -D-Galactosidase and Phospholipase C activity in the gel is shown in Fig. 25 and 26. In case of  $\beta$ -D-Galactosidase PAA-gel system possessed highest optical signal at pH 7.4. The absorbance curve reached its maxima at this pH.  $\beta$ -D-Galactosidase was less active at pH 6.0 than at pH 7.0. The specific Phospholipase C produced maximal optical signal at pH=7.4 during 60 minutes of reaction time.



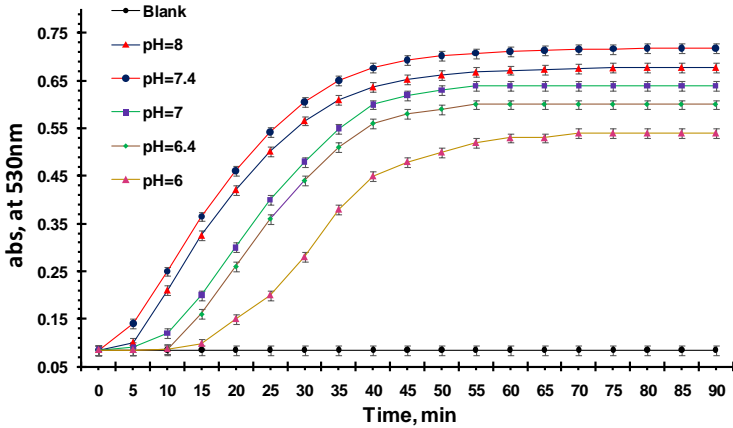


Figure 25 Influence of pH on production of  $\beta$ -D-Galactosidase in the gel. The mean absorbance values are presented. Spectrophotometrical measurements were carried out every 5min. Blank represents the gel without addition of  $\beta$ -D-Galactosidase. At pH=7.4 color formation occurred during 10 minutes and the absorbance value reached the detection threshold (0.25). Absorbance was measured at 530 nm wavelength.

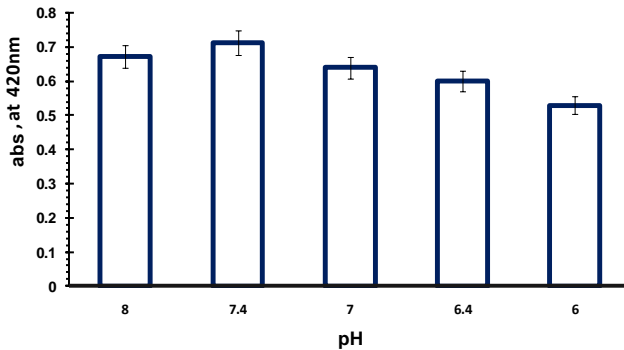
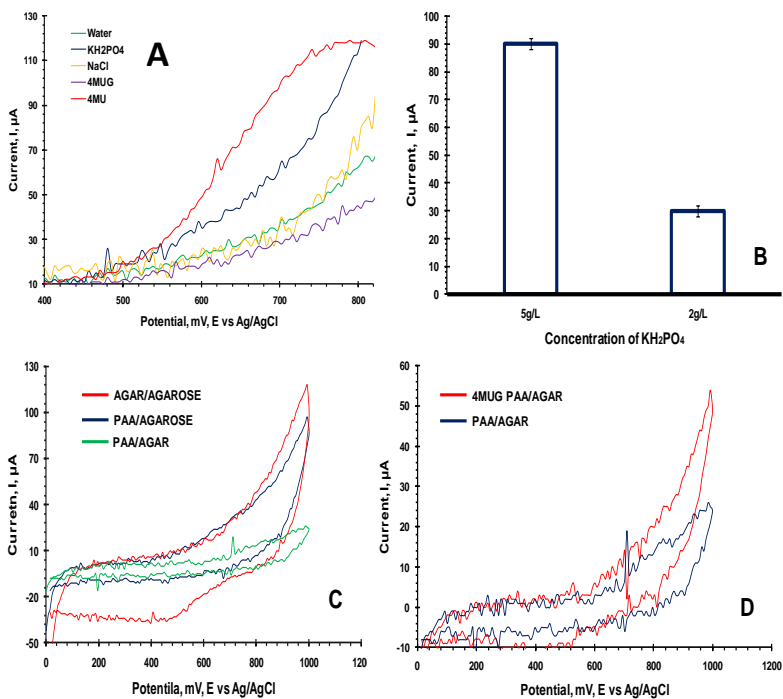


Figure 26 Influence of pH on production of Phospholipase C in the gel. Absorbance was measured at 420 nm wavelength specific for 4-NP.

### 5.3.2 Electrochemical characteristics of gel–electrode system

The electrochemical activity of the gel components is shown in Fig. 27A. At the optimized potential range varying from 0 to 800 mV, only 4-MU produced the inherent CV peak at ~750 mV. Other components including 4-MUG substrate did not produce any peak, however the intensity of current produced by  $\text{KH}_2\text{PO}_4$  reached the ~90  $\mu\text{A}$  at 750 mV potential. The current intensity of Gel-2 with optimized concentration of  $\text{KH}_2\text{PO}_4$  and  $\text{K}_2\text{HPO}_4$  decreased up to 30  $\mu\text{A}$  comparing to the gel before optimization (Fig. 27B). The redox behavior of three combinations of gels (without substrate) is shown in Fig. 27C. All three combinations of gels did not produce any redox peak that could interfere with signal produced by 4-MU, however the lowest intensity current was produced by combination of 1 g/L polyacrylamide and 10 g/L agar-agar in comparison with other two compositions (the same concentrations were tested). The redox behavior of the gel with and without substrate is shown in Fig. 27 D. Negligible change of anodic current intensity from 10  $\mu\text{A}$  to 17  $\mu\text{A}$  was noticed when the 4-mug was injected to the gel-electrode system. The comparison of CV curves produced by the Gel-2 (including all components) with the Gel-2 containing the target analyte is shown in Fig. 28 A. The Gel-2 with target analyte produced anodic signal at the already defined potential ~750 mV inherent for the oxidation of 4-MU. The gel containing only substrate did not show any electrochemical activity at the mentioned potential. The redox behavior of the agar/ polyacrylamide gel, in the potential

range inherent for 5,4-DDI, without any component and substrate is shown in Fig. 28B.



**Figure 27** A) The voltammetric signals produced by different components of the gel. B) The current intensities produced by different concentrations of K<sub>2</sub>HP0<sub>4</sub>. C) The electrochemical behavior of 3 combinations of gels. D) Influence of 4-MUG on electrochemical stability of PAA/AGAR gel.

In the potential range varying from -600 to 400 mV the agar-polyacrylamide gel did not produce any redox peak as well as the current intensity was at very low level ( $\sim 40 \mu\text{A}$  for the anodic current). The electrochemical behavior of the Gel-2 containing all components and 5,4-BCIG substrate is shown in Fig. 28B (dashed lines).

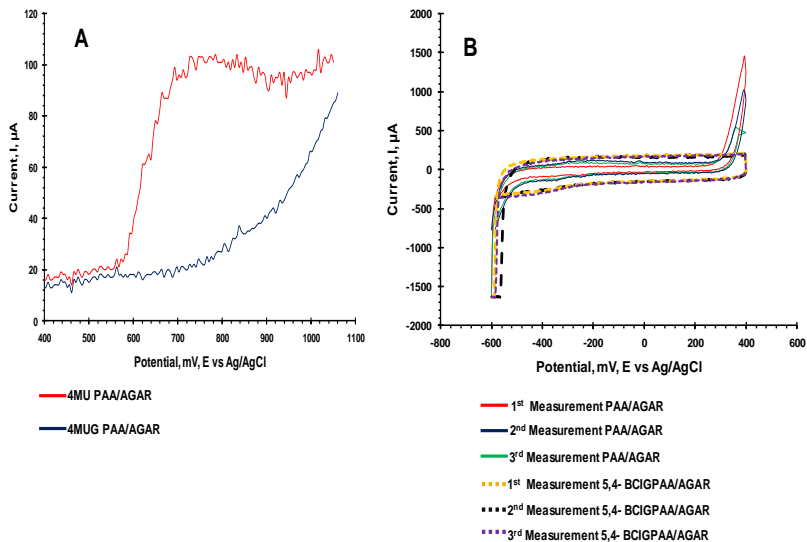


**Figure 28 Electrochemical signals produced by gels containing target analyte and substrate. B) Electrochemical behavior of the gels (with 5,4-BCIG dashed lines; only gel normal lines) at the potential range varied from -600 mV to 400 mV. All measurements were done in triplicate.**

Although, the increase of the current intestines from  $\sim 40 \mu\text{A}$  to  $150 \mu\text{A}$  occurred, the Gel-2 did not possess any redox activity in the defined potential range and did not produce any redox peaks at the potentials inherent for 5,4-DDI. The electrochemical behavior of redox probe  $\text{Fe}(\text{CN})_6^{3-/4-}$  on GR/PAAGC electrode is shown in Fig. 29 A.

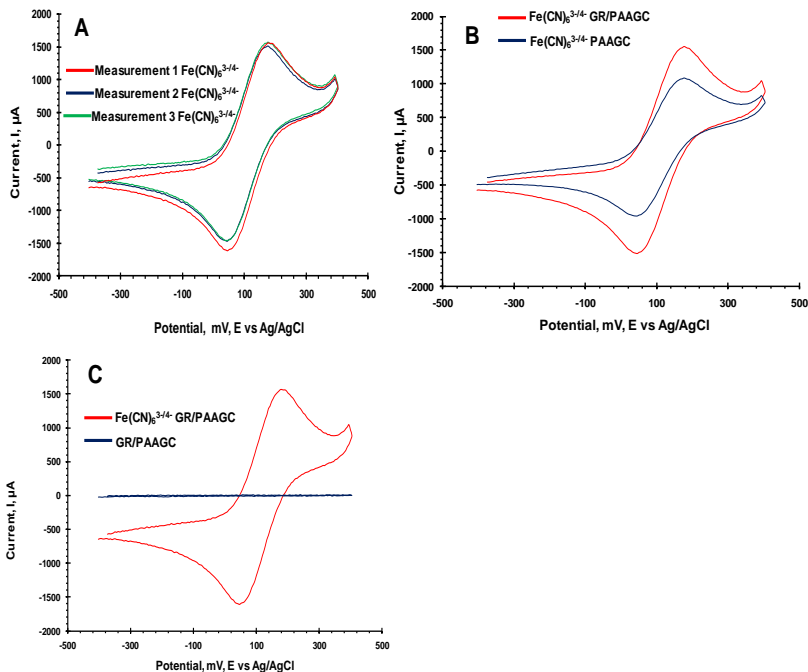


**Figure 29** Electrochemical properties of GR/PAAGC and PAAGC systems. A) CV signals produced by  $\text{Fe}(\text{CN})_6^{3-/4-}$  on GR/PAAGC electrode system. Red, dark blue and green curves represents three independent CV measurements. The anodic and cathodic current peaks for three measurements are  $I_{pa/m1} = 1556 \mu\text{A}$ ,  $I_{pa/m2} = 1548 \mu\text{A}$ ,  $I_{pa/m3} = 1503 \mu\text{A}$ ;  $I_{pc/m1} = -1587 \mu\text{A}$ ,  $I_{pc/m2} = -1450 \mu\text{A}$ ,  $I_{pc/m3} = -1473 \mu\text{A}$ . B) CV signals produced by  $\text{Fe}(\text{CN})_6^{3-/4-}$  on GR/PAAGC (red) and PAAGC (dark blue) electrode systems. The mean values of current peaks for GR/PAAGC and PAAGC were  $I_{pa/GPGC} / I_{pc/GPGC} = 1550/1514 \mu\text{A}$  and  $I_{pa/PAAGC} / I_{pc/PAAGC} = 1081/960 \mu\text{A}$  respectively ( $P < 0.05$ ). C) CV signals produced by GR/PAAGC system in presence (red) and absence (dark blue) of  $\text{Fe}(\text{CN})_6^{3-/4-}$ . Measurements were done at 50 mV/s scan rate and -400 mV to 400 mV potential range.

The three measurements showed very low deviation as well as very low noise disturbances. The comparative cyclic voltammograms of GR/PAAGC and PAAGC injected with  $K_3Fe(CN)_6$  solution are shown in Figure 29B. As shown in Fig 28C, GR/PAAGC gel did not possess any significant redox peaks. A cyclic voltammogram of 6-DI recorded from  $-600$  mV to  $+400$  mV potential range, at  $50$  mV/s scan rate is shown in Fig. 30A. Anodic peak ( $1420 \mu A$ ) at  $-200$  mV with cathodic peak ( $-1450 \mu A$ ) at  $-300$  mV have been detected. Also the second anodic peak ( $I_{an}=1340 \mu A$ ) at the  $E_{an} = 120$  mV was detected. Fig. 30 B shows the voltammograms of 6-DI with scan rates ( $v$ ) varying from  $50$  mV to  $200$  mV. Good linearity ( $R^2=0.98$  for anodic and  $R^2=0.99$  for cathodic) between increase of anodic and cathodic peak currents and applied scan rates were observed (Fig. 30 C). The electrochemical behavior of 4-MU on GR/PAAGC electrode is shown in Fig. 31A. On GR/PAAGC electrode 4-MU produced irreversible anodic peak  $\sim 700$  mV, which corresponds to the oxidation peak of 4-MU on carbon and GNPs modified carbon electrodes. The intensity of anodic currents produced by  $0.1$  mM of 4-MU was equal to  $200 \mu A$  and  $680 \mu A$  for unmodified and modified electrodes respectively. The CV peaks produced by 4-MU at scan rates varying from  $50$  mV/s to  $100$  mV/s are shown in Fig. 31B A linear relationship ( $R^2=0.99$ ) between increasing scan rates as well as their square roots and anodic currents was found (Fig. 31C, D). Oxidation peak potential was dependent on the scan rate. The  $E_{pa}$  shifted positively with the increase of scan rate. A linear relationship between  $E_{pa}$  and  $I_{an}$  was obtained. The redox peak produced by  $1$  mM 4-NP in PBS ( $pH=7.4$ ) solution is shown in Fig. 32 A. The  $1$  mM 4-Np produced irreversible anodic peak at the defined potential  $\sim 880$  mV. The intensity of peak

current produced by 4-NP on GR/PAAGC increased up to 650  $\mu\text{A}$  in comparison to bare carbon electrode  $\sim 350 \mu\text{A}$ .

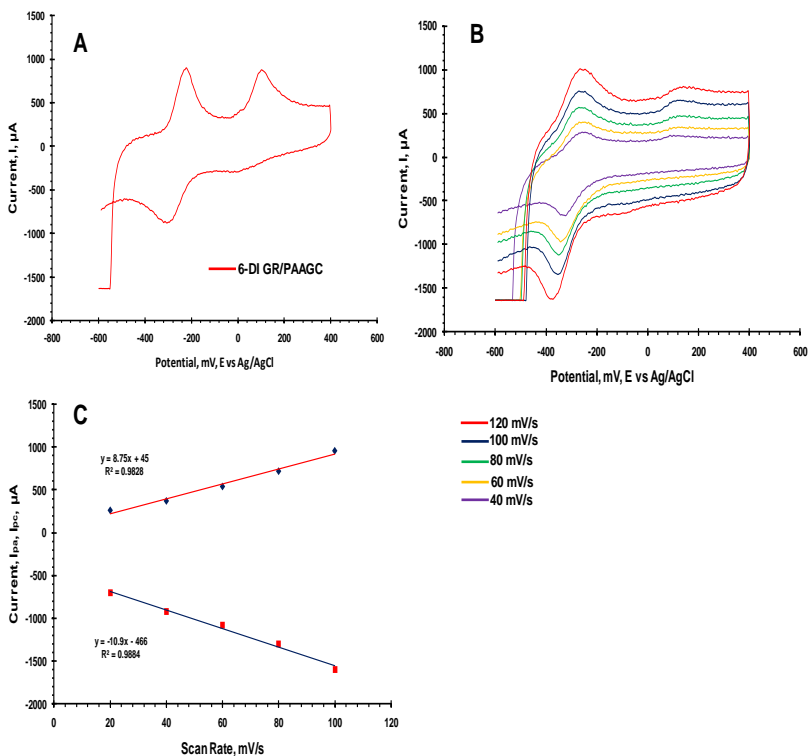


**Figure 30** A) Voltammetric curve produced by 6-DI on GR/PAAGC electrode. B) Peak currents produced by 6-DI at different scan rates. C) Correlation between scan rates and anodic and cathodic peak currents.

The electrochemical behavior of 4-NP on GR/PAAGC system at different scan rates was studied. The CV peaks produced by 4-NP at scan rates varying from 10 mV/s to 100 mV/s are shown in Fig. 32B.

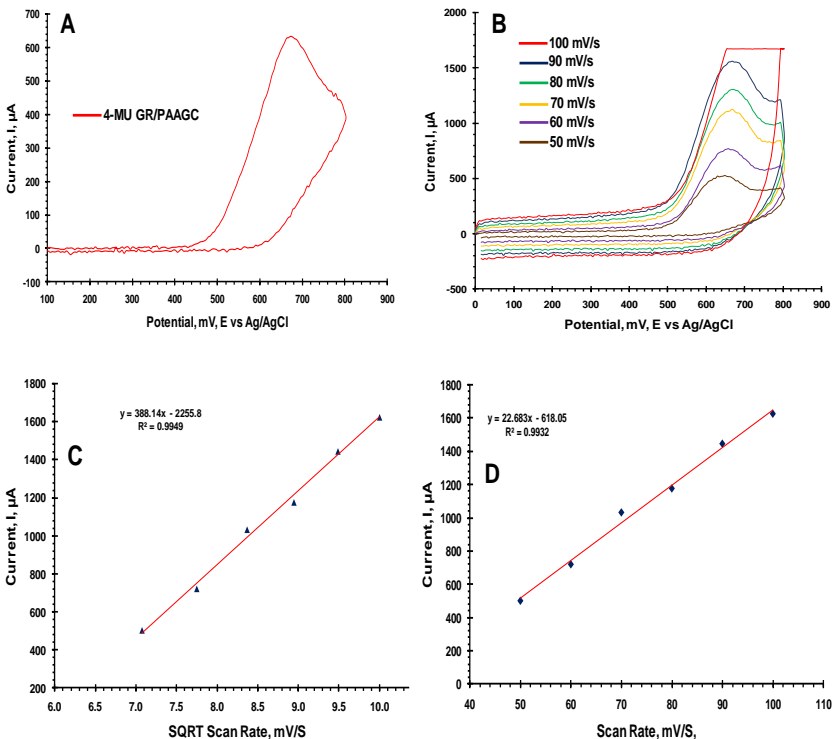


**Figure 31** A) Voltammetric curve produced by 4-MU on GR/PAAGC electrode. B) Peak currents produced by 4-MU at different scan rates. C) Correlation between scan rates and anodic and cathodic peak currents. D) Correlation between square roots of the scan rates and anodic and cathodic peak currents.

Linear relationships ( $R^2=0.99$  for scan rate and  $R^2=0.98$  for SQRT of scan rate) between increasing scan rates as well as their square roots and anodic currents were found (Fig. 32C, D). Oxidation peak potential was dependent on the scan rate. The slight positive shift of  $E_{pa}$  with the increase of scan rate was occurred.



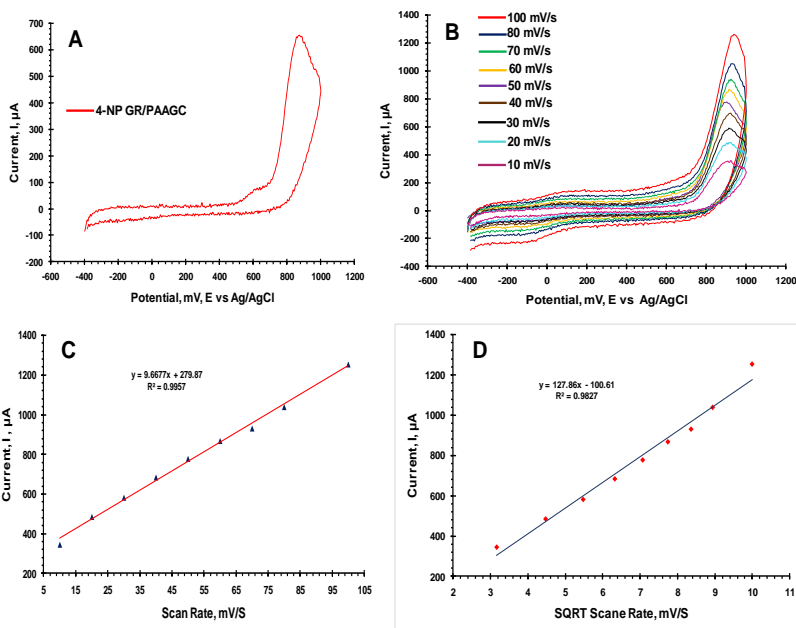


**Figure 32** A) Voltammetric curve produced by 4-NP on GR/PAAGC electrode. B) Peak currents produced by 4-NP at different scan rates. C) Correlation between scan rates and anodic and cathodic peak currents. D) Correlation between square roots of the scan rates and anodic and cathodic peak currents.

## 5.4 Detection of bacteria using developed GR/PAAGC electrode system in culture

The electrochemical behavior of  $\beta$ -Galactosidase /6-CIGP reaction mixture at scan rate 50 mV/s is shown in Fig. 33A. Irreversible anodic peak  $I_{an}=80 \mu\text{A}$  was detected at the 50 mV potential after 2 minutes reaction time. After 5 and 15 minutes the reduction of current down to 10  $\mu\text{A}$  occurred (Fig. 33B). Thereafter, the red color typical for the  $\beta$ -Galactosidase /6-CIGP reaction was

noticed in the gel. Good correlation ( $R^2=0.97$ ) between the decrease of the redox peak and parallel increase of absorbance values was observed (Fig. 33C, D). The CV acquired in the gel systems containing only  $\beta$ -D-Galactosidase and 6-CIPG did not exhibit any redox peak in at the defined potential range. Gel-electrode systems containing only 6-CIPG and  $\beta$ -D-Galactosidase did not produce any redox peak in the selected potential range (Fig. 34). The fast depletion of 6-chloro-3-indoxyl (due to its oxidation) in the gel caused the decrease of specific redox peak. In parallel increase of absorbance values and intensity of the specific color was occurred due to formation of 6-DI. A cyclic voltammogram of enzyme substrate mixture in the gel system recorded from  $-600$  mV to  $+400$  mV potential range, at  $50$  mV/s scan rate is shown in Fig. 35. In the tested potential range, two processes have been detected. The first one is quasi-reversible with anodic peak of  $1420$   $\mu$ A occurring at  $-200$  mV with correspondence cathodic peak of  $-1440$   $\mu$ A at  $-300$  mV. The second process occurred at  $+120$  mV (vs Ag/AgCl) potential and had an irreversible nature ( $I_{an}=1340$   $\mu$ A). The difference of cathodic and anodic potentials ( $\Delta E_p$ ) was equal to  $\approx 80$  mV. The ratio of cathodic and anodic peak currents ( $I_p^{red}/I_p^{ox}$ ) value was equal to 1. The comparison of CV curves produced by oxidation of pure 6-DI and 6-DI produced due to  $\beta$ -D-Galactosidase/ 6-CIGP reaction is shown in Fig. 35. The slight shift of two anodic (to the positive) and one cathodic (to negative) potentials was occurred in the CV curve produced by enzyme/substrate reaction in comparison with pure 6-DI.  $\beta$ -D-Galactosidase as well as 6-CIGP in the GR/PAA-gel system did not produce any redox peak in the selected potential range (Fig. 36 A). The CV curves produced due to reaction of different

concentrations of  $\beta$ -D-Galactosidase with 6-CIPG are shown in Fig. 36B. All studied concentrations exhibited similar electrochemical behavior with redox peaks corresponding to the 6-DI. The good linear relationship ( $R^2=0.98$  for anodic and  $R^2=0.99$  for cathodic) was found between increasing concentrations of  $\beta$ -D-Galactosidase and increasing anodic and cathodic peaks (Fig. 36C). Fig shows the dependence of the electrochemical signal produced by 6-DI on the incubation period of sensor with  $\beta$ -Galactosidase.

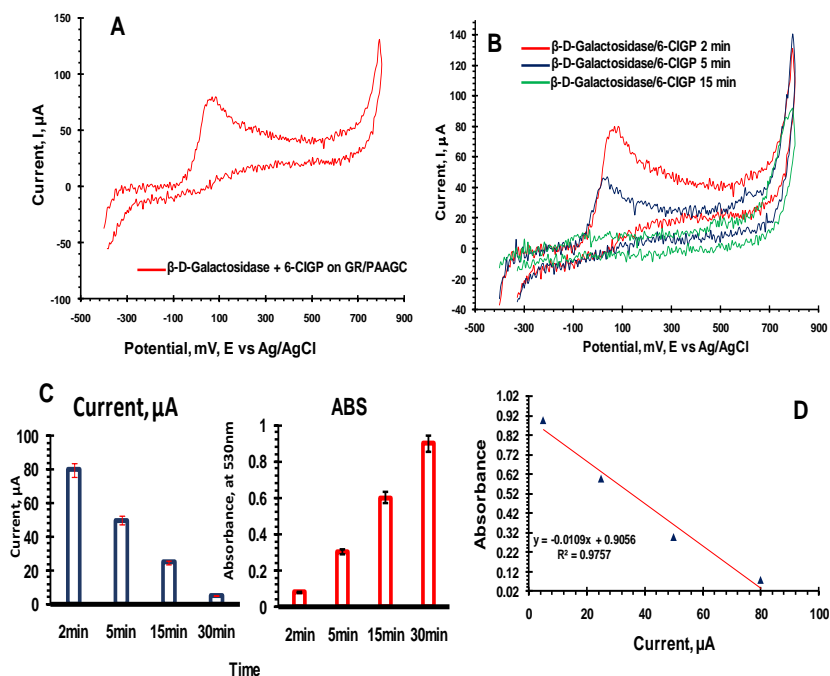


**Figure 33** A) Voltammetric signal produced due to  $\beta$ -D-Galactosidase/6-CIPG reaction. B) Voltammetric signals produced in 2, 5 and 30 minutes after  $\beta$ -D-Galactosidase/6-CIPG reaction C) Change of voltammetric signal intensity (blue columns) and optical signal intensity (absorbance at 530 nm) (red columns) during 30 minutes of  $\beta$ -

**D-Galactosidase/6-CIPG reaction. D) Correlation between electrochemical and optical signals.**

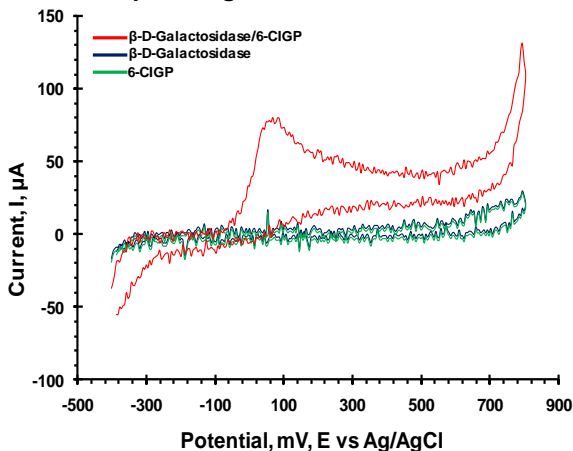


**Figure 34** Voltammetric curves generated by GR/PAAGC system containing  $\beta\text{-D-Galactosidase}$  and 6-CIPG (red); only  $\beta\text{-D-Galactosidase}$  (dark blue) and only 6-CIPG (green).

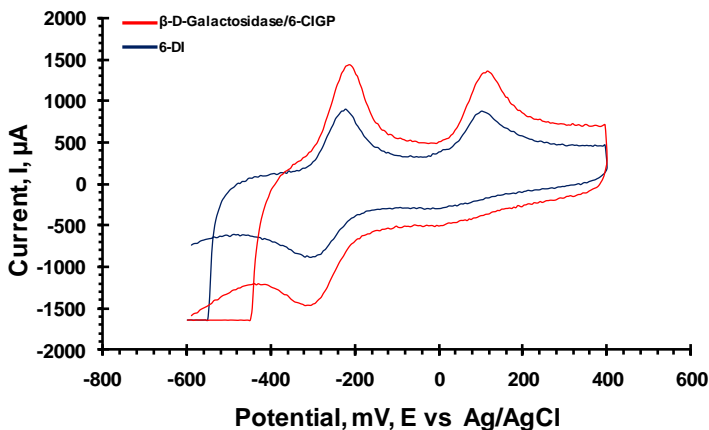


**Figure 35** Voltammetric signals produced by  $\beta\text{-D-Galactosidase}$  and 6-CIPG reaction (red); and 6-DI (dark blue).

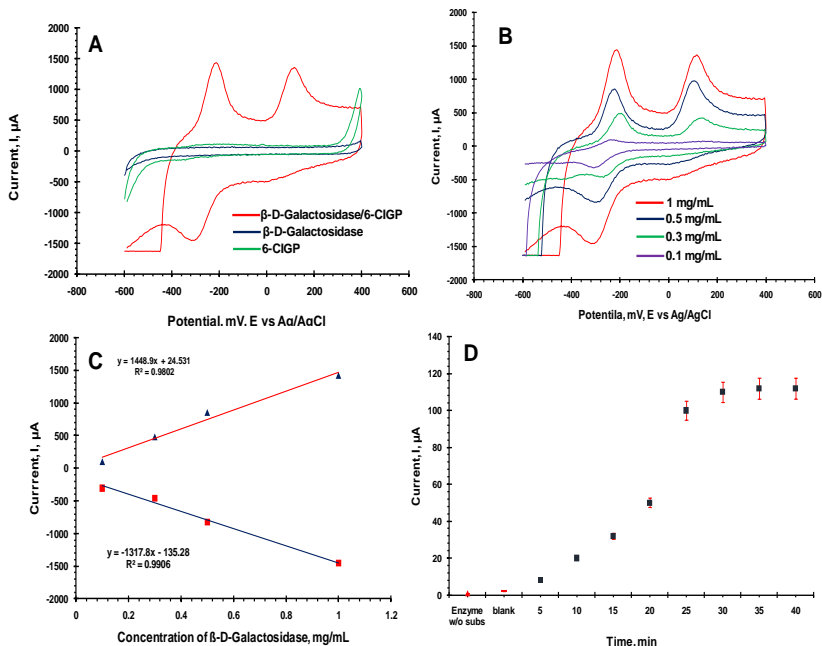


**Figure 36** A) Voltammetric signals produced by GR/PAAGC system containing  $\beta$ -D-Galactosidase and 6-CIPG,  $\beta$ -D-Galactosidase and 6-CIPG. B) Voltammetric signals produced due to reaction of different concentrations  $\beta$ -D-Galactosidase with 0.5 mg/mL 6-CIPG. C) Correlation between current intensities and concentrations of  $\beta$ -D-Galactosidase. D) Anodic current peaks produced at different reaction times of  $\beta$ -D-Galactosidase with 6-CIPG.

The increase of the anodic peak currents was noticed with the increasing reaction time. At the 35<sup>th</sup> minute of the reaction, the total conversion of substrate into the product occurred and the anodic peak reached 112  $\mu\text{A}$  (Fig. 36D). High expression of  $\beta$ -Gal by Coliform bacteria occurred after incubation with 0.2 mg/mL of IPTG and 0.005 mg/mL of ODTG (see 5.7).

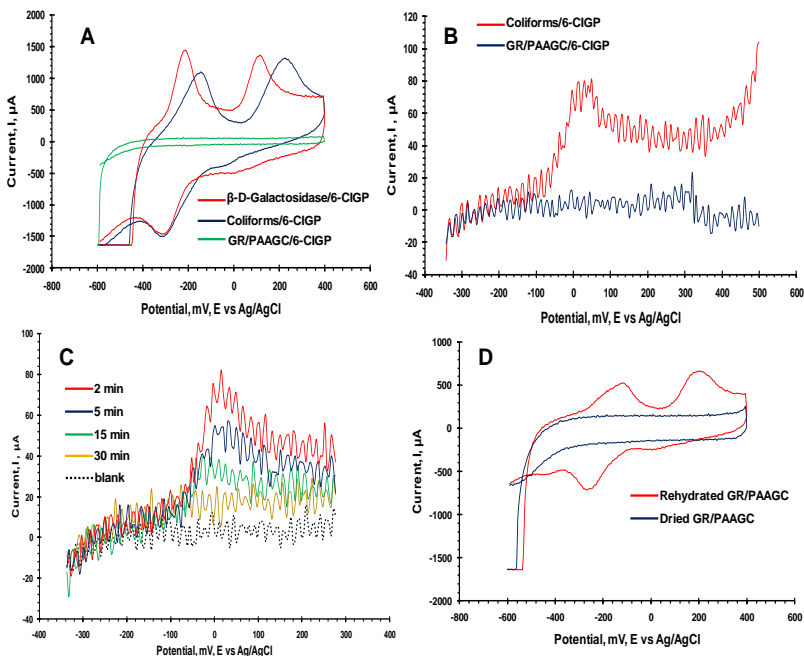


**Figure 37** A) Electrochemical signals produced by  $\beta$ -D-Galactosidase and Coliform mix culture (*E.coli* DSM 498, *E.coli* DSM 301, *Hafnia alvei* DSM 30163<sup>T</sup>, *Klebsiella pneumonia* DSM 30104). The potential range = - 600 mV to 400 mV, Scan rate = 50 mV/s; the electrochemical behavior of the blank is represented with the green line. B) Electrochemical signal produced by Coliform mix culture at the potential range varied from - 400 mV to 800 mV. C) Current peaks produced at different incubation times of Coliform mix culture with the GR/PAAGC sensor. D) Voltammograms of the dried GR/PAAGC sensor and its rehydrated stage.

A cyclic voltammograms, recorded from -600 mV to + 400 mV potential range, at 50 mV/s scan rate, generated due to reaction of 6.6 log<sub>10</sub>CFU/ml Coliforms (*E. coli* DSM 498, *E. coli* DSM 301, *Hafnia alvei* DSM 30163<sup>T</sup>, *Klebsiella pneumonia* DSM 30104) with 0.5

mg/ml 6-CIGP in the gel system is shown in Fig 37A. In the GR/PAAGC system Coliforms produced the redox peaks similar to peaks produced by the enzyme and target analyte. However, in case of Coliforms the positive shift of two anodic potentials was noticed. The GR/PAA-gel system containing the 6-CIGP substrate did not show any electrochemical activity at the selected potential range. The electrochemical behavior of Coliforms at potential range varied from -400 mV to 800 mV is presented in Fig. 37B. The anodic peak inherent for the 6-chloro-3-Indoxyl was detected during 2 min incubation of the sensor at 37 °C. The anodic peak occurred at the ~49 mV anodic potential confirming the results obtained from enzyme/substrate reaction. However, already after 5 minutes of incubation the decrease of the electrochemical signal occurred, which could be explained by depletion of the 6-chloro-3-Indoxyl. During 15 minutes of incubation the anodic peak current decreased from 80  $\mu$ A to ~20  $\mu$ A (Fig. 37C). The electrochemical behavior of dried and rehydrated gel-electrode systems is shown in Fig. 37D. The electrochemical behavior of the blank (GR/PAAGC sensor containing 6-CIGP substrate) is shown in Fig. 38. No redox peaks were detected at the potential range varying from -600 mV to 400 mV. Also no redox peaks were detected at the mentioned potential when the gel-electrode system was incubated at 42 °C for 3 h (Fig 38A). Five independent measurements of the blank confirmed the redox inactivity and stability of GR/PAAGC sensor without sample (Fig. 38B).

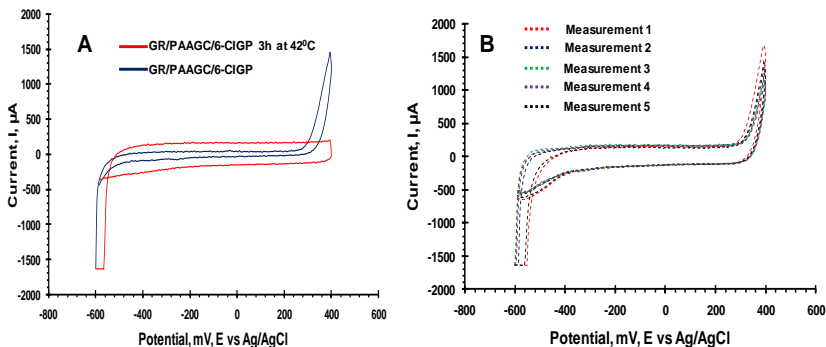


**Figure 38 A) Electrochemical behavior of the blank GR/PAAGC system containing 6-CIPG. B) Five independent CV measurements of the blank GR/PAAGC system.**

The formation of the redox peaks produced by Coliforms (*E. coli* DSM 498, *E. coli* DSM 301, *Hafnia alvei* DSM 30163<sup>T</sup>, *Klebsiella pneumonia* DSM 30104) on GR/PAAGC sensor during 60 minutes is shown in Fig. 39. At the 0 minute no electrochemical activity was observed. After 15 minutes the formation of cathodic peak current equal to  $\sim 700 \mu\text{A}$  at the potential  $E_{\text{cat}} = -435 \text{ mV}$  was noticed, which increased up to  $\sim 860 \mu\text{A}$  at the 30 minutes of incubation. No potential shift was detected. However, at 45 minutes of incubation the positive potential shift to  $-387 \text{ mV}$  occurred and the peak current increased up to  $1500 \mu\text{A}$ . At this time the formation of the anodic peak was observed at the potential  $E_{\text{an}} = -305 \text{ mV}$ , and the peak current was equal to  $370 \mu\text{A}$ . The positive potential shift to  $-140 \text{ mV}$  and  $-305 \text{ mV}$  occurred for the anodic and cathodic peaks respectively at the 60 minutes of incubation. No increase of cathodic current occurred in comparing to anodic current, which raised up to  $1084 \mu\text{A}$ .



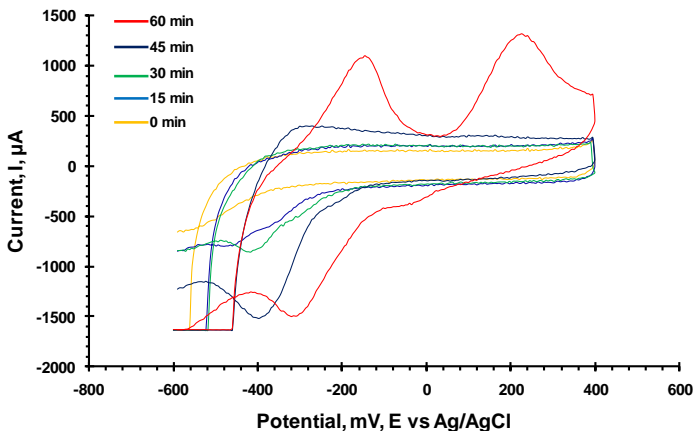


**Figure 39 The formation stages of CV curve inherent for produced by Coliforms on GR/PAAGC sensor.**

The voltammograms produced by different concentrations of Coliforms mix culture (*E. coli* DSM 498, *E. coli* DSM 301, *Hafnia alvei* DSM 30163<sup>T</sup>, *Klebsiella pneumonia* DSM 30104) suspensions are shown in Fig. 40A. The increase of anodic and cathodic current intensities in correlation with the increasing concentration of Coliform bacteria was demonstrated. Good linear relationship ( $R^2=0.99$  for anodic and  $R^2=0.99$  for cathodic currents) between increasing concentrations and anodic as well as cathodic peaks was obtained in the range from 2.1  $\log_{10}$ CFU/mL to 7.1  $\log_{10}$ CFU/mL (absolute number: 6 CFU to  $6 \times 10^5$  CFU) (Fig.40B).

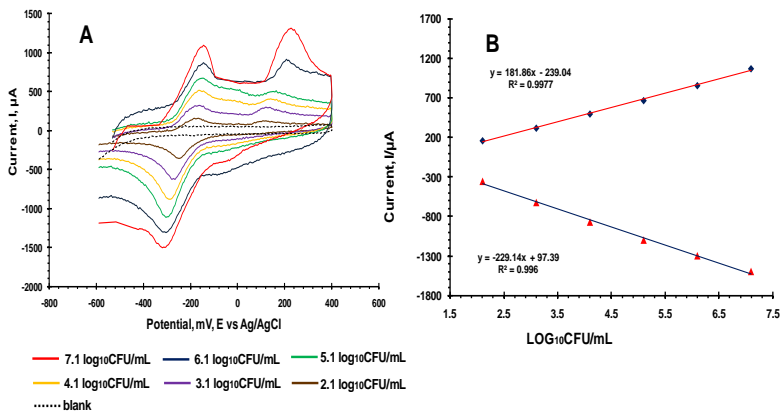


**Figure 40** A) Voltammetric signals produced by different concentrations of mixed Coliform culture. B) Correlation between anodic and cathodic current intensities and concentrations of Coliforms.

The CV peaks produced by the reaction of Coliforms (*E. coli* DSM 498, *E. coli* DSM 301, *Hafnia alvei* DSM 30163<sup>T</sup>, *Klebsiella pneumonia* DSM 30104) with the 0.5mg/mL and 5mg/ml concentration of substrate during 20 minutes of incubation is presented in Fig. 41. The cathodic peak current increased from 850  $\mu\text{A}$  to 1100  $\mu\text{A}$  by increasing the concentration of the substrate from 0.5 to 5 mg/mL respectively. The increase of anodic peak from 100  $\mu\text{A}$  to 270  $\mu\text{A}$  occurred.

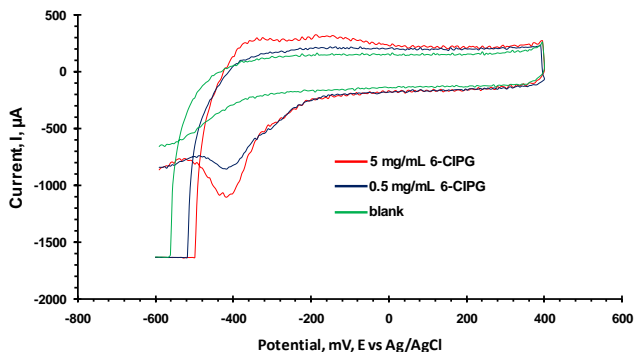


**Figure 41 Comparison of anodic and cathodic peak intensities of CV curve produced due to reaction of Coliforms with different concentrations of 6-CIPG.**

The influence of pH change of gel-electrode system on peak intensities and on potentials is shown in Table 2. After sixty minutes of incubation of the sensor with injected  $6\log_{10}\text{CFU/mL}$  of Coliform suspension (*E. coli* DSM 498, *E. coli* DSM 301, *Hafnia alvei* DSM 30163<sup>T</sup>, *Klebsiella pneumonia* DSM 30104), the change of pH from 7.4 to 5.5 was detected and the redox current values decreased from  $-90\ \mu\text{A}$  to  $-924\ \mu\text{A}$  and increased from  $53\ \mu\text{A}$  to  $530\ \mu\text{A}$  for the cathodic and anodic peaks respectively. The positive shift from  $-421\ \text{mV}$  to  $-245\ \text{mV}$  and  $-360\ \text{mV}$  to  $-120\ \text{mV}$  was noticed for the cathodic and anodic potentials respectively. The influence of the metabolic activity of total Coliforms on the electrochemical signal is shown in Fig 42A. During 1 h of incubation, no any redox peaks were produced by the gel-electrode system in the absence of specific substrate. The influence of the microbiota, found typically in food processing, on the voltammetric signals is shown in Fig. 42B. The strains, which lack any  $\beta$ -Galactosidase activity (*B. pumilus* DSM

029<sup>T</sup>, *Ps. fluorescence* DSM 50090 <sup>T</sup>), did not produce any redox peak. The effect of ferrocene redox couple (Fc/Fc<sup>+</sup>) on redox peak current intensities and oxidation rate is shown in Fig. 42C.

**Table 3 The influence of change of pH on electrochemical parameters of CV curve produced by coliform bacteria on GR/PAAGC sensor.**

Incubation time/min	pH	Mean ± SD*			
		Anodic potential (Ea/ mV)	Cathodic potential (Ec/ mV)	Anodic peak current (Ipa/μA)	Cathodic peak current (Ipc/μA)
10	7.4	-382 ± 2	-421 ± 2	53 ± 2	-90 ± 1
20	7.0	-375 ± 2	-418 ± 2	271 ± 2	-542 ± 2
40	6.5	-232 ± 2	-305 ± 2	373 ± 2	-752 ± 2
60	5.5	-120 ± 2	-251 ± 2	529 ± 1	-925 ± 1

\*Standard deviation of three measurements

The ferrocene caused only the potential shift to more positive values from -380 mV to -350 mV and from -395 mV to -320 mV for anodic and cathodic potentials respectively. Voltammetric signals produced at the potential  $E_{cat} = -113$  mV by mixed Coliform culture (*E. coli* DSM 498, *E. coli* DSM 301, *Hafnia alvei* DSM 30163<sup>T</sup>, *Klebsiella pneumonia* DSM 30104) and *Lactobacillus acidophilus* DSM 20079 on the GR/PAAGC sensor containing L-Alanyl-p-nitroanilide substrate is shown in Fig. 42 D.

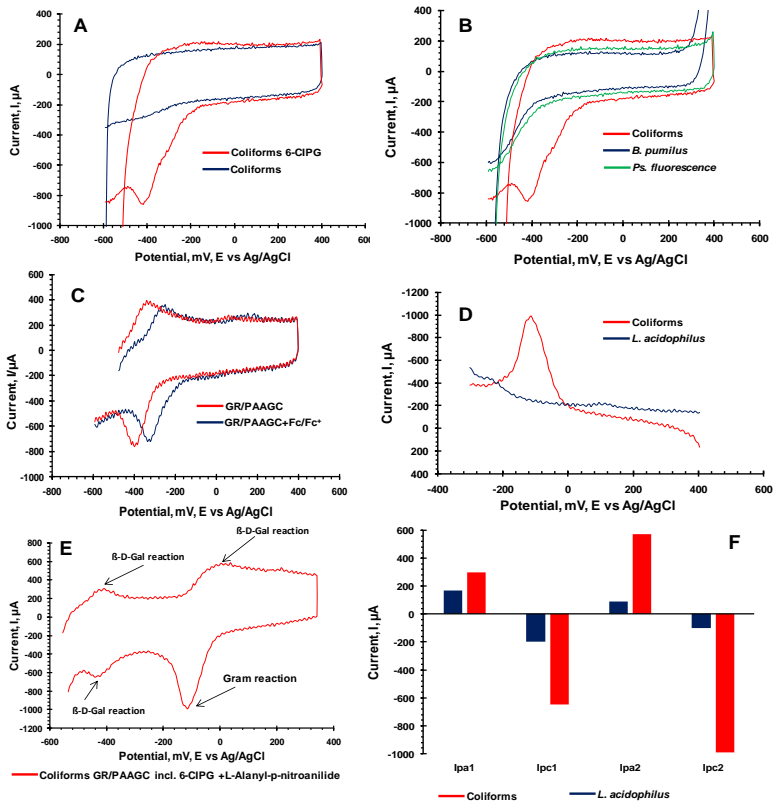


**Figure 42** A) Voltammetric signals produced by Coliforms on GR/PAAGC sensor with and without 6-CIPG during 1 h incubation. B) Voltammetric signals produced by Coliforms, *B. pumilus* and *P. fluorescence* on GR/PAAGC sensor during 1 h incubation. C) Influence of Fc/Fc<sup>+</sup> redox prob on the intensity of the signal produced by Coliform bacteria. D) Electrochemical signal specific for the gram-reaction produced by Coliforms during reverse cycle at the  $E_{cat} = -113$  mV potential. E) Voltammetric signals produced by Coliforms on GR/PAAGC dual substrate system containing both 6-CIPG and L-Alanyl-p-nitroanilide. F) Current intensities of CV curves produced by Coliforms and *L. acidophilus* at the potential range inherent for  $\beta$ -D-Galactosidase activity.

*L. acidophilus* DSM 20079 did not produce any redox peak at the tested potential in the gel-electrode system during 3h of incubation. That clearly indicates that *L. acidophilus* DSM 20079 does not possess L-Alanine aminopeptidase activity as expected. Fig. 42E shows the redox signals produced due to simultaneous reaction of Coliforms (*E. coli* DSM 498, *E. coli* DSM 301, *Hafnia alvei* DSM 30163<sup>T</sup>, *Klebsiella pneumonia* DSM 30104) with 6-CIPG and L-Alanyl-p-nitroanilide in one gel-electrode system. The CV peaks inherent for 6-DI (produced due to reaction of Coliforms and 6-CIPG) were produced at the previously defined potentials, while scanning from -600 mV to 400 mV, at the 50 mV scan rate. The negative shift from -200 mV to -400 mV, 200 mV to 20 mV and ~-300 mV to - 420 mV occurred for the two anodic and one cathodic peaks respectively. The cathodic peak inherent for p-nitroaniline (produced due to reaction of coliforms and L-Alanyl-p-nitroanilide) was produced at the potential  $E_{cat}=-113$  mV.

During 3 h of incubation *L. acidophilus* DSM 20079 produced small redox signals inherent for  $\beta$ -D-Galactosidase activity at the negatively shifted anodic and cathodic potentials.

Current intensities of the anodic and cathodic peaks of voltammogram produced by *L. acidophilus* DSM 20079 reached 168  $\mu$ A and -200  $\mu$ A values respectively, which was significantly lower ( $P<0.05$ ) than the anodic and cathodic peaks produced by Coliform bacteria (Fig. 42F). Due to the reaction of  $\beta$ -D-Galactosidase, produced by *L. acidophilus* DSM 20079 and 6-CIPG substrate there was no occurrence of the second anodic peak intrinsic for the redox reaction of 6-DI. The current intensity equal to 90  $\mu$ A (less than current intensity produced by the blank gel 100  $\mu$ A) was produced,

which was significantly lower compared to the anodic peak produced by Coliforms (*E. coli* DSM 498, *E. coli* DSM 301, *Hafnia alvei* DSM 30163<sup>T</sup>, *Klebsiella pneumonia* DSM 30104) ( $P < 0.05$ ). The production of the second cathodic peak, inherent for the p-nitroaniline (gram negative reaction), by *L. acidophilus* DSM 20079 was also not detected in two-substrate gel electrode system in comparison with Coliforms, which were detected.

### **5.5 Detection of other bacteria with GR/PAAGC sensor platform in culture**

The CV curve produced due to incubation (at 44 °C) of 7.8 log<sub>10</sub>CFU/mL *E. coli* DSM 301 in the GR/PAAGC sensor, containing 0.5 mg/mL 5,4-BCIPG substrate, is shown in Fig. 43. After 20 to 30 min of incubation the cathodic peak was formed at potential  $E_{cat} = -40$  mV, when scanning from -600 mV to 400 mV, at the 50 mV/s scan rate (Fig. 43A). After 3h of incubation the CV peaks inherent for redox reaction of 5,4-DDI were formed (Fig 43B). The irreversible CV curve produced by reaction of *E. coli* DSM 301 with the 4-MUG (0.5 mg/ml) injected to the gel-electrode system is shown in Fig. 43C. The anodic signals produced by different concentrations of *E. coli* DSM 301 in the culture varying from 1.8 log<sub>10</sub>CFU/ml to 7.8 log<sub>10</sub>CFU/ml are shown in Fig. 43 D. The good linear relationship ( $R^2=0.99$ ) was observed between increasing concentration of *E. coli* DSM 301 and anodic peak currents (Fig. 43E). All tested concentrations of *E. coli* DSM 301 produced anodic signals at the defined potential  $E_{an} \sim 720$  mV during 3h incubation of the gel-electrode sensor at 44 °C. The blank gel-electrode system containing 0.5mg/mL substrate, accelerating reagent and inducer and injected

by sterile culture media (free of *E. coli*) did not produce any electrochemical signal in the defined potential range. The CV curve produced due to incubation of 7.6 log<sub>10</sub>CFU/ml *St. aureus* DSM 799 in the gel-electrode system at 37 °C for 3 h is shown in Fig. 44A. The anodic peak typical for the oxidation of 4-NP was detected at the previously defined potential range ~880 mV. The five independent measurements of the blank gel-electrode system at the defined potential varying from -400 to 1000 mV at the 50 mV/s scan rate did not show any electrochemical activity (Fig. 44B). The redox peaks produced by *St. aureus* DSM 799 ranging from 2.6 log<sub>10</sub>CFU/mL to 7.6 log<sub>10</sub>CFU/mL are shown in Fig. 44C. The linear relationship ( $R^2=0.98$ ) was observed between increasing concentrations of *St. aureus* DSM 799 and anodic peak currents (Fig. 44D).

## 5.6 Detection of bacteria on stainless steel surfaces

The voltammograms produced by Coliform bacteria (*E. coli* DSM 498, *E. coli* DSM 301, *Hafnia alvei* DSM 30163<sup>T</sup>, *Klebsiella pneumonia* DSM 30104) grown on stainless steel surfaces are shown in Fig. 45A. The specific reversible redox peaks were detected at the determined potential ranges. The peak currents increased with the increasing concentration of Coliform bacteria (*E. coli* DSM 498, *E. coli* DSM 301, *Hafnia alvei* DSM 30163<sup>T</sup>, *Klebsiella pneumonia* DSM 30104). Good linearity was observed between the peak current and bacteria concentrations in the range from 0.6 log<sub>10</sub>CFU/cm<sup>2</sup> to 6.6 log<sub>10</sub>CFU/cm<sup>2</sup> (Fig. 45B). The CV curves produced by two set of increasing concentrations of Coliforms (*E.coli* DSM 498, *E.coli* DSM 301, *Hafnia alvei* DSM 30163<sup>T</sup>, *Klebsiella*



*pneumonia* DSM 30104) ranging from 3 log<sub>10</sub>CFU/cm<sup>2</sup> to 7 log<sub>10</sub>CFU/cm<sup>2</sup> (10<sup>3</sup> CFU/cm<sup>2</sup> to 10<sup>7</sup> CFU/cm<sup>2</sup>) and from 2 log<sub>10</sub>CFU/cm<sup>2</sup> to 6log<sub>10</sub>CFU/cm<sup>2</sup> (10<sup>2</sup> CFU/cm<sup>2</sup> to 10<sup>6</sup> CFU/cm<sup>2</sup>) are presented in Fig. 46 A and B. In 30 minutes of incubation, only cathodic peaks inherent for 6-DI were detected at the cathodic potential equal to ~420 mV. In both cases, the cathodic current intensities increased with the increasing concentrations of Coliforms (*E. coli* DSM 498, *E.coli* DSM 301, *Hafnia alvei* DSM 30163<sup>T</sup>, *Klebsiella pneumonia* DSM 30104), however slightly positive shift of cathodic potential with the increasing concentrations was noticed.

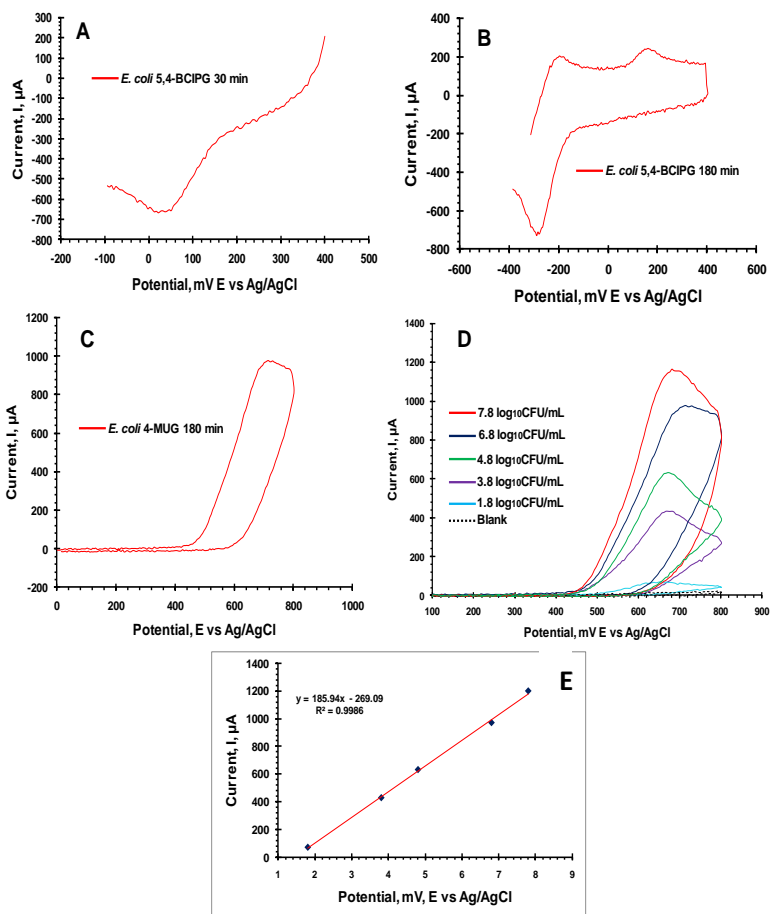


**Figure 43** A) Voltammetric signal produced by *E. coli* DSM 301 on GR/PAAGC sensor during 30 minutes. B) Current peaks inherent for 5,4-DDI produced by *E. coli* DSM 301 on GR/PAAGC sensor during 180 minutes. C) Irreversible voltammogram produced by *E. coli* DSM 301 on GR/PAAGC sensor containing 4-MUG substrate. D) Current peaks produced by different concentrations of *E. coli* DSM 301 on GR/PAAGC. E) Correlation between currents and concentrations of *E. coli*.

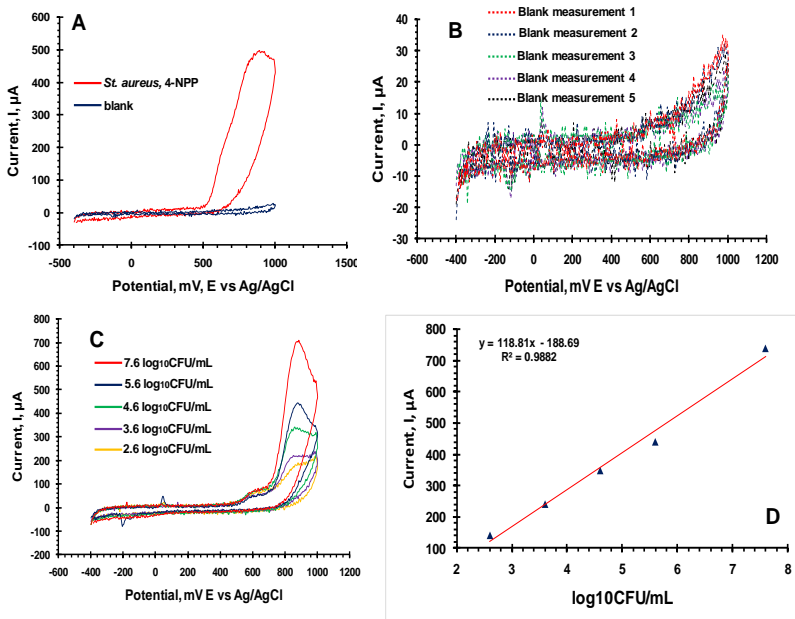


**Figure 44** A) Voltammetric current peak produced by *St. aureus* DSM 799 on GR/PAAGC sensor. B) Electrochemical behavior of GR/PAAGC-gel system containing 4-NPP. C) Current peaks produced by different concentrations of *St. aureus* DSM 799 at the defined anodic potential  $E_{\approx 880}$  mV. D) Correlation between current peaks and concentrations.

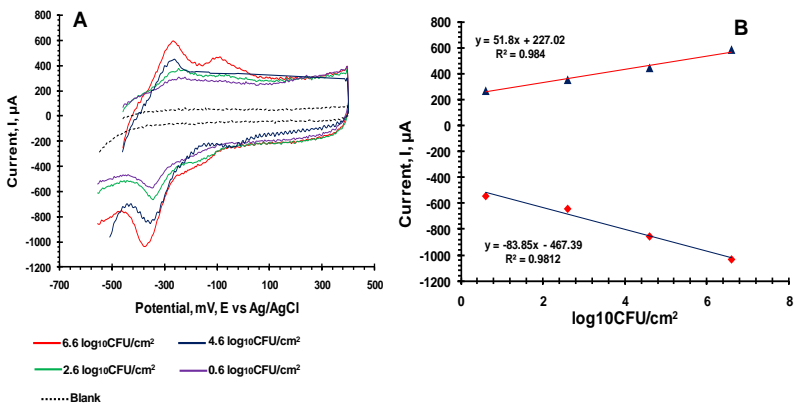


**Figure 45 A) Voltammetric signals produced by different concentration of Coliforms sampled from stainless steel surfaces. B) Correlation between anodic and cathodic peak currents and concentrations of Coliforms.**

The reduction peaks produced due to incubation of gel-electrode system with the Coliforms (*E. coli* DSM 498, *E. coli* DSM 301, *Hafnia alvei* DSM 30163<sup>T</sup>, *Klebsiella pneumonia* DSM 30104) ranging from 0.6  $\log_{10}\text{CFU}/\text{cm}^2$  to 6.6  $\log_{10}\text{CFU}/\text{cm}^2$  are shown in Fig. 46C. The reduction signals occurred at the cathodic potential equal to  $\sim 430$  mV. Good linear relationship ( $R^2=0.99$ ) was observed between increasing concentrations of Coliforms and cathodic peak currents (Fig. 46D). However, a slight negative and positive shift of peak potentials produced by different bacterial concentrations was noticed. The cyclic voltammograms produced by Coliform bacteria (*E. coli* DSM 498, *E. coli* DSM 301, *Hafnia alvei* DSM 30163<sup>T</sup>, *Klebsiella pneumonia* DSM 30104) ranging from 0.6  $\log_{10}\text{CFU}/\text{cm}^2$  to 6.6  $\log_{10}\text{CFU}/\text{cm}^2$  during 30 minutes of incubation are presented in Fig. 47A. The formation of anodic peak currents was occurred. The anodic and cathodic peaks formed within 30 minutes on gel-

electrode system containing 5mg/mL substrate showed negative potentials. The positive and negative shift from 360 mV to 300 mV and from -420 mV to -450 mV occurred for the anodic and cathodic potentials respectively. Good linear relationship ( $R^2=0.98$  for anodic and  $R^2=0.99$  for cathodic) was observed between the redox peak currents and increasing concentrations of Coliform bacteria (Fig. 47B).

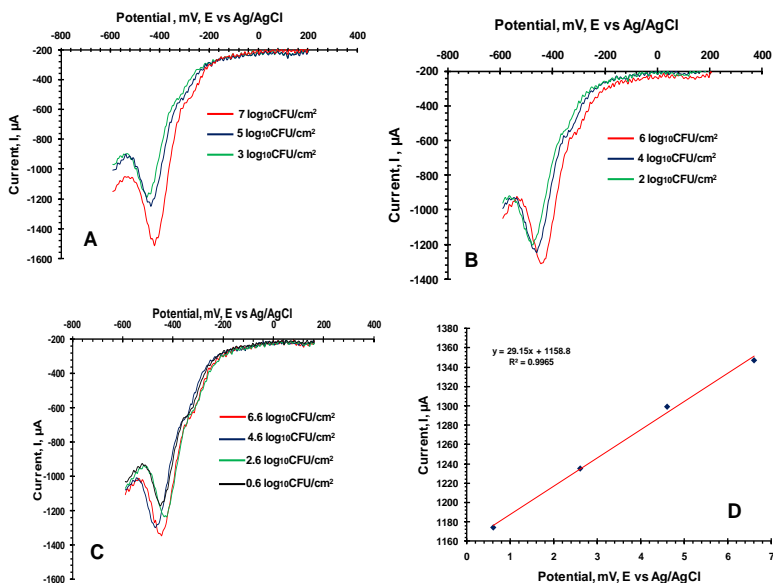


**Figure 46 A),B), C) Cathodic current peaks produced by different concentrations of Coliforms during 30 min of incubation on GR/PAAGC-gel system. Coliforms were sampled from stainless steel surfaces. D) Correlation between voltammetric signals and concentrations.**

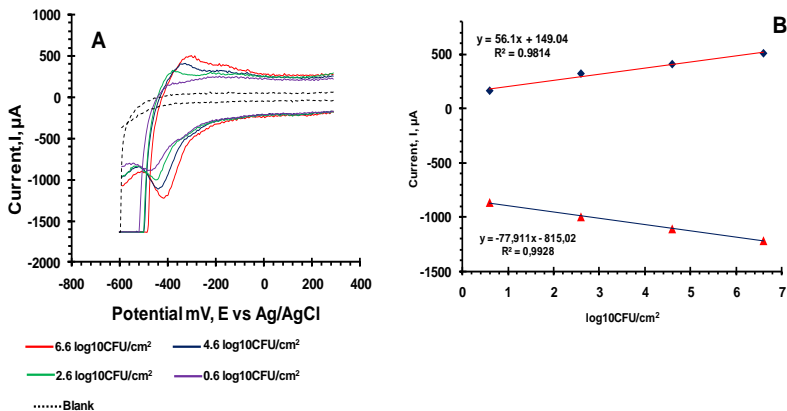


**Figure 47** A) Voltammetric signals produced by Coliforms, sampled from stainless steel surfaces, GR/PAAGC-gel sensor containing 5 mg/mL 6-CIPG substrate. Incubation time = 30 min. B) Correlation between produced anodic and cathodic peaks and concentrations of Coliforms.

The electrochemical behavior of Coliforms (*E. coli* DSM 498, *E. coli* DSM 301, *Hafnia alvei* DSM 30163<sup>T</sup>, *Klebsiella pneumonia* DSM 30104) on stainless steel surfaces in heavy-soiled conditions is shown in Fig. 48A. Coliforms (*E. coli* DSM 498, *E. coli* DSM 301, *Hafnia alvei* DSM 30163<sup>T</sup>, *Klebsiella pneumonia* DSM 30104) exhibited well-defined redox peaks in the already determined potential range. The soil (meat juice) without Coliform bacteria did not produce any redox peak. The electrochemical signals produced by 6.6  $\log_{10}\text{CFU}/\text{cm}^2$  Coliforms (*E. coli* DSM 498, *E. coli* DSM 301, *Hafnia alvei* DSM 30163<sup>T</sup>, *Klebsiella pneumonia* DSM 30104) on clean (without any meat residues) stainless steel surfaces are shown

in Fig. 48B. The current intensity of the cathodic peak was equal to 1160  $\mu\text{A}$  after the first 4 h of incubation, which corresponds to 4.4  $\log_{10}\text{CFU}/\text{cm}^2$ . After disinfection of stainless steel surface with 3% hydrogen peroxide the cathodic current decreased down to 960  $\mu\text{A}$  (80  $\text{CFU}/\text{cm}^2$ ) (Fig. 48B). The gel-electrode system used for sampling of not inoculated surface did not produce any cathodic signal as well as no significant current ( $\approx 200$  mV) at the defined potential range (Fig 48C). The comparison of swabbing method and developed sensor is presented in Fig. 48D. Good correlation ( $R^2=0.99$ ) was noticed between numbers of Coliforms (*E. coli* DSM 498, *E. coli* DSM 301, *Hafnia alvei* DSM 30163<sup>T</sup>, *Klebsiella pneumonia* DSM 30104) detected by classical swabbing method and developed GR/PAA-gel carbon sensor. The results of comparison of classical method and developed sensor for monitoring of Coliforms (*E. coli* DSM 498, *E. coli* DSM 301, *Hafnia alvei* DSM 30163<sup>T</sup>, *Klebsiella pneumonia* DSM 30104) on stainless steel surfaces at simulated food processing working conditions are shown in Fig. 49. The detected cathodic currents at every hour are presented in Fig. 49A.

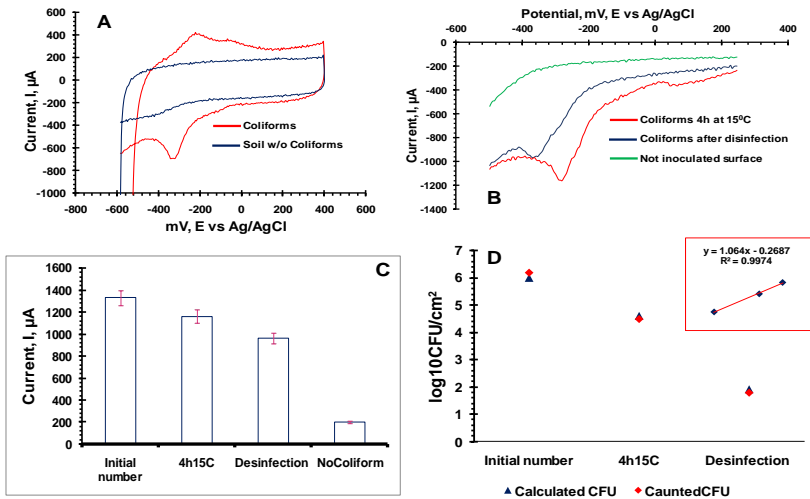


**Figure 48 A) Voltammetric signals produced by Coliforms on stainless steel surfaces in dirty conditions. B) Cathodic peaks produced by Coliforms after surviving on stainless steel surfaces at 15°C and disinfection. C) Comparison of current peaks produced by Coliforms at different conditions. D) Correlation between numbers of Coliforms obtained by classical microbiological method and counted from the current values obtained by the developed sensor.**

The increase of current values with the time is noticed. The comparison of results obtained with the two methods is presented in Fig. 49B. The good linear relationship ( $R^2=0.99$ ) (Fig. 49C) was observed between increasing number of Coliforms ( $\log_{10}\text{CFU}/\text{cm}^2$ ) quantified by designed sensor and cultural method. The CV peaks produced by different concentrations of *E. coli* DSM 301 sampled from stainless steel surfaces on GR/PAAGC-gel sensor containing 5,4-BCIPG substrate are shown in Fig. 50A. The good linear relationship ( $R^2=0.99$ ) was observed between increasing concentrations of *E. coli* DSM 301 and cathodic current intensities



(Fig. 50B). The blank did not produce any electrochemical signal at the tested potential range. The CV peaks produced by *E. coli* DSM 301, on GR/PAAGC-gel sensor containing 4-MUG substrate, sampled from stainless steel surfaces within 30 minutes of incubation are shown in Fig. 51A.

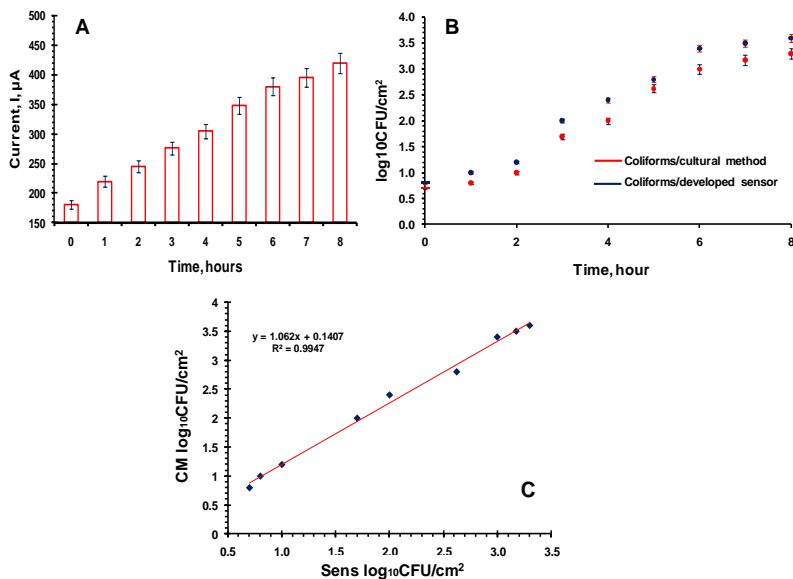


**Figure 49** A) Current peaks produced by Coliforms on stainless steel surfaces at continuous re-soiling conditions during 8h period. B) Comparison of Coliforms obtained by classical microbiological method and counted from the current values obtained by the developed sensor. C) Correlation between numbers of Coliforms obtained by plate counting method (CM) and counted from the current values obtained by the developed sensor (Sens).

The anodic currents occurred at the already defined potential  $E_{an} = \sim 700$  mV. The good linear relationship ( $R^2=0.99$ ) was observed between increasing concentrations of *E. coli* DSM 301 and cathodic peak currents (Fig. 51B). The anodic signals produced by *St. aureus*

DSM 799, during 30 minutes, sampled from stainless steel surfaces are shown in Fig. 52A. The good linear relationship ( $R^2=0.99$ ) was found between increasing concentrations of *St. aureus* DSM 799 and anodic peak currents (Fig. 52B). The anodic signals formed at the potential  $E_{an} = \sim 1080$  mV. However, the positive shift of the anodic potential from was occurred in comparison with detection of *St. aureus* in culture within 3 h of incubation. Electrochemical signal produced, within 3h of incubation, by *St. aureus* DSM 799 sampled from stainless steel surface is shown in Fig. 53A. The anodic peak current occurred at the  $E_{an} = \sim 900$  mV. After 30 minutes of incubation the pH of the gel electrode system was around 7.2, however after 3 h of incubation it decreased up to 6.0 (Fig. 53B).

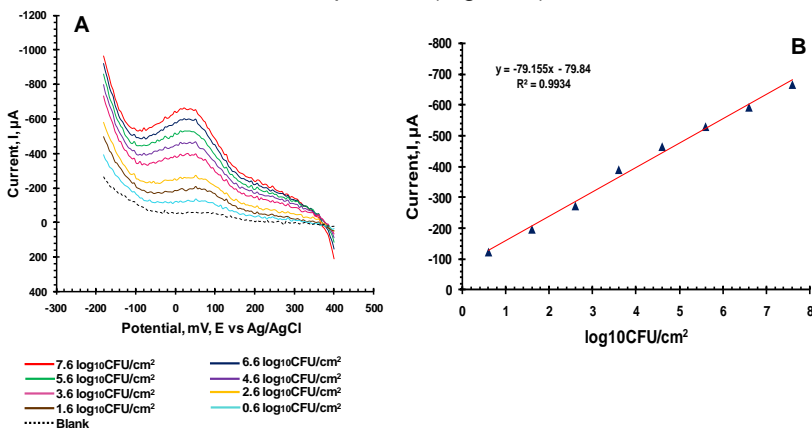


**Figure 50 A) Cathodic peaks produced by *E. coli* DSM 301, sampled from stainless steel surfaces, within 30 minutes. The GR/PAAGC-gel sensor contains 5 mg/mL of 5,4-CIPG. B) Correlation between current peaks and detected concentrations.**

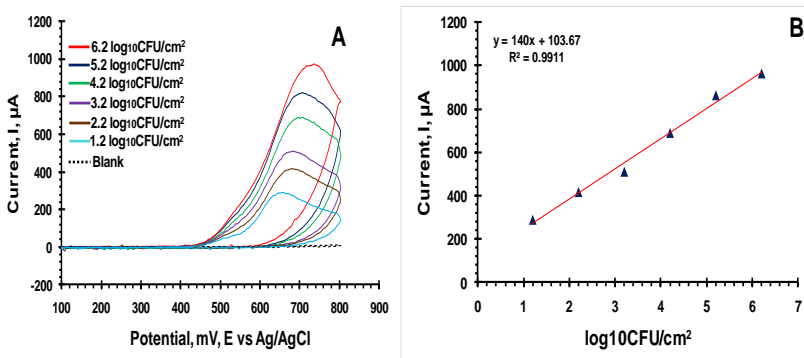


Figure 51 A) Anodic peaks produced by *E. coli* DSM 301, sampled form stainless steel surfaces, within 30 minutes. The GR/PAAGC-gel sensor contains 5 mg/mL of 4-MUG. B) Correlation between current peaks and detected concentrations.

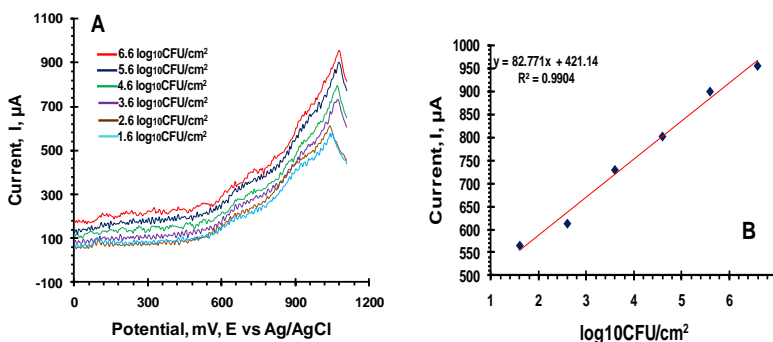
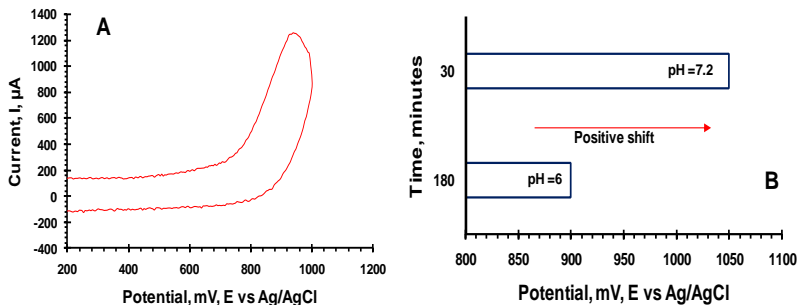


Figure 52 A) Anodic peaks produced by *St. aureus* DSM 799, sampled form stainless steel surfaces, within 30 minutes. The GR/PAAGC-gel sensor contains 5 mg/mL of 4-NPP. B) Correlation between current peaks and detected concentrations.



**Figure 53** A) Anodic peak produced by *St. aureus* DSM 799, sampled from stainless steel surfaces, within 3 hours. The GR/PAAGC-gel sensor contains 5 mg/mL of 4-NPP. B) The influence of pH and incubation time on the anodic potential of the produced peaks.

## 5.7 Colorimetric properties of the gel system

The optimization of the exact wavelength where the gel showed maximal absorbance due to production of 6-DI is presented in Fig 54. As shown in Fig 54A the absorbance values reached their maximum at 530 nm wavelength at visible spectrum. Within 30 minutes of reaction the absorbance value increased from 0.3 to 0.6 (Fig 54B). The dense rose color occurred at 30 minutes of incubation at 37 °C, however the color formation could already been detectable at 5<sup>th</sup> minute of incubation (Fig. 54C).

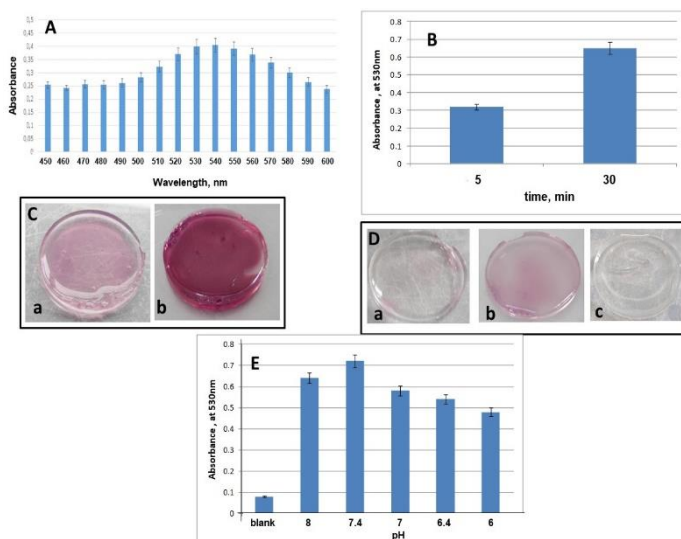


**Figure 54** A) Detection of maximum absorbance of produced 6-DI at different wavelengths. B) Absorbance produced in 5 and 30 minutes of enzyme reaction in the gel system. C) Color produced in 5 and 30 minutes of enzyme reaction in the gel system. D) Color produced at different pH values of the gel, a) pH = 7; b) pH = 7.4; c) pH = 6.4. E) Absorbance values detected at different pHs of the gel.

As shown in Fig 54D and Fig 54E the PAA gel system possessed highest optical signal at pH 7.4. The optical signals produced b-d-glucuronidase activity are shown in Fig 55. The maximum absorbance of the gel, due to b-d-glucuronidase activity was observed at 620 nm wavelength (Fig. 55A).

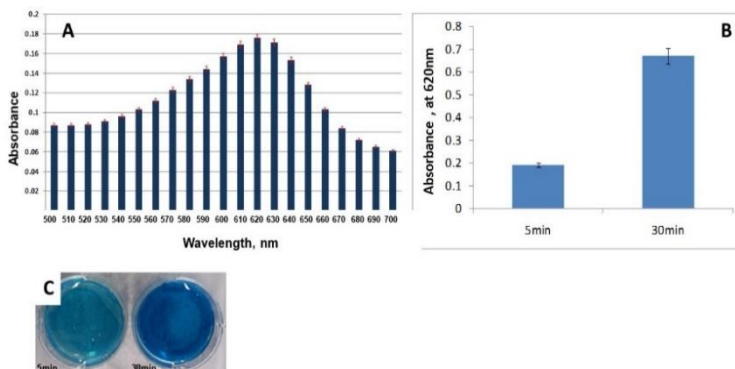


**Figure 55 A) Detection of maximum absorbance of produced 5,4-DDI at different wavelengths. B), C) Absorbance at specific wavelength (620 nm) and specific color produced in the gel system in 5 and 30 minutes of reaction.**

The optical density of the gel reached the 0.2 after 5 min of enzyme substrate reaction and within 30 minutes it increased up to 0.65 (Fig 55B). These results were confirmed by the visual examination of the gels (Fig. 55C). The reaction of  $\beta$ -d-Glucuronidase and 4-MUG substrate produced the maximum fluorescence at 370nm excitation and 450 nm emission (Fig.56 A, B). The fluorescence already occurred after 6 minutes of reaction and reached the maximum values within 30 minutes (Fig. 56C). The obtained results were confirmed by the examination of the PAA gel in the UV chamber under UV light (Fig56D). The reactions of  $\beta$ -d-Glucuronidase with 5,4-BCIPG and 4-MUG substrates in optimized PAA gel systems during 1h period are shown in Fig. (57A, B). The saturation of 1mg/mL  $\beta$ -d-Glucuronidase with 0.5mg/mL substrates occurred after 48 and 45 minutes of reaction for the 5,4-BCIPG and 4-MUG respectively. The 6 log<sub>10</sub>CFU/ml of Coliform suspension (*E. coli* DSM

498, *E.coli* DSM 301, *Hafnia alvei* DSM 30163<sup>T</sup>, *Klebsiella pneumonia* DSM 30104) produced the maximum optical signal (abs=2.8, at 530 nm), within 3 h of incubation with 0.5 mg/mL 6-CIPG and 0.2 mg/mL IPTG (Fig. 58A). The other tested concentrations produced significantly lower signals. The optical signals produced by 4-MU formed due to incubation of 10<sup>6</sup>CFU/mL *E. coli* DSM 301 suspension with the 0.5mg/mL 4-MUG and different concentrations of OBDG are shown in Fig. 58B.

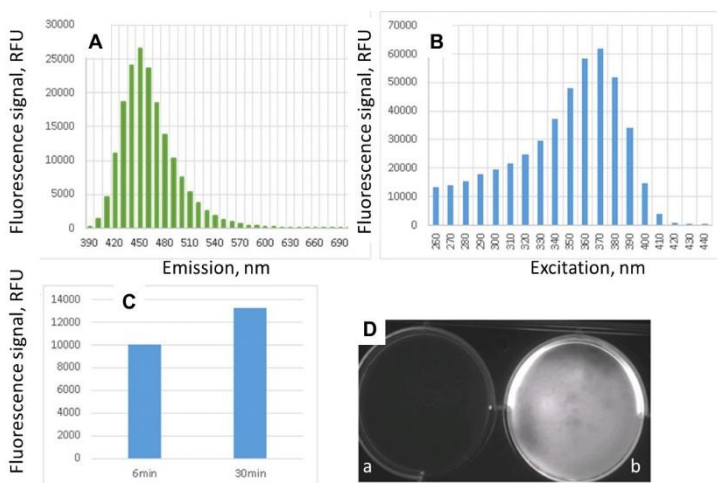


**Figure 56A), B) Emission and excitation values where the gel produced the maximum fluorescence signals. C), D) Fluorescence signals at specific EX/EM values and specific fluorescence produced in the gel system in 6 and 30 minutes of reaction.**

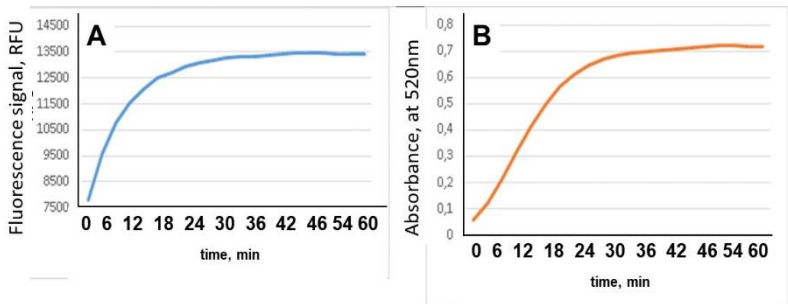


**Figure 57** The reaction of  $\beta$ -d-Glucuronidase and A) 4-MUG and B) 5,4-BCIGP substrates during 60 minutes.

The reaction mixture containing 0.2 mg/mL OBDG produced the highest fluorescent signals ~11500RFU at 450 nm emission within 3 h reaction time. mixture containing 0.2 mg/mL OBDG produced the highest fluorescent signals ~11500RFU at 450 nm emission within 3 h reaction time.

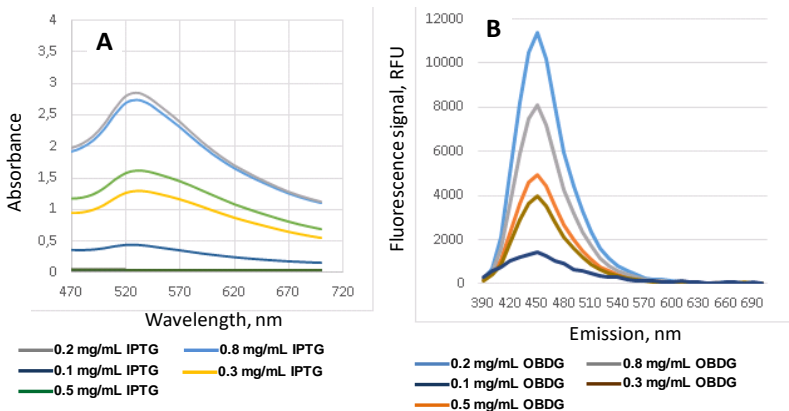


**Figure 58** Fluorogenic (A) and chromogenic(b) and signals produced in the gel system in the presence of different concentrations of A) IPTG and B) OBDG.

The colorimetric signals produced in presence of different acceleration reagents are shown in Fig. 59A. In case of Coliforms (*E.*



*coli* DSM 498, *E. coli* DSM 301, *Hafnia alvei* DSM 30163<sup>T</sup>, *Klebsiella pneumonia* DSM 30104) the PAA gel system produced the highest optical signals (abs =0.634; 530 nm) within 1h of incubation of 10<sup>6</sup>CFU/mL bacterial suspension with 0.5 mg/mL 6-CIPG, 0.2 mg/mL IPTG and 0.005 mg/mL ODTG. In case of *E. coli* DSM 301 highest fluorescent signal formed due to incubation with 0.2 mg/ml of OBDG and 0.005mg/ml of OBG (Fig59B). Within 1 h of incubation the fluorescent signal produced by reaction mixture containing OBG was equal to ~8000 RFU. The fluorescent signals equal to 818 RFU and 2140 RFU were produced by the PAA gel with and without permeabilization reagent (OBG) respectively (Fig. 59 C).

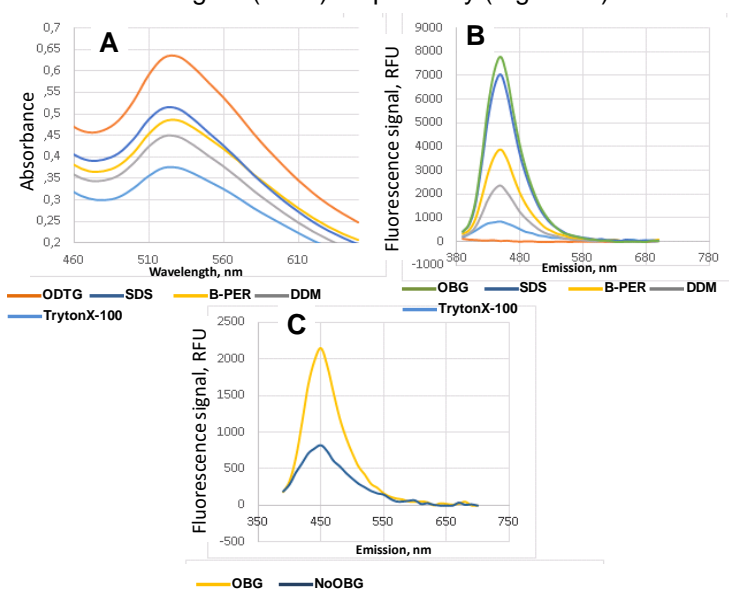


**Figure 59 Influence of different accelerator reagents on production of chromogenic and fluorogenic signals by *E. coli* and Coliforms. A) Coliforms/ODTG absorbance, B) *E. coli* DSM 301/OBG Fluorescence, C) Comparison of signal intensity produced by *E. coli* DSM 301 in the gel system with and without OBG.**

The reaction of  $10^6$ CFU/mL Coliforms (*E. coli* DSM 498, *E. coli* DSM 301, *Hafnia alvei* DSM 30163<sup>T</sup>, *Klebsiella pneumonia* DSM 30104) and *E. coli* DSM 301 suspensions with the B-Per, ODTG and OBG is shown in Fig.60. No color formation as well as no fluorescence was occurred in the reaction mixture of Coliforms (*E. coli* DSM 498, *E. coli* DSM 301, *Hafnia alvei* DSM 30163<sup>T</sup>, *Klebsiella pneumonia* DSM 30104) and *E. coli* DSM 301 with B-Per reagent within 5min. In comparison, in the reaction tubes containing the OBG and ODTG, the distinguishable rose color, weak cyan color as well as strong fluorescence inherent for 6-DI, 5,4-DDI, and 4-MU respectively, occurred within the same time period (Fig 60A, E, F).

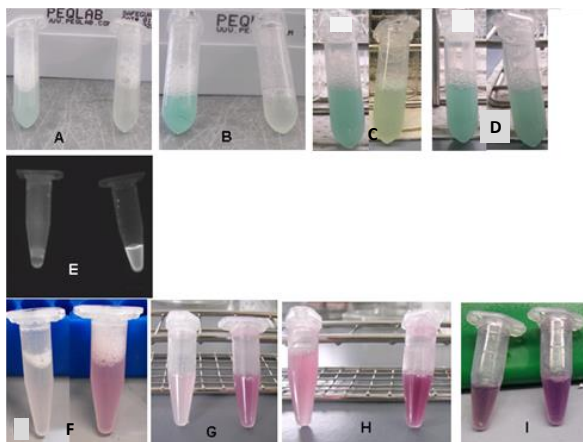


**Figure 60 Influence of different accelerator reagents on production of chromogenic and fluorogenic signals by *E. coli* and Coliforms.**

After 15 minutes of reaction no visible color change, due to  $\beta$ -D-glucuronidase activity, was noticed in the tube with the B-Per reagent. The increase of color density in the reaction tube containing OBG was noticed after 15 minutes. In case of Coliforms (*E. coli* DSM 498, *E. coli* DSM 301, *Hafnia alvei* DSM 30163<sup>T</sup>, *Klebsiella pneumonia* DSM 30104), the formation of weak rose color was observed after 15 minutes of reaction with 6-CIPG substrate in the presence of B-Per. The reaction mixture containing the ODTG reagent produced strong rose color within 15 minutes (Fig.60B, G). In the reaction tube containing B-Per reagent the formation of weak cyan color and distinguishable rose color was noticed after 30 minutes for the *E. coli* DSM 301 and Coliforms (*E. coli* DSM 498, *E. coli* DSM 301, *Hafnia alvei* DSM 30163<sup>T</sup>, *Klebsiella pneumonia* DSM 30104) respectively (Fig. 60C, H). Within 60 minutes, the intensities of colors, formed due to influence of both group of reagents were almost equal, although higher color densities formed by OBG and ODTG could be noticed in comparison with B-Per (Fig. 60D, I). The influence of the different concentrations of 4-MUG fluorogenic substrate, varying from 1 mg/mL to 8 mg/mL, on fluorescent signal intensity was investigated (Fig. 61A). The PAA gel with the highest substrate concentration produced the optical signal with maximum intensity equal to 1111 RFU. The good linear

relationship was observed between increasing concentration of the substrate and fluorescent intensity (Fig. 61B).

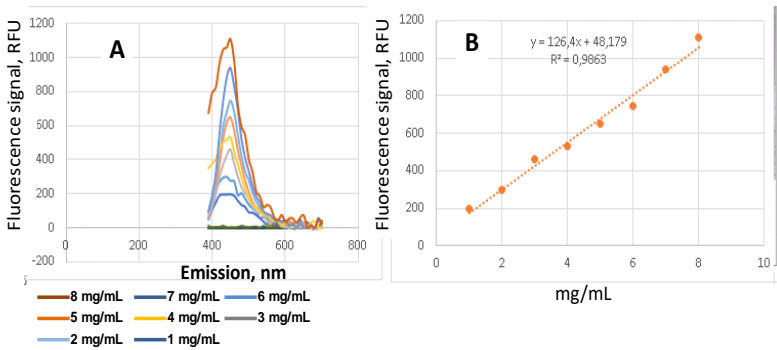


**Figure 61 Influence of different concentration of 4-MUG substrate on fluorescence signal intensity produced by *E. coli* DSM 301 in the gel system.**

Color production by Coliforms sampled from stainless steel surfaces using PAA gel with optimized concentrations of OBG and IPTG is shown in Fig. 62. The visual control showed that signal already occurred after 20 minutes of reaction of Coliforms with 5mg/mL 6-CIPG substrate. After 30 minutes the increase of the color density was observed. Strong rose color was observed after 60 minutes of reaction.

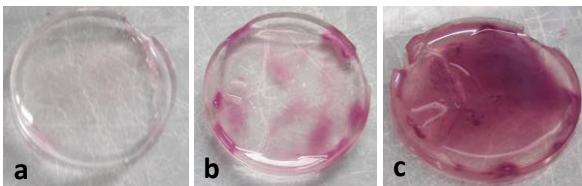


**Figure 62 Production of specific color by Coliforms sampled from stainless steel surfaces in A) 20, B) 30 and C) 60 minutes of incubation.**

Color formation by Coliforms (*E. coli* DSM 498, *E. coli* DSM 301, *Hafnia alvei* DSM 30163<sup>T</sup>, *Klebsiella pneumonia* DSM 30104), *E. coli* DSM 301 and *E. coli* DSM 498 sampled from stainless steel surfaces is shown in Fig. 63. The formation of optical signals specific for both group of bacteria observed within 30 minutes (Fig63 A, C, E). Strong color formation and diffusion through the PAA gel was observed within 3h hours for all tested bacteria (Fig. 11 B, D, F).

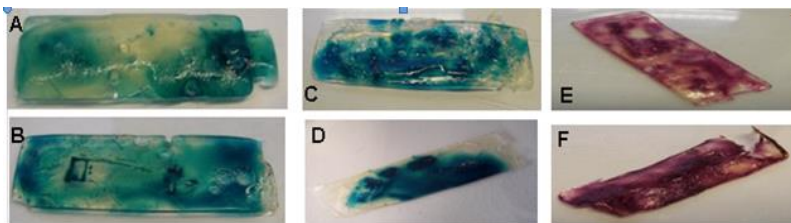


**Figure 63 Production of specific color by Coliforms, *E. coli* DSM 301 and *E. coli* DSM 498 sampled from stainless steel surfaces in A), C), E) 30 minutes and B),D),F) 180 minutes of incubation.**

The production of fluorometric signals by the *E. coli* (sampled from stainless steel surfaces) during 30 and 180 minutes was also studied. The generated fluorescence signals are shown in Fig. 64A. After 30 minutes of incubation in the developed gel system *E. coli* produced ~4000 RFU at 450 nm emission. After 180 minutes. of incubation the fluorescence value significantly increased up to ~11000 RFU. The fluorescence signals produced by *E. coli* at the above mentioned incubation times at the excitation/emission range specific for the 4-MUG are shown in Fig. 64B.

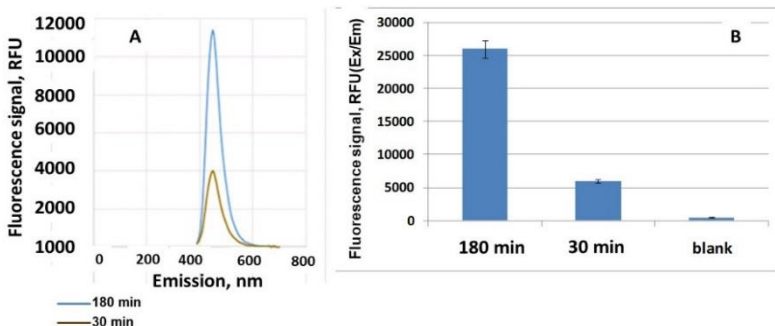


**Figure 64 Production of specific fluorescence by *E. coli* DSM 301 sampled from stainless steel surfaces in 30 and 180 minutes of incubation. A) Emission spectra, B) Excitation/Emission spectra.**

The combined optical and electrochemical behavior of  $6 \log_{10}$ CFU/cm<sup>2</sup> Coliforms, *E. coli* DSM 301 and *St. aureus* DSM 799 on PAACGRG sensor platforms is shown in Fig 65. The blank gel-electrode systems containing target substrate for each group of bacteria did not produce any optical or electrochemical signals (Fig.65 a). Production of specific chromogenic, fluorogenic and electrochemical signals for Coliforms (*E. coli* DSM 498, *E. coli* DSM 301, *Hafnia alvei* DSM 30163<sup>T</sup>, *Klebsiella pneumonia* DSM 30104), *E. coli* DSM 301, *St. aureus* DSM 799, Gram –negative bacteria is shown in Fig 65 (b,c,d,e,f and g). Optical and electrochemical behavior of different concentrations of Coliforms (*E. coli* DSM 498, *E. coli* DSM 301, *Hafnia alvei* DSM 30163<sup>T</sup>, *Klebsiella pneumonia* DSM 30104) sampled from food contact surfaces is shown in Fig. 66. Developed sensor could detect  $1 \log_{10}$ CFU/cm<sup>2</sup> Coliform bacteria on food contact surfaces within 30 minutes both optically and electrochemically. The sharp and distinguishable curves were obtained for each tested concentration.

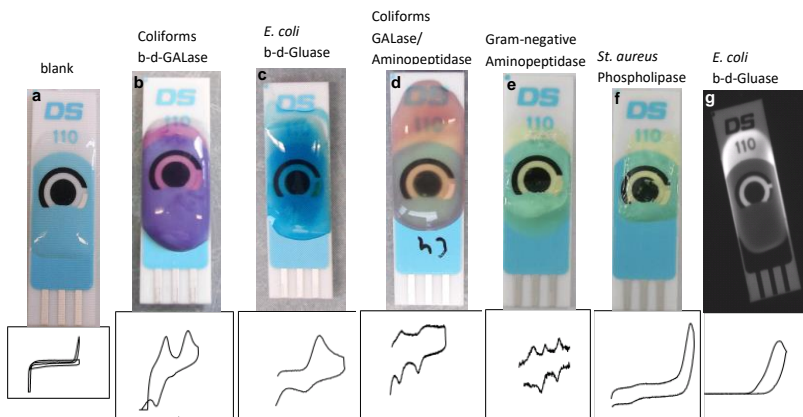


**Figure 65** Production of optical and electrochemical (curves in boxes) signals by different bacteria sampled from stainless steel surfaces. Bacterial concentration =  $10^6$  CFU/cm<sup>2</sup>. Detection time = 30 minutes.

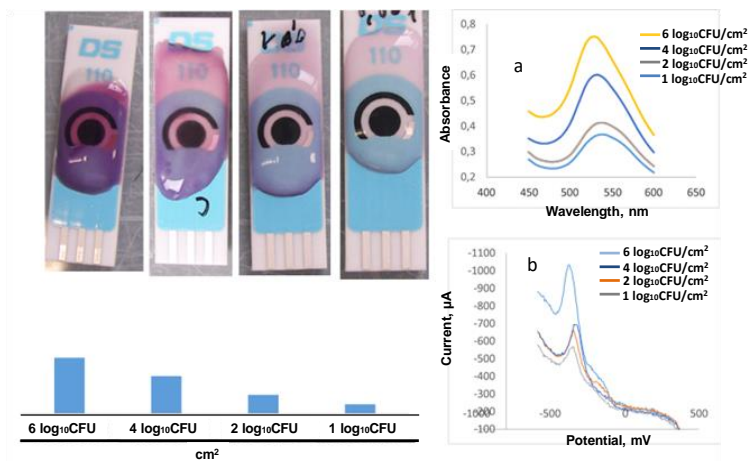


**Figure 66** Optical (a) and voltammetric (b) signals produced by different concentrations of Coliforms sampled from stainless steel surfaces within 30 minutes. Each of concentration was obtained by dilution of the highest bacterial concentration ( $6 \log_{10}$ CFU/cm<sup>2</sup>). The preparation the highest bacterial concentration and appropriate dilution are described

in the section 4.4. After dilution, each inoculum also was validated by additional plate count and swabbing methods (in case of stainless steel coupons).

## 6 Discussion

### 6.1 Electrochemical detection of target analytes

Three groups of target analytes namely indoxyl, coumarin, and phenol based substances were tested in this section. The first, second and third groups include 5,4-DDI/6,6-DI, 4-MU, and 4-NP respectively. The indoxyl and coumarin based substances were selected as target analytes for detection of Coliforms and *E. coli*. 4-nitrophenol was selected for the detection of *St. aureus* as it is a known chromogenic reporter of Phospholipase activity specific for some pathogens including *St. aureus* (Berete et al. 1980, Sakiñç et al. 2007). These substances have never been investigated as electroactive indicators of mentioned bacteria and their specific enzymes. In order to study the electrochemical properties of 5,4-DDI cyclic voltammetry analyses (CV) of the mentioned substance were carried out initially on gold thereafter on carbon screen printed electrodes. Different potential ranges have been applied both to gold and carbon electrodes to fully understand the voltammetric behavior of mentioned substance and to obtain the well-optimized CV curves. In case of gold electrode, initial potential was selected within 50 mV and 1200 mV range (Fig.11 in Results). The difference of cathodic and anodic potentials ( $\Delta E_p$ ) was equal to  $\approx 400$  mV, which is almost 6 times the value inherent for reversible CV curves. The change of the potential range cause the negative and positive shifts of the



anodic and cathodic potentials (Fig. 11B in Results). The decrease of difference of anodic and cathodic potentials ( $\Delta E_p$ ) occurred, however it did not reach the ranges of reversible cyclic voltammogram. CV curve possessed quasi-reversible properties when the potential decreased from 1200 mV to 300 mV. The anodic potential (~200 mV) was equal to potential detected in previous curve, which could proof that the 5,4-DDI oxidized on gold electrode at  $E_{an}$  ~200 mV potential (Fig. 12A in Results).

The next step of optimization included the study of behavior of 5,4-DDI on carbon screen printed electrode (Fig 12B in Results). Negative shift of anodic and cathodic potentials occurred in case of carbon electrode. Although, gold electrodes have excellent electro catalytic ability and are very sensitive, however they show self-oxidation peak in low potential ranges. As the potential shifted to more negative values the usage of screen printed carbon electrodes became important due to their wide electrochemical window especially in the negative potentials. To confirm that the electrodic process is associated with oxidation of 5-4-DDI, in all 4 cases the different concentrations (ranging from 5 to 15  $\mu$ M) of 5-4-DDI were tested in the previously selected potential ranges, at 50 mV/s scan rate and in PBS solution containing only target analyte. All concentrations showed CV curves inherent for 5-4-DDI (Fig 13 in Results). Obtained results indicated that we could find several potential ranges where 5-4-DDI possess good quasi-reversible redox peaks and it could be base to continue with understanding the mechanisms laying behind the redox reaction of 5-4-DDI and to continue with enzyme substrate analyses taking the obtained curves as a positive control.

However, one more optimization step (third step) still had to be performed before moving on with next steps. The third step, which is one of the main issues for the analytical methods, especially during development of novel technique, is the optimization of the blank. Sanagi et al. (Sanagi et al. 2009) showed the importance of blank determination during estimation of limit of detection and limit of quantification of analytical methodology. Electrochemical behavior of the substrate 5-4-BCIG in PBS, without 5-4-DDI, was studied in the previously tested potential ranges at 50 mV/s scan rate, on gold and carbon electrodes, in order to see if the substrate produce any CV peak at the same potential as the target analyte (Fig14 in Results). The electrochemical activity of blank solutions on gold electrodes was detected, which could be explained by identity of structures of substrate and target analyte. The building molecule of both compounds (5-Bromo-4-chloro-1*H*-indol-3-yl  $\beta$ -D-glucopyranosiduronic acid and ( $\delta$ -2,2'-biindole)-3,3'-dione) is the indole ring. In comparison with colorimetric techniques, where device can detect only colored molecule of indigo molecule, which is dimerized form if two indoxyl molecules (enol isomer and keto isomer), the electrochemical high sensitive technique can detect signals produced by indole molecules (Belghiti et al. 2016). When tested in the range varying from 50 to 1200 mV on gold electrode at scan rate 50 mV/s the irreversible CV peak occurred at  $\sim$ 800 mV was inherent to oxidation of amino group of 5,4-DDI. The similar results were obtained by Castaño-Álvarez et al. (Castaño-Álvarez et al. 2004), where they could detect the irreversible oxidation peak of amino group of indigo carmine on gold disk electrodes. The detected redox peak also was produced by substrate 3-Indoxylphosphate. On

the carbon electrode 5-4-DDI produced reversible CV peaks one at  $E_{an} = +100$  mV and the second cathodic at  $E_{an} = -100$  mV, which could be explained by oxidation of hydroxy groups and correspond to process that involves two protons and two electrons. The 5-4-BCIG possessed the most stable behavior ( $I_{an}=0$ ,  $I_{cat}=-15$ ) at mentioned low potential range. Thus, the future experiments were continued with carbon screen printed electrodes at more negative potential ranges. The negative shift of anodic and cathodic potentials was noticed when applied potential decreased up to - 600 mV. The formed CV curve had a quasi-reversible ( $I_{an}/I_{cat} = 0.3$ ,  $\Delta E_p = 63$  mV) nature and blank solution did not produce any redox peaks (Fig. 15A,B in Results). Linear increase of anodic and cathodic peak currents with increasing concentrations of 5,4-DDI was noticed (Fig. 16A, B in Results). Such behavior is inherent for quasi-reversible electrochemical systems (Heinze 1981). Obtained good correlation ( $R^2 > 0.98$ ) proved that the anodic/cathodic currents, occurred and increased at the same and already defined potentials, were intrinsic to the redox reaction of 5-4-DDI.

The influence of scan rate on electrochemical behavior of released 5-4-DDI on carbon electrode was studied (Fig. 17 in Results). The scan rate of the experiment controls how fast the applied potential is scanned. Faster scan rates lead to a decrease in the size of the diffusion layer; as a consequence, higher currents are observed (Compton 2007). The scan rates ranging from 50 mV/s to 120 mV/s were tested. The shift of the oxidation and reduction peak potentials ( $E_p^{ox}/E_p^{red}$ ) to more positive and negative values respectively has been noticed with the increase of the scan rate. For a quasi-reversible system, the anodic peak is shifted to more positive

potentials and the cathodic peak to more negative potentials. The quasi-reversible CV parameters can be summarized as (i)  $E_p$  is dependent on scan rate, (ii)  $\Delta E_p$  depends on scan rate and increases with scan rate, (iii)  $I_p$  depends on square root of the scan rate in a non-linear way and (iv)  $I_p$  is linearly dependent on concentration (Elgrishi et al. 2018). The potential range varying from -600 mV to 400 mV, where the 5-4-DDI produced sharp and well defined quasi-reversible (based on preliminary data) redox peaks and the blank did not show any electrochemical activity, was selected as a target potential range for the reminder experiments with indoxyl based substances.

The second group of target analytes especially 7-hydroxy-4-methyl-coumarin or 4-methylumbelliferone undergone initial optimization procedures including detection of specific and most efficient potential range, optimization of the blank/substrate, and characterization of inherent CV curve. The optimization procedures were started with the detection of specific potential range for 4-MU. The carbon screen printed electrode was selected for the measurement of 4-MU redox activity. The electrochemical behavior of 4-MU on wide potential range starting from -600 mV to 800 mV was tested at 50 mV/s scan rate. In phosphate buffer (pH=7.4) the 4-MU produced the irreversible peak at ~700 mV anodic potential at the potential starting from 0 to 1000 mV (Fig. 18 in Results).

Based on the initial results the experiments continued with only positive potential ranges. Wu et al. (Wu et al. 2001) performed cyclic voltammetry of a 1 mM umbelliferone solution (pH 6.8). In their experiments the potential varied from 0.2 V to 1.2 V at a scan rate of 20 mV/s. They obtained that umbelliferone exhibits an irreversible

oxidation peak at  $\approx 700$  mV potential for the oxidation of the phenol. Irreversibility was indicated by the lack of any corresponding reduction peak on the reverse cycle. Similar results were obtained during CV studies of the other coumarins. Oxidation potential was referred to the coumarin structure. The oxidation of umbelliferone occurred due to oxidation of two hydroxyl groups on benzyl ring. The substitutions occurred on the pyran and benzyl rings, thus the pyran was hard to oxidize and benzyl ring had a lower oxidation potential. The 4-methyl substitution had little, if any, effect on the oxidation potential. The similar results were obtained by Carrazon et al. (Pingarron Carrazon et al. 1989). They showed that coumarin based substance umbelliferone produced voltammetric peaks at the potentials ranging from 616 mV to 840 mV on glassy carbon electrodes. The cyclic voltammetric behavior of 7-OH coumarin at the bare activated glassy carbon electrode also was studied by Dempsey et al. (Dempsey et al. 1993). They showed that the 7-OH-coumarin exhibited an irreversible anodic oxidation peak at  $E_{an} = 660$  mV in 0.1 M phosphate buffer (pH 7.4).

To confirm that the observed CV peaks correspond to oxidation of 4-MU different concentrations of the mentioned compound ranging from 1  $\mu$ M to 8  $\mu$ M were tested at carbon electrode at the 50 mV/s scan rate at the already applied potential range (0 to 1000 mV) (See Fig.19 in Results). The good linear relationship ( $R^2 > 0.98$ ) between anodic peaks and concentrations confirmed the nature of the irreversible CV signal. The CV experiments carried out at the potential range varied from 0 to 800 mV, 50 to 1200 mV and 0 to 1000 mV indicated that the anodic peak current occurred at the same potential  $E_{an} = \sim 700$  mV at

all 3 cases. Thus, the potential range could be shortened by reducing the end potential from 1000 to 800 mV and also it would reduce the electrochemical window (potential range where the target analyte is neither oxidized or reduced). However, because the developed system was interfering with bacterial metabolism where the pH of environment could vary from 7.5 to 5.5 the influence of pH on anodic peak potential is important factor to know. Wu et al. (Wu et al. 2001) have shown that anodic peak potential of 4-MU depends on pH values. They investigated pH behavior of the coumarins in 0.1 M PBS with pH range of 2 to 12. They found that at the target pH values (5.5 to 7.0) the anodic potential varied from 750 to 680 mV. The mentioned results were confirmed with another study conducted by Wang et al. (Wang et al. 2015). The effect of the solution's pH on the oxidation process of 4-MU was investigated in the range of 2.0–7.0. Peak potential shifted negatively in case of increase of pH.

Our experiments indicated that pH value of the system, due to reaction of b-d-glucuronidase of *E. coli* with 4-MUGLUC substrate, during 3 h dropped to 6.5, which corresponds to anodic potential equal to ~ 700 mV. Thus, the potential range varying from 0 to 800 mV considered optimal for the future experiments. The final optimization step included the study of electrochemical activity of the blank in the selected potential range (Fig. 19C, in Results). Based on the results obtained from all optimization steps, potential range varying from 0 to 800 mV was selected as a target potential range of 4-MU for the future experiments.

The initial optimization steps were also conducted for the third group of target analytes phenols particularly 4-nitrophenol. Detection of specific and most efficient potential range, optimization

of the blank/substrate, and characterization of inherent CV curve was performed. The carbon screen printed electrode was selected for the testing of electrochemical activity of 4-NP. To detect the redox peaks produced by 4-NP in phosphate buffer solution, pH=7.4, the CV scans at the potential starting from -400 mV to 1000 mV at 50 mV/s scan rate were performed (Fig. 20, in Results). Wang et al. (Wang et al. 2015) investigated the electrochemical behavior of 4-NP at glassy carbon electrode by cyclic voltammetry. They did not find any redox signals in PBS without 4-NP in the selected potential range. After 4-NP was added into PBS, an obvious oxidation peak was obtained at  $E_{an}=914$  mV. It was no any doubt that the oxidation peak should be attributed to the oxidation of 4-NP. In their experiments no corresponding reduction peak was observed in the following reverse scan, implying that the oxidation of 4-NP is a totally irreversible electrode process. The good linear relationship ( $R^2>0.98$ ) between increasing anodic peaks and concentration of 4-NP (Fig. 21 A,B, in Results) as well as production of CV peaks of the same shape and at the same anodic potential confirmed that the generated peaks were inherent to oxidation of 4-NP. The blank (4-NPP in PBS) did not show any electrochemical activity at the selected potential range, thus allowing us to select the optimized potential range (-400 to 1000 mV) for the future experiments based on 4-NP detection.

## **6.2 Detection of target analytes on graphene modified carbon electrodes**

The next step of the optimization process, which is the constitutive of whole procedure of development of the sensor

platform, was the increasing of the signals produced by target analytes at the already defined potential ranges. The graphene based materials were selected for the modification of the screen-printed carbon electrodes. The important features graphene and graphene based materials such as high mechanical strength, excellent electrical and thermal conductivities as well as other electrochemical properties (e.g. signal amplification) allows to use them as a construction material for high performance electrodes (Filip et al. 2015). In the current work, the graphene nanoplateletes were selected for the modification of screen-printed carbon electrodes. The modification of different types of electrodes by GNPs for the increasing the sensitivity, is relatively new procedure comparing to other graphene materials (e.g. graphene, graphene oxide). Several authors showed the advantages of graphene nanoplateletes and nanomaterials for electrochemical sensing (high sensitivity, reproducibility, and signals) over other materials (Ma et al. 2017, Wahyuni et al. 2018, Zou et al. 2018).

To our knowledge, GNPs were used for the fabrication of rapid bacterial detection platform in this work for the first time. All three groups of target analytes were tested on GNPs modified carbon screen printed electrodes. On graphene GNPs modified carbon electrodes 5,4-DDI, 4-MU and 4-NP showed significantly higher peak currents comparing to bare carbon SPEs (Fig. 22 in Results). For the confirmation of better electrochemical performance of GNPs modified SPE the pure electrochemical active substance 4-aminophenol was tested on both SPE and GNPs modified SPE electrodes. 4-AP showed higher current intensities comparing to bare carbon electrodes (Fig. 22D, in Results). These results confirm



the work of other authors who used another electrochemical active redox probe such as ferrocyanide and potassium ferricyanide. In the first work conducted by AlAqad et al. (AlAqad et al. 2018) showed the electrochemical properties of graphene-modified carbon-paste electrode by studying behavior of the ferrocyanide redox couple by cyclic voltammetry. The modified electrode showed voltammetric responses with a higher level of sensitivity and a lower background current compared to the carbon paste electrode. In the second work conducted by Ntsendwana et al. (Ntsendwana et al. 2012) cyclic voltammetry was used to study the electrochemical properties of the prepared graphene modified glassy carbon electrode using potassium ferricyanide as a redox probe. The prepared graphene modified glassy carbon electrode exhibited more facile electron kinetics and enhanced current of about 75% when compared to the unmodified glassy carbon electrode. The GNPs modified carbon electrode was selected for the future experimental steps.

## **6.3 Development of Gel-electrode system**

### **6.3.1 Gel characteristics**

A testing of the attachment efficiency of Coliforms to different types of gels, used for the construction of sensor platform, was performed. After a detailed review of the literature, the two gel forming substances, namely agar-agar and polyacrylamide were investigated in this study. Four different gel combinations (Gel-1, Gel-2, Gel-3 and Gel-4) with different nutrient compositions (see 4.5) were tested to obtain the most efficient bacterial attachment. After

series of optimization experiments, the optimal concentrations of substances were selected. In comparison with agar-agar polyacrylamide gel is a new substrate for the bacterial attachment and growth. Polyacrylamide hydrogels can be used as a new class of polymers for microbiological studies and good substrates for bacterial cell culture (Tuson et al. 2012). The gel containing polyacrylamide possessed significantly higher efficiency compared to the other three gels especially for lower concentrations of Coliforms (>80% for all selected inoculum levels  $P < 0.05$ ) (Fig. 23, in Results). Polyacrylamide hydrogel system possessed high mechanical strengths, excellent shape recoverability as well as good cell adhesion properties (Li et al. 2014). Thereafter, the polyacrylamide gel with optimized formula was applied to *Staphylococcus aureus* cells. In case of *St. aureus* the Gel-2 also possessed the best attachment properties in comparison with other formulas (72% only for lowest inoculum 4CFU/cm<sup>2</sup> and >80% for remaining inoculums). The efficiency of the developed Gel-2 is compatible with number of commercial touching based (usually contain agar material) environmental sampling systems. Commercial Rodac plates showed 76% and 54% efficiency of recovering of Gram-positive cocci and Gram-negative rods from surfaces respectively (Lemmen et al. 2001). In the other study the Rodac showed a 70% recovery rate for both Gram-positive and Gram-negative bacteria (Gouveia et al. 2015). Pinto et al. (Pinto et al. 2009) studied the recovery efficiency of the commercial contact plates. The efficiency of the tested commercial contact plates for 2.2 log<sub>10</sub>CFU (160 CFU) of *St. aureus* was about 58%, which is lower in comparison with the efficiency of the developed Gel-2 (72% for 2 log<sub>10</sub>CFU (100 CFU)). Another

type of commercial agar based sampling system known as a dispslide showed 20% recovery of total bacterial count from stainless steel surface at inoculum level equal to  $1 \log_{10}\text{CFU}/\text{cm}^2$  (Salo et al. 2000). In comparison, the Gel-2 showed >80% efficiency in case of  $1.6 \log_{10}\text{CFU}/\text{cm}^2$  inoculum level. The high recovery efficiency of the Gel-2 could be explained by inclusion of PAA (which possess efficient adhesive properties) in the gel and optimized formula of PAA, agar and other components, which increases adhesion properties of the mentioned gel and thus enhances its efficiency (Baït et al. 2012). Thus, developed Gel-2 could be an alternative for existing commercial systems and could be implemented for the construction of environmental sampling systems. To optimize the pH of the most efficient gel system (Gel-2), different pH values ranging from 6.0 to 8.0 were investigated. Optical signals in the gel, produced by specific enzymes of Coliforms and *St. aureus*, were tested.  $\beta$ -D-Galactosidase and Phospholipase C possessed the highest activities at neutral pH values (near 7.4). These results suggested that  $\beta$ -D-Galactosidase works better under neutral pH environments than to acidic pH. The similar results were obtained by Tomizawa et al. (Tomizawa et al. 2016). Results of another work showed that maximal Phospholipase C (isolated from *P. aeruginosa*) activity was recorded at pH varying from 7 to 8 (Elleboudy et al. 2014). The pH=7.4 was selected for all remaining experiments with  $\beta$ -D-Galactosidase (positive control) for Coliforms and Phospholipase C for *St. aureus*.

### **6.3.2 Electrochemical characteristics of gel–electrode system**

Every component of gel-electrode system was subjected to CV analysis to detect the electrochemical activity that can interfere with the electrochemical signal produced by the target analyte, enzyme or bacteria at the defined potential range. Electrochemical properties of all components of Gel-2 have been studied. The electrochemical activity of the gel components was compared with the redox signals produced by 4-MU. Among all components, only  $\text{KH}_2\text{PO}_4$  produced signals that could interfere with signal produced by target analyte (Fig. 27 A, in Results), especially when lower concentrations of bacteria should be detected. Thus, the concentrations of  $\text{KH}_2\text{PO}_4$  and  $\text{K}_2\text{HPO}_4$  decreased from 5 g/L to 2 g/L, which reduced the anodic current intensity. The electrochemical behavior of different combinations of gels (agar-agar, acrylamide, agarose) without any component has been tested at the previously optimized potential ranges. Based on obtained results the above mentioned combination (agar-agar + polyacrylamide) was selected for the future optimization steps. For the confirmation of the electrochemical stability and inactivity of the selected and optimized Gel-2 the electrochemical behavior of the mentioned gel was tested in the potential range varying from -600 to 400 mV and from 0 to 1000 mV inherent for the oxidation of 5,4-DDI and 4-MU respectively. In addition, the influence of the specific substrate on the behavior of the selected gels was studied. The three independent measurement of the agar/polyacrylamide gel on carbon electrodes showed that the agar-gel system produced stabile, reproducible and

electro-inactive CV curves in the both potential ranges. The substrates had no interfering effect on the electrochemical stability of the gel. The agar-polyacrylamide gel was selected for the fabrication of the graphene modified electrochemical system.

Two types of electrochemical systems, namely graphene/polyacrylamide-gel modified carbon (GR/PAAGC) and polyacrylamide-gel modified carbon electrodes (PAAGC) have been compared (Fig 29, in Results). The charge transfer properties of the tested GR/PAAG and PAAG coated SPEs systems were studied by using redox couples of  $\text{Fe}(\text{CN})_6^{3-/4-}$  as probes. Measurements were done at the scan rate of 50 mV/s by cyclic sweep between a potential of -400 mV and 400 mV. Well-defined, typical duck shape CV graphs were observed on gel-modified electrode system. The redox peak currents were larger at the GR/PAAG covered electrode compared with those of PAAG. This is due to the excellent electrical conductivity and high surface area of graphene/polyacrylamide gel modified carbon electrode. Combination of graphene with polyacrylamide is a promising approach to design novel generation of highly sensitive and conductive polymers (Tungkavet et al. 2015, Alam et al. 2016, Li et al. 2016, Alam et al. 2017). Due to the presence of carboxylic groups graphene-based materials provide high electroactive surface area to SPEs and was successfully used to construct various biosensors for enhancing the electrochemical signals (Wang et al. 2015, Cheng et al. 2017, Jaiswal et al. 2017, Zhang et al. 2017). The CV measurements of the GR/PAAGC gel modified system were performed without redox active compounds to assess the electrochemical behavior of the developed gel on the carbon electrodes. The obtained results showed that without active

redox substances the GR/PAAGC gel did not show any electrochemical activity. Based on obtained results, GR/PAA-gel system was selected for the future analyses.

The electrochemical behavior of all target analytes (6-DI, 4-MU and 4NP) on the GR/PAA-gel system was tested. The CV measurements of 6-DI was conducted at the same potential range as 5,4-DDI. In the tested potential range, two processes have been detected. The first one is reversible with anodic and correspondence cathodic peak. The other process, which occurred, had an irreversible nature. The electrochemical behavior of indigo on electrode can be explained by two processes (Božič et al. 2009). The first electrodic process corresponds to the oxidation of the conjugated enol groups of the leuco-indigo to yield indigo. The second electrodic process involves the oxidation of indigo through the -NH groups of the indol structures to yield dehydro-indigo. The similar electrochemical behavior (two separate electrodic processes) of indigo and indigogenic substrates has been studied by several authors (Govaert et al. 1999, Komorsky-Lovrić 2000, Arvand et al. 2017, Manjunatha 2018).

The influence of the scan rate on the electrochemical behavior of released 6-DI on GR/PAAGC electrode was studied. Several parameters (the difference of cathodic and anodic potentials ( $\Delta E_p = 57-59$  mV), the ratio of cathodic and anodic peak currents ( $I_p^{\text{red}}/I_p^{\text{ox}} = 1$ ), good linearity between scan rates and peak currents ( $R^2 > 0.95$ )) determine the reversible nature of the CV curve (Elgrishi et al. 2018). Analysis of the CV voltammogram, generated by the redox reaction of 6-DI on GR/PAA –gel modified carbon electrode, showed that the mentioned CV curve possessed

reversible behavior ( $\Delta E_p = 60$  mV;  $I_p^{\text{red}}/I_p^{\text{ox}} = 0.98$ ;  $R^2 \geq 0.98$ ). Reversible CV peaks at the similar potential ranges was recorded (Fernández-Sánchez et al. 2000, Bengoechea Álvarez et al. 2002). Although, the anodic and cathodic peak currents were linearly proportional to scan rates a very slight shift of the reduction peak potential to more positive values were noticed with the increase of the scan rate. The CV measurements of 4-MU were conducted at the previously optimized range varying from 0 to 800 mV. The GR/PAAGC electrode increased the signal intensity of the generated peak. The obtained results correspond to the studies conducted by Wang et al. (Wang et al. 2015). They measured the electrochemical behavior of 4-MU at different electrodes. At the bare glassy carbon electrode, a small anodic peak was observed. The significantly higher peak current was observed when the graphene modified glassy carbon electrode was used.

In the present work the influence of the scan rate on the electrochemical behavior of 4-MU on GR/PAAGC was studied. The anodic peak currents were linearly proportional to scan rates as well as their square root. The results indicated that the electrode process was controlled by both diffusion and adsorption. The oxidation peak potential was also dependent on the scan rate and slightly shifted positively with the increase of scan rate. A good linear relationship ( $R^2=0.99$ ) between  $E_{pa}$  and scan rate was obtained. The electrochemical behavior of 4-NP on GR/PAAGC electrode was studied in the previously optimized potential range varying from -400 to 1000 mV. The intensity of peak current produced by 4-NP on GR/PAAGC was significantly higher ( $p<0.005$ ) in comparison with bare carbon electrode. Similar results were obtained by Wang et al.

(Wang et al. 2015). They found that the graphene modified glassy carbon electrode exhibited enhanced electrocatalytic activity toward the 4-NP reduction when compared to the bare glassy carbon electrode. The electrochemical behavior of 4-NP on GR/PAAGC system at different scan rates was studied. The results indicated that the electrode process was controlled by both diffusion and adsorption.

#### **6.4 Detection of bacteria using developed GR/PAAGC electrode system in culture**

In this section, the results of optimization of GR/PAAGC electrode system for the detection of indicator and pathogenic bacteria in culture conditions were described. The experiments on the optimization of GR/PAAGC electrode system for detection of the mentioned target bacterial groups was performed initially on Coliforms and then the already optimized and ready platform was applied to detect and quantify other bacterial species. The detection of Coliforms was based on the indirect electrochemical sensing of  $\beta$ -Galactosidase activity. The redox signals, produced due to  $\beta$ -Galactosidase activity of the pure enzyme on the developed GR/PAAGC electrode used as a positive control for the further experiments with Coliforms. The commercially available chromogenic 6-CIGP substrate, known as rose-Gal, was used in commercial media as well as in rapid chromogenic kits for the optical detection of  $\beta$ -D-Galactosidase activity for many years. During catalytic hydrolysis of 6-Chlor-3-indoxyl- $\beta$ -D-Galactopyranoside the 6-chloro-3-Indoxyl is formed. The latest is converted to 6,6'-Dichloro-



Indigo (6-DI), which stains the bacterial colony or media with rose color. To our knowledge, the electrochemical detection of CIPG has never been reported in the literature. Thus, the electrochemical features of 6-CIPG and 6-chloro-3-Indoxyl was first investigated in this section. For that purpose, the CV measurements of the substrate and reaction product were performed. The reaction of 0.1 mg/ml  $\beta$ -Galactosidase with 0.5 mg/ml 6-CIPG was studied in PBS (pH 7.4). The electrochemical measurements were done in the potential range varying from -400 to 800 mV, where the redox signals specific for the oxidation of 6-DI was previously detected. In order to investigate the observed phenomena, obtain information about redox system as well as the nature of the detected irreversible voltammetric signal the CV measurements of the  $\beta$ -D-Galactosidase /6-CIPG reaction mixture were done every 5 minutes. Obtained results together with the results of measurements of blank GR/PAAGC system confirmed that the produced CV peaks were inherent to  $\beta$ -D-Galactosidase /6-CIPG reaction. The formation of ultrafast irreversible electrochemical < 2 minutes signal could be explained by the  $\beta$ -Galactosidase /6-CIPG reaction mechanism. The mentioned reaction consists from two steps: formation of 6-chloro-3-indoxyl due to  $\beta$ -Galactosidase and 6-CIPG reaction and the second the formation of 6-DI due to oxidation of 6-chloro-3-Indoxyl (Figure 67). The 6-chloro-3-indoxyl in colorless product, which after oxidation is transformed to color product 6-DI. The redox peak formed at ~50 mV potential was inherent to 6-chloro-3-indoxyl.

Obtained results showed that the initial product of  $\beta$ -Galactosidase/6-CIPG reaction possessed electrochemical activity and the signal can be detected much earlier (<2 minutes) than optical one. Thus,

obtained electrochemical signal could be used for more rapid detection  $\beta$ -Galactosidase activity and subsequently of Coliform bacteria in comparison with optical signals at the same reaction conditions. The next measurement was carried out using the same potential range, varying from 600 mV to 400 mV, used for oxidation of 6-DI. The potentials, and shapes of the peaks produced due to enzymes substrate reaction was similar to the peaks formed during oxidation of pure 6-DI on GR/PAAGC system.

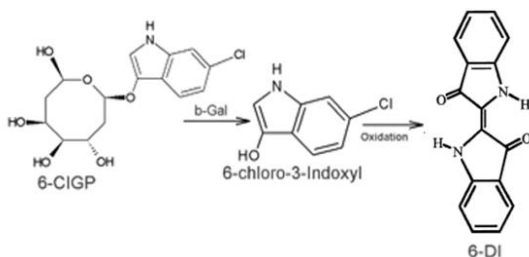


**Figure 67 Mechanism of formation of 6-DI due to reaction of  $\beta$ -D-Galactosidase with 6-CIPG.**

The depletion 6-Chlor-3-indoxyl and formation of 6-DI consists of two stages. At the first step the formation of 6,6'-Dichloro-Indigo white (6-DI) or leuco-indigo (colorless) takes place, which later on oxidizes to 6,6'-Dichloro-Indigo that has specific rose color. The possible reaction mechanism, which generates the specific redox peaks, on GR/PAA-gel modified carbon electrode is shown in Figure 68. The second anodic peak was formed due to redox reaction between 6-DI and Dehydro-6-DI. Thus, the formation of the second colorless product leuco-indigo, which possessed redox activity was observed, before formation of color product, which also had electrochemical activity. Obtained results are clearly indicating that the formation of

quasi-reversible and irreversible redox peaks is due to enzyme reaction initiated by addition of  $\beta$ -Galactosidase. To confirm that the produced CV peaks corresponds to  $\beta$ -Galactosidase activity the different concentrations of mentioned enzyme was tested on the GR/PAAGC system. All studied concentrations exhibited similar electrochemical behavior with redox peaks corresponding to the 6-DI. The  $\beta$ -Galactosidase activity on GR/PAAGC sensor was studied during different periods. The increase of the anodic peak currents was noticed with the increasing reaction time. The obtained results confirmed that the two anodic and one cathodic peaks were inherent for the  $\beta$ -Galactosidase reaction.

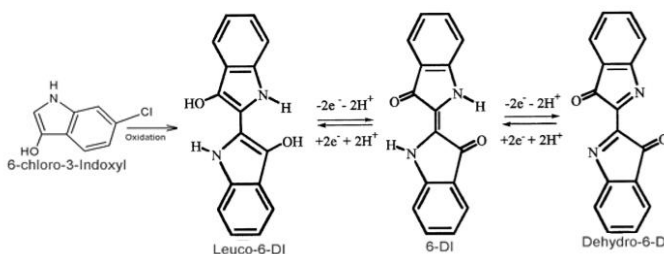


**Figure 68 Mechanism of formation of 6-DI, and leuco- as well dehydro-forms of 6-DI.**

The result also showed that electrochemical approach could be a good alternative to optical methods for detection of  $\beta$ -Galactosidase enzyme activity. In recent years simple, sensitive and rapid electrochemical methods for detection of bacterial  $\beta$ -Galactosidase and the their advantages over optical analogues were shown by Chen et al. and Manibalan et al. (Chen et al. 2015, Manibalan et al. 2015). Three specific peaks ( $I_{pa}^1$ ,  $I_{pa}^2$  and  $I_{pc}$ ), produced both by target analyte and  $\beta$ -Galactosidase enzyme (positive controls), were chosen as analytical response for detection of *Coliforms* in the future

experiments. Since, the proposed approach bases on single step detection of Coliform bacteria, the all components, including accelerators were incorporated in the gel-electrode system. The designed GR/PAA-gel modified carbon electrode sensor was used for detection and quantification of Coliform bacteria grown in culture media. The initial measurement of voltammetric signal was performed with only  $7.1 \log_{10}$ CFU/ml suspension. To confirm the formation of electrochemical signal, produced by initial product 6-chloro-3-Indoxyl, formed due to reaction of  $\beta$  -Galactosidase and 6-CIGP, and redox peaks were observed at the potential range varying from -400 mV to 800 mV. However, already after 5 minutes of incubation the decrease of the electrochemical signal occurred, which could be explained by depletion of the 6-chloro-3-Indoxyl. Although, the observed electrochemical signal produced by the intermediate product 6-chloro-3-Indoxyl had rapid and sensitive nature, the lack of stability and high disappearance rate would create difficulties in detection of Coliforms in real samples. The future optimization steps as well as detailed investigation of electrochemical properties of the 6-chloro-3-Indoxyl by other electrochemical techniques are required. In comparison with the signal produced by 6-chloro-3-Indoxyl the CV peaks formed due to oxidation of leuco-indigo and 6-DI possessed good stability. The stability of GR/PAAGC sensor, inoculated with Coliforms, was investigated by drying the GR/PAA gel. The completely dried gel did not show any specific redox peak. However, after rehydration the redox peaks inherent for the 6-DI were recovered. For biosensors, many factors must be taken into account for developing novel interface materials. Two main requisites for electrode materials are

to present high conductivity and the long-term stability (Li et al. 2015).

The incubation temperature of Coliform bacteria did not influence on electrochemical behavior of GR/PAAGC sensor. No peak occurred during incubation of GR/PAAGC sensor without Coliform bacteria. The series of CV measurements of the blank (GR/PAAGC sensor containing 6-CIGP substrate) was performed, in order to detect any electrochemical signal produced by blank that can interfere with the redox peaks produced by the sample. Five independent measurements of the blank confirmed the redox inactivity and stability of GR/PAAGC sensor without sample. Graphene-based materials exhibit lower noise and thus can be used for development of biosensors for sensitive assays (Yang et al. 2010). The optimization of the blank was also important step for the quantitative detection of Coliforms in the future, especially when the calculation of the sensitivity and limit of the detection was performed. The formation process of the redox peaks produced by Coliforms on GR/PAAGC sensor was investigated during 60 minutes. The formation of redox peaks corresponded to oxidation of leuco-6-DI started already after 15 minutes of incubation however the distinguishable anodic and cathodic peaks occurred at the 45 minutes of incubation and the complete reversible redox curve was observed at the 60 minute of incubation. After 60 minutes of incubation the formation of the second anodic peak at the potential  $E_{an} = 231$  mV with the anodic peak current equal to 1305  $\mu$ A occurred in parallel with formation of red color specific for the oxidation of 6-DI. Thus, the electrochemical signal produced by Coliforms on the GR/PAAGC sensor was detected much earlier in comparison with

the optical signal. Among sensors, enzyme-based electrochemical sensors provide high, steady, and reproducible signal amplification (Chen et al. 2015).

Developed GR/PAAGC sensor platform, detected 2.1 log<sub>10</sub>CFU/mL ( $\approx$  100 CFU/mL, 6 CFU) Coliform suspension during 3 h of incubation. However, the specific cathodic signals were already detected after 20 to 30 min of incubation. Mittelmann et al. (Mittelmann et al. 2002) developed amperometric enzyme biosensor based on the electrochemical detection of  $\beta$ -D-Galactosidase activity, using *p*-amino-phenyl- $\beta$ -d-galactopyranoside as substrate, for determining the density of Coliforms, represented by *Escherichia coli* and *Klebsiella pneumoniae*. They could detect 1000 CFU/mL within 60–75 min. In another study the detection of 100 CFU/mL of *E. coli* cells was achieved after 7h of enrichment. They used 4-aminophenyl- $\beta$ -galactopyranoside as an electrochemical substrate (Wang et al. 2017).

The influence of the substrate 6-CIPG concentration on the current intensities of redox signals produced by Coliform bacteria in GR/PAAGC sensor was studied. Significant difference ( $p < 0.05$ ) between anodic peak currents produced by 0.5mg/mL and 5mg/mL of 6-CIPG was noticed. Thus, 5mg/mL 6-CIPG was used for the future optimization steps of the developed sensor for the detection of low concentration of Coliforms. The change of pH of the gel system during  $\beta$ -D-Galactosidase activity of Coliform suspension as well as the influence of the changing pH on peaks has been monitored. The decrease of pH value from 7.4 to 5.5 due to  $\beta$ -Galactosidase activity of Coliform bacteria caused a positive shift of anodic and cathodic

potentials ( $E_{pa}$  and  $E_{pc}$ ) as well as the increase of the anodic and cathodic currents ( $I_{pa}$  and  $I_{pc}$ ).

The influence of the metabolic activity of total Coliforms on the electrochemical signal was investigated. The results clearly indicated that the redox peaks were formed by 6-DI produced during specific reaction of  $\beta$ -Galactosidase with 6-CIGP. Thus, other metabolites of Coliform bacteria did not influence on and interfere with the target redox peaks. The influence of the microbiota, found typically in food processing, on the voltammetric signals was also studied. These results confirmed that the reversible redox peaks occurred at determined potential range inherent only for 6-DI produced by reaction of  $\beta$ -Galactosidase of Coliform bacteria with the specific 6-CIGP substrate. Investigation of influence of bacterial flora, prevalent for concrete environment, on electrochemical signal is an important step for the development of novel sensors for specific bacterial groups. Obtained results correspond to the work conducted by Shoaie et al. (Shoaie et al. 2018). They found that other prevalent uropathogenic bacteria did not produce remarkable CV response. Thus, confirming the high specificity of developed biosensor. The specificity of the developed sensor was also studied in another work conducted by Wang et al. (Wang et al. 2017). The results demonstrated that only samples containing *E. coli* resulted in a significant signal. The electrochemical signal obtained for other bacteria had no significant difference with the control (no bacteria). In our study the effect of ferrocene redox couple ( $Fc/Fc^+$ ) on redox peak current intensities and oxidation rate was investigated. No influence on oxidation rate or redox peak height was detected.

Gram-positive bacteria particularly lactic acid bacteria should be strongly considered during development of enzyme/ $\beta$ -D-Galactosidase – based rapid methods and sensors for the detection of Coliforms/*E.coli* especially at food environments. The first important feature of lactic acid bacteria is the production of  $\beta$ -D-Galactosidase enzyme. Some genera of gram-positive bacteria especially lactic acid bacteria are able to produce  $\beta$ -Galactosidase enzyme. Gheyntanchi et al. (Gheyntanchi et al. 2010) and Sangwan et al. (Sangwan et al. 2015) showed the production of  $\beta$ -Galactosidase by *Lactobacillus spp.* (incl. *L. acidophilus*) and *Streptococcus thermophilus*. Devi et al. (Devi et al. 2011) reported the method of studying the  $\beta$ -Galactosidase production by *Lactobacillus spp.* using indoxyl based 5-bromo-4-chloro-3-indolyl-b-D-galactopyranoside substrate. Galat et al. (Galat et al. 2016) developed a novel method using chromogenic agar media (containing indoxyl based substrates) to enumerate lactic acid bacteria from a complex milk mixture. The second not less important factor is the prevalence lactic acid bacteria in food processing factories, especially in dairy, wine and meat industries. For dairy and meat industries, they are used as a starter cultures but also can act as a causative agent of food spoilage. *Lactobacillus spp.* are one of the extensively used genera to ferment various sausage types (Foschino 2009). Lactic acid bacteria actively involved in the spoilage of processed meats (Kalschne et al. 2015). They can be present on the equipment and food contact surfaces of the fermentation area and spread to the other processing sectors via cross contamination. Thus, distinguishing between lactic acid bacteria and Coliform bacteria will allow to avoid false-positive results. As the Coliforms are Gram-negative bacteria, the Gram



differentiation principle was considered the most suitable method to use. Enzyme based Gram differentiation technique incorporated directly to the gel-electrode system was used to detect Gram-negative reaction of the tested Coliforms. The identification of specific types of aminopeptidase activity in microorganisms has proved useful in diagnostic microbiology (Cellier et al. 2014). L-alanine aminopeptidase was selected as a target enzyme. L-Alanine aminopeptidase activity can differentiate between Gram-negative and Gram-positive bacteria (Orenga et al. 2009). This enzyme is ubiquitous in Gram-negative microorganisms whereas, in contrast, it is generally absent from most Gram-positive microorganisms. There are a diverse range of chromogenic aminopeptidase substrates. In these substrates, hydrolysis of the amide bond by an appropriate aminopeptidase enzyme liberates the corresponding colored amine. L-Alanyl-p-nitroanilide 1 (AA = L-alanyl) liberates yellow p-nitroaniline in the presence of Gram-negative microorganisms (Cellier et al. 2014). Comparing to colorimetric properties of L-Alanine aminopeptidase/ L-Alanyl-p-nitroanilide reaction the electrochemical behavior of the mentioned reaction has never been studied.

The results of the current work showed that the p-nitroaniline, which was formed due to reaction of Coliforms with L-Alanyl-p-nitroanilide in graphene modified gel-electrode system, produced reduction peak at  $E_{cat} = -113$  mV, in the potential range varying from -800 mV to 400 mV, at 50 mV/s scan rate during 3h of incubation at 37 °C. Different studies showed similar results of reduction of p-nitroaniline on modified electrodes. In most cases the p-nitroaniline produce irreversible reduction peak at the negative potentials (Rachida 2014). Another works conducted by Zhao et al. and Laghrib et al. (Zhao et

al. 2007, Laghrib et al. 2017, Laghrib et al. 2018) indicated that 4-nitroaniline exhibited irreversible reduction responses at - 200 mV, - 260 mV and -750 mV at silver and gel modified carbon-paste electrodes respectively. They found that the peak potential shifted in negative direction when the scan rate increases, meaning that the electrochemical reaction is irreversible. The total number of electrons transferred during reduction of 4-NA was equal to 4.

According to results of current work *Lactobacillus acidophilus* DSM 20079 did not produce any redox peak at the tested potential in the gel-electrode system during 3h of incubation due to the lack of p-nitroaniline in the system, which clearly indicated that *Lactobacillus spp.* did not possess L-Alanine aminopeptidase activity. The obtained results have shown that for the robust detection of Coliforms with the enzyme (especially  $\beta$ -Galactosidase) based methods, only  $\beta$ -D-Galactosidase activity based measurements is not enough due to present other  $\beta$ -D-Galactosidase positive bacteria that could produce some electrochemical as well as optical signals giving false-positive results. Thus, inclusion of the second enzyme (in this case aminopeptidase) in the system would increase the specificity and robustness of the developed method. This is critical especially for the rapid electrochemical and/or optical methods/sensors designed for detection, quantification and distinguishing the Coliforms in food processing environment, where there is a lack of standard confirmation methodology.

## 6.5 Detection of other bacteria with GR/PAAGC sensor platform in culture

The developed and optimized GR/PAAGC sensor platform was applied for the detection of *E. coli* and *St. aureus*. The detection of *E. coli* was based on electrochemical detection of 5,4-DDI and 4-MU formed during chromogenic and fluorogenic reaction of b-d-glucuronidase with 5,4-BCIPG and 4-MUG substrates respectively. The electrochemical behavior of both target analytes was studied and described in details in the previous sections. After 3 h of incubation the CV peaks inherent for redox reaction of 5,4-DDI were formed. Developed GR/PAAGC sensor platform could detect the *E. coli* cells already after 20 min of incubation. However, in case of *E. coli* the 4MUG was selected as the target substrate, which would allow the electro-fluorogenic detection of 4MU by developed sensor. The CV measurements were carried out at the already defined potential range varying from 0 mV to 800 mV. The irreversible CV peak at the anodic potential equal to 720 mV (typical for oxidation of 4MU) produced by  $7.8 \log_{10}\text{CFU/mL}$  *E. coli* in the GR/PAAGC sensor platform at 44 °C within 3 h of incubation. The CV curves produced by *E. coli* correspond to signals produced by the b-d-glucuronidase enzyme (used as a positive control) with the shape and potential of the peaks.

Developed platform could detect low numbers of *E. coli* in culture  $\sim 1.7 \log_{10}\text{CFU/mL}$  (60 CFU/mL, 3 CFU) within 3h of incubation. Developed platform possessed higher sensitivity comparing to other electrochemical sensors for detection of *E. coli*. For example, Rochelet et al. (Rochelet et al. 2015) could detect  $4 \log_{10}\text{CFU/mL}$  *E.*

*coli* in culture during 3 h by indirect amperometric quantification of the  $\beta$ -D-Glucuronidase activity using *p*-aminophenyl- $\beta$ -D-glucopyranoside electrochemical substrate. Ettenauer et al. (Ettenauer et al. 2016) showed the detection of 1 CFU/ml of *E. coli* within 10h based on detection of  $\beta$ -D-Glucuronidase activity using 8-hydroxyquinoline-glucuronide electrochemical substrate.

The developed sensor platform was also applied for the detection of *St. aureus* cultures. The detection principle was based on electrochemical behavior of 4-NP produced due to reaction Phospholipase C and 4-NPP substrate. The electrochemical behavior of 4-NP was studied and described in details in the previous section. The shape and potential of the peak were conform to the peak potential and shape produced by Phospholipase C enzyme, which was selected as a positive control. The developed sensor platform was successfully applied also for detection of low numbers of *St. aureus*  $2.6 \log_{10}$ CFU/mL (400 CFU/mL, 20 CFU) within 3 h. The principle of detection of *St. aureus* cells was based on the detection of activity of Phospholipase C (PLC). A variety of pathogenic bacteria produces Phospholipase C (Titball 1993). The PLCs are responsible for the pathogeneses and toxin production of well-known pathogenic bacteria such *St. aureus*, *Clostridium perfringens*, *Listeria monocytogenes*, *Bacillus cereus* and *Pseudomonas aeruginosa* (Songer 1997). There was no any study on PLC -based voltammetric detection of pathogenic bacteria (including *St. aureus*) using 4-NPP substrate.

## 6.6 Detection of bacteria on stainless steel surfaces

The applicability of designed GR/PAAGC sensor to detect Coliform bacteria on stainless steel surfaces was studied. The specific reversible redox peaks were detected at the determined potential ranges. Both cathodic and anodic peaks exhibited good sensitivity. The same experiment was performed with shorter incubation times. Two set of concentrations ranging from 3  $\log_{10}\text{CFU}/\text{cm}^2$  to 7  $\log_{10}\text{CFU}/\text{cm}^2$  and from 2  $\log_{10}\text{CFU}/\text{cm}^2$  to 6  $\log_{10}\text{CFU}/\text{cm}^2$  were selected. After 30 minutes of incubation only cathodic peaks inherent for 6-DI were detected. In both cases, the cathodic current intensities increased with the increasing concentrations of Coliforms. However, the slight negative and positive shift of peak potentials produced by different bacterial concentrations was noticed. This can be explained by the not stable pH of the system at the early stages of incubation. Overall, at 30 minutes of incubation the cathodic peaks occurred at more negative potentials comparing to peaks formed at the 3h of incubation. Although the absence of anodic peaks at the 30 minutes of incubation, formation of clearly distinguishable and sharp cathodic peaks reflected the bacterial activity. The detection of Coliforms bacteria on stainless steel surfaces was performed with higher substrate concentration (5 mg/mL). The formation of anodic peak currents was occurred. This correspond to the results obtained during substrate optimization experiments. The formation of anodic peak can be explained by increased substrate concentration, which accelerates the  $\beta$ -d-Galactosidase activity and thus increasing the redox reaction rate between leuco-6-DI and 6-DI. The limit of

detection of the Coliform bacteria on stainless steel surfaces during 30 minutes of incubation time for the proposed sensor was  $0.5 \log_{10}\text{CFU}/\text{cm}^2$ , which is equal to  $\sim 3 \text{ CFU}/\text{cm}^2$ . The developed gel-electrode platform with increased substrate concentration could produce both oxidation and reduction signals even when small numbers of Coliforms on stainless steel surfaces were tested. For comparison, the commercially available enzyme based bioluminogenic detection device (MicroSnap™) intended also for food contact surfaces could detect  $\sim 2 \log_{10}\text{CFU}$  Coliforms during 8h of incubation (Meighan 2014).

The applicability of designed GR/PAA-gel carbon sensor to detect Coliform bacteria on stainless steel surfaces in simulated meat processing conditions was studied. Three processing scenarios were simulated including (i) heavy-soiled conditions of a food contact surfaces (excess of organic matter) that was not subjected to clean for long time, (ii) cleaned and dried food contact surfaces and (iii) food contact surfaces used for whole working shift. The obtained results showed that the high quantity of organic matter present on food contact surfaces for more than 48 hours did not hamper the voltammetric signal inherent for  $\beta$ -d-Galactosidase activity of Coliforms. The second scenario covered the detection of the Coliforms on washed and disinfected food contact surfaces during working period. The obtained results were confirmed by the classical swabbing methodology. The good correlation was noticed between numbers of Coliforms at different stages of processing detected by classical swabbing method and developed GR/PAA-gel carbon sensor.

To simulate the working conditions in food processing industry the re-soiling cycles (with meat juice) at every 1.5 hour were performed. The growth of Coliform bacteria on stainless steel soiled surfaces during 8 hours was studied. The increase of current values after each hour is noticed. Considering obtained results on no influence of soiling on current intensity produced by Coliforms, it could be proposed that the increase of current was due to increase of bacterial number on stainless steel surface during 8-hour period. To confirm this, the sampling of stainless steel surfaces with traditional agar touching method was performed during selected time frame. Concentration of Coliform bacteria determined by proposed method was nearly the same comparing with the cultural methods. However, a small difference was noticed between both methods. Similar results were obtained during testing the electrochemical sensor for detection of *E. coli* in water samples (Rochelet et al. 2015). They detected higher numbers of *E. coli* cells in water by electrochemical sensor compared to classical methods. The designed sensor was applied for the rapid detection of *E. coli* on stainless steel surfaces. The peak currents, produced by *E. coli* on developed gel-electrode system, containing indoxyl based b-d-glucuronidase substrate, within 30 minutes of incubation at 44°C, occurred at the already defined potential, typical for short incubation times. The limit of detection of *E. coli* cells with the designed sensor was equal to 0.5 log<sub>10</sub>CFU/cm<sup>2</sup>, which is equal to ≈ 3 CFU/cm<sup>2</sup>. There are number of hygiene monitoring commercial kits available to the food industry. For example, ATP bioluminescence can provide a rapid estimate of total surface contamination, however, ATP bioluminescence can only differentiate between bacterial and soil ATP if non-bacterial ATP is

removed enzymatically before the assay (Vanne et al. 1996), also there is no indication of the types of organisms present. Additionally, previous studies have suggested that, in the absence of soil, ATP bioluminescence is unable to detect the presence of low numbers of bacteria on a surface ( $<10^3$  cfu/cm<sup>2</sup> (3 log<sub>10</sub>CFU/cm<sup>2</sup>)) and protein detection methods are incapable of detecting even very high levels of microbial contamination (Moore et al. 2001).

In contrary, the developed sensor platform could distinguish the signals produced by 1.7 log<sub>10</sub>CFU/cm<sup>2</sup> (50 CFU/cm<sup>2</sup>) Coliforms in heavy soiled conditions as well as detect low numbers of Coliforms (1.9 log<sub>10</sub>CFU/cm<sup>2</sup> (80 CFU/cm<sup>2</sup>)) on cleaned (absence of the soil), disinfected and dry surfaces. Moore et al. 2002 et al. (Moore et al. 2002) compared several available kits for detecting of *E. coli* on dry stainless steel surfaces. Coliform petrifilm, sampling sponge, dipslides, ColiformSwab-Check, ColiformPath-Check and ColiTrace could detect 5.5 log<sub>10</sub>CFU/cm<sup>2</sup> ( $3 \times 10^5$  CFU/cm<sup>2</sup>), 6 log<sub>10</sub>CFU/cm<sup>2</sup> ( $10^6$  CFU/cm<sup>2</sup>), 2.5 log<sub>10</sub>CFU/cm<sup>2</sup> ( $2 \times 10^2$  CFU/cm<sup>2</sup>), 3.8 log<sub>10</sub>CFU/cm<sup>2</sup> ( $7 \times 10^3$  CFU/cm<sup>2</sup>), 3 log<sub>10</sub>CFU/cm<sup>2</sup> ( $10^3$  CFU/cm<sup>2</sup>) and 4 log<sub>10</sub>CFU/cm<sup>2</sup> ( $10^4$  CFU/cm<sup>2</sup>) of *E. coli* cells after 24, 48, 18 and 6 hours respectively. In comparison, the developed sensor chips could detect 0.6 log<sub>10</sub>CFU/cm<sup>2</sup> (4CFU/cm<sup>2</sup>) and 1.2 log<sub>10</sub>CFU/cm<sup>2</sup> (16 CFU/cm<sup>2</sup>) *E. coli* cells within 30 minutes with 5,4-CIPG and 4-MUG substrates respectively. Considering the obtained results the developed sensor platform could compete with commercial hygienic systems and could be used in food processing factories for detection of Coliforms and *E.coli* at different processing conditions as well as for assessing the cleanliness and effectiveness of sanitizing programs. The detection and enumeration of indicator



organisms is widely used to assess the efficiency of sanitation programs (Ingham et al.2000, Exum et al. 2017). Detection of *E. coli* cells on stainless steel surfaces using developed sensor platform with coumarin based 4-MUG substrate was also performed. The anodic currents occurred at the already defined potential which was correspond to the obtained results on detection of *E. coli* in cultures with 4MUG substrate. The limit of detection of *E. coli* cells with the designed sensor was equal to  $1\log_{10}\text{CFU}/\text{cm}^2$ , which is equal to  $\approx 10\text{CFU}/\text{cm}^2$ . The designed sensor platform was applied also for rapid detection of *St. aureus* on stainless steel surfaces. Within 30 minutes, the limit of detection of *St. aureus* cells with the designed sensor was equal to  $1.5\log_{10}\text{CFU}/\text{cm}^2$ , which is equal to  $\approx 32\text{CFU}/\text{cm}^2$ . The anodic signals formed at the potential  $E_{\text{an}} = \sim 1080\text{ mV}$ , which is correspond to the results obtained by Pavitt et al. (Pavitt et al. 2017) on oxidation of 4-Nitrophenol. However, in current work, the positive shift of the anodic potential from was occurred in comparison with detection of *St. aureus* in culture within 3h of incubation. The shift of anodic potential from  $\sim 880\text{ mV}$  to  $\sim 1080\text{ mV}$  was due to reduction of incubation time from 3h to 30min respectively. This hypothesis was confirmed by testing the electrochemical signal produced by *St. aureus* sampled from stainless steel surface, within 3h of incubation. The anodic peak current was occurred at the  $E_{\text{an}} = \sim 900\text{ mV}$ , similar to anodic potential of pure 4-NP, reaction of Phospholipase C and 4-nitrophenylphosphocholine substrate and *St. aureus* in the culture. The positive shift of the anodic potential within the short detection times could be explained by the change of the pH of the system. After 30 minutes of incubation the pH of the gel electrode system

was around 7.2, however after 3h of incubation it decreased up to 6.0 (Fig. 53B). Thus, the oxidation potential increased with decreasing pH. This finding corresponds to the study conducted by Arvinte et al. (Arvinte et al. 2011). They obtained that oxidation peak potential of 4-NP is shifted to positive potential with increasing pH value.

## **6.7 Colorimetric properties of the gel system**

The optical signals produced by  $\beta$ -D-Galactosidase activity have been investigated. The initial experiments were performed with pure  $\beta$ -D-Galactosidase enzyme. The red colored 6-DI was formed due to reaction of  $\beta$ -D-Galactosidase with the 6-CIPG substrate. For the spectrophotometrical analyses the exact wavelength, where the absorbance reached the maximum values, was optimized. The formation of rose color as well as the production of optical signal at already optimized wavelength have been examined during 30 minute period. To optimize the pH of the PAA gel-system, different pH values ranging from 6.0 to 8.0 have been investigated. The absorbance curve as well as the color intensity reached their maximums at mentioned pH value, which was selected for the future experiments. The optical signals produced by b-d-glucuronidase (the target enzymes for the *E. coli*) on the already optimized gel systems was also investigated using 5,4-BCIGP and 4-MUG substrates for colorimetric and fluorometric signals respectively. The fluorogenic properties of the PAA gel were studied. The reaction of b-d-glucuronidase and 4-MUG substrate in the gel was studied during 1h period. The developed PAA gel showed good optical properties. No

inhibition of target enzymes substrate reactions was occurred during 1 h of period.

Application of the gels or hydrogels for the investigation of bacterial enzyme activity is the relatively new approach. The Ebrahimi et al. (Sadat Ebrahimi et al. 2015) developed the chitosan-based thin hydrogels for the rapid detection of b-d-glucuronidase activity. Under optimized conditions, the 4-methylumbelliferyl- $\beta$ -D-glucuronide-functionalized hydrogel reported the presence of  $\beta$ -GUS within 15 minutes with a limit of detection of <1 nM. However, the detection of bacteria itself in that case *E. coli* was achieved within 24 h. The enzyme substrate reaction in the PAA gel system was used as a positive control for the detection of target bacteria from stainless steel surface. The next step of the optical analyses was the optimization of the enzyme inducers and membrane permeabilization reagents for each target bacteria. The IPTG and OBDG were used as inducers of b-d-Galactosidase and b-d-glucuronidase for Coliforms and *E. coli* respectively. The influence of different concentrations of IPTG (varied from 0.1 mg/ml to 0.8 mg/ml) on  $\beta$  - Galactosidase activity produced by Coliforms was studied. The influence of different concentrations of OBDG varying from 0.1 mg/mL to 0.8 mg/mL on production of optical signal by *E. coli* using target fluorogenic substrate was studied. The influence of different bacterial cell permeabilization reagents on colorimetric and fluorogenic signals produced by Coliforms and *E. coli* was tested. In case of Coliforms the PAA gel system produced the highest optical signals (abs =0.634; 530 nm) within 1h of incubation of 6 log<sub>10</sub>CFU/mL bacterial suspension with 0.5 mg/mL 6-CIPG, 0.2 mg/mL IPTG and 0.005 mg/mL ODTG. Thus, the right

concentrations of permeabilization reagents and inducers significantly increased the values of the optical signals produced by  $10^6$  CFU/ml Coliforms and *E. coli* in the PAA gel systems reagents. An optimal concentration of IPTG is necessary to increase the  $\beta$ -D-Galactosidase activity (Laczka et al. 2010, Noh et al. 2015). Several authors studied different cell permeabilization components, including SDS, B-PER, Triton X-100 for the extraction of target enzymes from *E. coli* and Coliforms (Noh et al. 2015, Rochelet et al. 2015, Gunda et al. 2016). Among tested acceleration reagents the new membrane permeabilization reagents octyl-b-d-glucopyranoside and octyl-b-d-galactopyranoside were the most efficient for the *E. coli* and Coliforms respectively. For the confirmation of the obtained results the efficiency of the optimized accelerating reagents in the bacterial cultures were tested. The influence of OBG and ODTG on the color production by *E. coli*, Coliforms was assessed using 0.5 mg/mL (the lowest concentration) from each 6-CIPG, 5,4-BCIGP and 4MUG substrates. The formation of colors and fluorescence was studied during different time periods. The visual assessment of the efficiencies of two groups of permeabilization reagents showed that the OBG and ODTG were more efficient (Absorbance<sub>OBG</sub>=0.65; Absorbance<sub>B-PER</sub>=0.5; RFU<sub>ODTG</sub>=8000, RFU<sub>B-PER</sub>=3500) for detection of colorimetric and fluorometric signals produced by Coliforms and *E. coli*, than B-per reagent particularly at the early stages of the reaction. Thus, the PAA gel system with higher substrate concentrations could be used for detection of low number of target bacteria, especially when applied to stainless steel surfaces. The fluorescence signals produced by *E. coli* during tested

detection times were correspond to colorimetric signals at the same periods.

The optimized graphene-gel modified electrodes containing both optical and electrochemical specific substrates were tested for simultaneous detection of Coliforms, *St. aureus* and *E. coli* on stainless steel surfaces. The simultaneous generation of optical and electrochemical signals were occurred. Within 30 minutes of incubation of each gel-electrode system the optical and electrochemical signals specific for the 6-DI, 5,4-DDI, 6-DI+4-NL, 4-NL, 4-NP and 4-MU produced by each bacterium were detected. Production of both chromogenic and voltammetric signals was noticed among different concentrations of Coliforms sampled from food contact surfaces, which indicates the good performance ability of the developed sensor platform. The electrochemical and optical signals were produced at the same time point for all tested concentrations. However, the detection limit of the combined sensor platform was slightly increased from 0.5 log<sub>10</sub>CFU/cm<sup>2</sup> to 0.9 log<sub>10</sub>CFU/cm<sup>2</sup> (3 CFU/cm<sup>2</sup> to 8 CFU/cm<sup>2</sup>) within 30 minutes of detection time. It could be explained by higher sensitivity if electrochemical sensor comparing to optical one. Nevertheless, the combined sensor platform is more efficient (rapid (30 minutes) and sensitive (10 CFU/cm<sup>2</sup>)) comparing with hygienic systems for Coliforms available on market. Additionally, dual signal production by developed sensor platform provides more accuracy to the method, which is important for industrial implementation. However, the optical and electrochemical properties of the sensor could be used also separately to construct different sensors. In case of Coliforms, developed sensor platform produces additional signal responsible for

the Gram-reaction of the detected bacteria. Mentioned feature makes the developed sensor platform very specific for the Coliforms comparing to other systems available on market. The developed combined sensor (both optical and electrochemical) platform could detect *E. coli*, *St. aureus*, Gram- negative bacteria during 30 minutes, however the sensitivity should be optimized for the lower concentrations. In the future colorimetric signals could be replaced by fluorometric signals (as it was done for *E. coli*) to provide more sensitive detection. The developed sensor platform also could be used for detection and quantification of general Gram-negative bacteria. The signals produced on developed sensor chips were measured by the separate equipment, potentiostat for the electrochemical signals and microplate reader for optical (colorimetric and fluorometric) signals. In the future the special reader for the developed sensor chips should be constructed and programmed to have completely separate and ready system for the market.

## 7 Conclusion and outlook

The colorimetric and voltammetric sensor platforms were developed for detection and enumeration of Coliforms, *E. coli* and *St. aureus*. Thereafter, the both platforms were combined in the one system. The 6-CIGP, 5,4-BCIGP, 4-MUG, 4-NPP and 4-NLD were successfully used as new electrochemical reporters for  $\beta$ -D-Galactosidase,  $\beta$ -D-Glucuronidase and Phospholipase C activity. The main results of initial optimization steps have shown that gold screen printed electrodes had a self-oxidation peak in low potential ranges. The carbon screen printed electrodes were used for the future construction of the voltammetric chips due their wide electrochemical window especially in the negative potential ranges. The findings also indicated significant electrochemical activity of blank solutions on gold electrodes comparing to carbon electrodes. Thus, the initial experiments on optimization of electrode materials as well as the electrochemical activity of the blank are critical steps that prevent the whole further development process from the significant errors and ensure the accuracy of the developed sensor. The main results of construction of gel-electrode system indicated that the gel containing polyacrylamide possessed significantly higher bacterial attachment efficiency compared to the other three gels especially for lower concentrations of tested bacteria. Polyacrylamide containing agar gel was chosen among different types of tested gels, for its low electrochemical background at the defined potential ranges. The concentrations of all components of the polyacrylamide –agar gel were optimized to obtain electrochemically inactive gel system, at the defined potential ranges, which is also very important

and critical aspect for the development of the novel detection system. The performed procedures resulted in electrochemically inactive gel with high bacterial attachment efficiency and pH values optimal for target enzymes specific for tested bacterial groups. The electrochemical properties (peak currents, electrochemical stability, reproducibility, electrical conductivity) of the developed gel-electrode system were improved by modifying the gel with previously tested graphene nanoplatelets. Results of the initial optimization step have shown that the pH of the gel-electrode system is the second critical factor that could influence on specific enzyme-substrate reaction, bacterial attachment and electrochemical properties. The change of the pH during incubation could influence on voltammetric signals causing the slight deviations of peak potentials. Gel-electrode system without optimized pH can cause errors in further measurements. Constructed graphene polyacrylamide agar gel electrodes were successfully tested for detection of voltammetric signals produced by the target analytes, specific enzyme/substrate reactions, target bacteria in cultures and on stainless steel surfaces. In case of Coliforms, the intermediate rapid (~2 min) electrochemical signals were observed and confirmed. Further investigation of the detected signals and mechanism can be lead to the construction of ultrafast sensor. Integration of second substrate, responsible for Gram-negative reaction, in to the developed gel-electrode system increased the specificity of the sensor for Coliforms and resulted in dual signal system, that can detect and differentiate Coliforms in multi-bacterial environment. Detection and quantification of low numbers (up to  $0.6 \log_{10}\text{CFU}/\text{cm}^2$ ) of target bacteria (Coliforms, *E. coli* *St. aureus*) in the culture and on stainless steel surfaces, by



GR/PAAGC electrode system was achieved from 30 min to 3 h period. Detection of Coliforms by developed sensor in simulated food processing conditions (heavy soiled, disinfected, processing) was successfully performed. The main findings of the colorimetric/fluorometric experiments have shown that right and optimized concentrations of permeabilization reagents and inducers (0.005 mg/mL and 0.2 mg/mL IPTG ODTG) significantly increased the speed and values of the produced optical and electrochemical signals. In the result, the optically active PAA hydrogel developed, which possessed uniformly distribution of specific color across the whole gel. Application of the gels or hydrogels for the investigation of bacterial enzyme activity is the relatively new approach. Sampling, detection and quantification of target bacteria from stainless steel surfaces by combined electrochemical and optical sensor system was successfully performed. The detection time varied from 30 min to 3 hours. The developed technique was applied in the other project as a proof of concept for detection of Coliforms in water samples (the sampling system was changed and designed for water analysis). The sensor could detect 1 log<sub>10</sub>CFU/mL to 8 log<sub>10</sub>CFU/mL Coliforms within 3 hours. The voltammetric and colorimetric peaks were produced at the defined potential and wavelength ranges, specific for the target analytes.

In the future, the sensitivity and detection speed can be improved by printing the carbon electrodes directly on the gels. The microfluidics technique could be applied to the gels for the dispersion of inducers and accelerating reagents. The time to detection principle also can be applied to get the correlation between bacterial concentration and detection time. The signals produced on developed sensor chips

were measured by the separate equipment, open source potentiostat for the electrochemical signals and microplate reader for optical (colorimetric and fluorometric) signals. In the future the special reader (combining both measurements) for the developed sensor chips should be constructed and programmed to have a sensitive, separate and ready system. Finally, the more validation experiments at different processing environments as well as for different strains of tested bacteria are necessary to perform.

## 8 Bibliography

Abdallah, M., C. Benoliel, C. Jama, D. Drider, P. Dhulster and N. E. Chihib (2014). "Thermodynamic prediction of growth temperature dependence in the adhesion of *Pseudomonas aeruginosa* and *Staphylococcus aureus* to stainless steel and polycarbonate." J Food Prot **77**(7): 1116-1126.

Adams, M. (2009). 22 - *Staphylococcus aureus* and other pathogenic Gram-positive cocci. Foodborne Pathogens (Second Edition). C. d. W. Blackburn and P. J. McClure, Woodhead Publishing: 802-819.

Adator, E. H., M. Cheng, R. Holley, T. McAllister and C. Narvaez-Bravo (2018). "Ability of Shiga toxigenic *Escherichia coli* to survive within dry-surface biofilms and transfer to fresh lettuce." Int J Food Microbiol **269**: 52-59.

Adell, A. D., F. O. Mardones and A. I. Moreno Switt (2018). "Preface: New Tools to detect and Prevent Foodborne Outbreaks from Farm to Fork." Food Microbiology **75**: 1.

Adeolu, M., S. Alnajar, S. Naushad and R. S. Gupta (2016). "Genome-based phylogeny and taxonomy of the 'Enterobacteriales': proposal for Enterobacterales ord. nov. divided into the families Enterobacteriaceae, Erwiniaceae fam. nov., Pectobacteriaceae fam. nov., Yersiniaceae fam. nov., Hafniaceae fam. nov., Morganellaceae fam. nov., and Budviciaceae fam. nov." International Journal of Systematic and Evolutionary Microbiology **66**(12): 5575-5599.

Ahmed, A., J. V. Rushworth, N. A. Hirst and P. A. Millner (2014). "Biosensors for Whole-Cell Bacterial Detection." Clinical Microbiology Reviews **27**(3): 631.

Alam, A., H.-C. Kuan, Z. Zhao, J. Xu and J. Ma (2017). "Novel polyacrylamide hydrogels by highly conductive, water-processable graphene." Composites Part A: Applied Science and Manufacturing **93**: 1-9.

Alam, A., Q. Meng, G. Shi, S. Arabi, J. Ma, N. Zhao and H.-C. Kuan (2016). "Electrically conductive, mechanically robust, pH-sensitive

graphene/polymer composite hydrogels." Composites Science and Technology **127**: 119-126.

AlAqad, K. M., R. Suleiman, O. C. S. Al Hamouz and T. A. Saleh (2018). "Novel graphene modified carbon-paste electrode for promazine detection by square wave voltammetry." Journal of Molecular Liquids **252**: 75-82.

Allata, S., A. Valero and L. Benhadja (2017). "Implementation of traceability and food safety systems (HACCP) under the ISO 22000:2005 standard in North Africa: The case study of an ice cream company in Algeria." Food Control **79**: 239-253.

APHA (2005). Standard methods for the examination of water and wastewater. APHA-AWWA-WEF, American Public Health Association, American Water Works Association and Water Environment Federation. **APHA-AWWA-WEF, 2005.**

Arvand, M., M. Saberi, M. S. Ardaki and A. Mohammadi (2017). "Mediated electrochemical method for the determination of indigo carmine levels in food products." Talanta **173**: 60-68.

Arvinte, A., M. Mahosenaho, M. Pinteala, A. Sesay and V. Virtanen (2011). "Electrochemical oxidation of p-nitrophenol using graphene-modified electrodes, and a comparison to the performance of MWNT-based electrodes." Microchim. Acta **174**: 337-343.

Baït, N., B. Grassl, A. Benaboura and C. Derail (2012). "Tailoring adhesion properties of polyacrylamide-based hydrogels. Application for skin contact." Journal of Adhesion Sciences and Technology **27**.

Exum, N. G., M. N. Kosek, M. F. Davis and K. J. Schwab (2017). "Surface Sampling Collection and Culture Methods for Escherichia coli in Household Environments with High Fecal Contamination." Int J Environ Res Public Health **14**(8).

Baldrich, E., F. X. Muñoz and C. García-Aljaro (2011). "Electrochemical Detection of Quorum Sensing Signaling Molecules by Dual Signal Confirmation at Microelectrode Arrays." Analytical Chemistry **83**(6): 2097-2103.

Barlow, S. M., A. R. Boobis, J. Bridges, A. Cockburn, W. Dekant, P. Hepburn, G. F. Houben, J. König, M. J. Nauta, J. Schuermans and D. Bánáti (2015). "The role of hazard- and risk-based approaches in ensuring food safety." Trends in Food Science & Technology **46**(2, Part A): 176-188.

Belghiti, D. K., E. Scorsone, J. de Sanoit and P. Bergonzo (2016). "Simultaneous detection of indole and 3-methylindole using boron-doped diamond electrodes." physica status solidi (a) **213**(10): 2662-2671.

Bengoechea Álvarez, M. J., M. T. Fernández Abedul and A. n. Costa García (2002). "Flow amperometric detection of indigo for enzyme-linked immunosorbent assays with use of screen-printed electrodes." Analytica Chimica Acta **462**(1): 31-37.

Berete, Y. J., W. Schaeg, J. Bruckler and H. Blobel (1980). "[Lipase and phospholipase C from Staphylococcus aureus of different origin. I. Determination and occurrence (author's transl)]." Zentralbl Bakteriol A **248**(2): 229-233.

Bhattacharya, S., S. Nandi and R. Jelinek (2017). "Carbon-dot–hydrogel for enzyme-mediated bacterial detection." RSC Adv. **7**.

Bjelkhagen, H. I. (2004). "Color vision and colorimetry: theory and applications, SPIE press monograph Vol. PM105: Daniel Malacara-Hernandez, Centro de Investigaciones en Optica, A.C. (Mexico), SPIE Press, April 2002, pp. 176, ISBN 0-8194-4228-3." Optics and Lasers in Engineering **42**(4): 490-491.

Blackburn, C. d. W. (2007). 1 - Microbiological testing in food safety and quality management. Microbiological Analysis of Red Meat, Poultry and Eggs. G. C. Mead, Woodhead Publishing: 1-32.

Božič, M., M. Díaz-González, T. Tzanov, G. M. Guebitz and V. Kokol (2009). "Voltametric monitoring of enzyme-mediated indigo reduction in the presence of various fibre materials." Enzyme and Microbial Technology **45**(4): 317-323.

Buzón-Durán, L., C. Alonso-Calleja, F. Riesco-Peláez and R. Capita (2017). "Effect of sub-inhibitory concentrations of biocides on the architecture and viability of MRSA biofilms." Food Microbiology **65**: 294-301.

Carrington, N., L. Yong and Z.-L. Xue (2006). "Electrochemical Deposition of Sol-gel Films for Enhanced Chromium(VI) Determination in Aqueous Solutions." Analytica chimica acta **572**: 17-24.

Castaño-Álvarez, M., M. T. Fernández-Abedul and A. Costa-García (2004). "Gold Electrodes for Detection of Enzyme Assays with 3-Indoxylphosphate as Substrate." Electroanalysis **16**(18): 1487-1496.

Cellier, M., A. L. James, S. Orenga, J. D. Perry, A. K. Rasul, S. N. Robinson and S. P. Stanforth (2014). "Novel chromogenic aminopeptidase substrates for the detection and identification of clinically important microorganisms." Bioorg Med Chem **22**(19): 5249-5269.

Chen, J., Z. Jiang, J. D. Ackerman, M. Yazdani, S. Hou, S. R. Nugen and V. M. Rotello (2015). "Electrochemical nanoparticle-enzyme sensors for screening bacterial contamination in drinking water." The Analyst **140**(15): 4991-4996.

Cheng, C., S. Li, A. Thomas, N. A. Kotov and R. Haag (2017). "Functional Graphene Nanomaterials Based Architectures: Biointeractions, Fabrications, and Emerging Biological Applications." Chemical Reviews **117**(3): 1826-1914.

Cheng, Y., Y. Liu, J. Huang, Y. Xian, W. Zhang, Z. Zhang and L. Jin (2008). "Rapid amperometric detection of coliforms based on MWNTs/Nafion composite film modified glass carbon electrode." Talanta **75**: 167-171.

Cho, I. H. and S. Ku (2017). "Current Technical Approaches for the Early Detection of Foodborne Pathogens: Challenges and Opportunities." **18**(10).

Ciobanu, M., J. P. Wilburn, M. L. Krim and D. E. Cliffel (2007). 1 - Fundamentals. Handbook of Electrochemistry. C. G. Zoski. Amsterdam, Elsevier: 3-29.

- Compton, R. (2007). "Elements of Molecular and Biomolecular Electrochemistry. An Electrochemical Approach to Electron Transfer Chemistry. By Jean-Michel Savéant." Angewandte Chemie International Edition **46**(9): 1367-1367.
- Daugherty, S. and M. G. Low (1993). "Cloning, expression, and mutagenesis of phosphatidylinositol-specific phospholipase C from *Staphylococcus aureus*: a potential staphylococcal virulence factor." Infection and Immunity **61**(12): 5078.
- De Acha, N., C. Elosúa, M. J. Corres and J. F. Arregui (2019). "Fluorescent Sensors for the Detection of Heavy Metal Ions in Aqueous Media." Sensors **19**(3).
- De Buyser, M.-L., S. Dragacci and J.-A. Hennekinne (2012). "Staphylococcus aureus and its food poisoning toxins: characterization and outbreak investigation." FEMS Microbiology Reviews **36**(4): 815-836.
- Dempsey, E., C. O'Sullivan, M. R. Smyth, D. Egan, R. O'Kennedy and J. Wang (1993). "Differential pulse voltammetric determination of 7-hydroxycoumarin in human urine." J Pharm Biomed Anal **11**(6): 443-446.
- Devi, M., N. s. Meera, P. Charantheja and S. D.V.R (2011). "Production and optimization of  $\beta$ -galactosidase enzyme from probiotic *Lactobacillus* sps." BioTechnology: An Indian Journal **5**: 153-159.
- Dhahi, T., U. Hashim, N. Alrawi and A. Taib (2010). "A review on the electrochemical sensors and biosensors composed of nanogaps as sensing material." Journal of Optoelectronics and Advanced Materials **12**: 1857-1862.
- Ding, T., Y.-Y. Yu, D. W. Schaffner, S.-G. Chen, X.-Q. Ye and D.-H. Liu (2016). "Farm to consumption risk assessment for *Staphylococcus aureus* and staphylococcal enterotoxins in fluid milk in China." Food Control **59**: 636-643.
- Duke, R., E. Veale, F. Pfeffer, T. Gunnlaugsson and P. Kruger (2010). "Colorimetric and fluorescent anion sensors: an overview of recent developments in the use of 1,8-naphthalimide-based chemosensors." Chemical Society Reviews **39**: 3936.

Elgrishi, N., K. J. Rountree, B. D. McCarthy, E. S. Rountree, T. T. Eisenhart and J. L. Dempsey (2018). "A Practical Beginner's Guide to Cyclic Voltammetry." Journal of Chemical Education **95**(2): 197-206.

Elleboudy, N. S., M. M. Aboulwafa and N. A. Hassouna (2014). "Phospholipase C from *Pseudomonas aeruginosa* and *Bacillus cereus*; characterization of catalytic activity." Asian Pac J Trop Med **7**(11): 860-866.

Espinoza, E. M., J. A. Clark, J. Soliman, J. B. Derr, M. Morales and V. I. Vullev (2019). "Practical Aspects of Cyclic Voltammetry: How to Estimate Reduction Potentials When Irreversibility Prevails." Journal of The Electrochemical Society **166**(5): H3175-H3187.

Ettenauer, J., K. Zuser, K. Kellner, T. Posniecek and M. Brandl (2016). "8-hydroxyquinoline-glucuronide Sodium Salt Used as Electroactive Substrate for a Sensitive Voltammetric Detection of *Escherichia Coli* in Water Samples." Procedia Engineering **168**: 143-146.

EU (2018). "The European Union summary report on trends and sources of zoonoses, zoonotic agents and food-borne outbreaks in 2017." EFSA Journal **16**(12): e05500.

Fernández-Sánchez, C. and A. Costa-García (2000). "Voltammetric studies of indigo adsorbed on pre-treated carbon paste electrodes." Electrochemistry Communications **2**(11): 776-781.

Filip, J., P. Kasák and J. Tkac (2015). "Graphene as a signal amplifier for preparation of ultrasensitive electrochemical biosensors." Chemicke zvesti **69**(1): 112-133.

Flores-Díaz, M., L. Monturiol-Gross, C. Naylor, A. Alape-Girón and A. Flieger (2016). "Bacterial Sphingomyelinases and Phospholipases as Virulence Factors." Microbiology and Molecular Biology Reviews **80**(3): 597.

FNES4 (2017). Standard Method for Detection and Enumeration of Bacteria in Swabs and other Environmental Samples. Public Health England. **FNES4**.



Foschino, R. (2009). "James M. Jay, Martin J. Loessner, David A. Golden Modern food microbiology." Annals of Microbiology **56**(1): 81-81.

Galat, A., J. Dufresne, J. Combrisson, J. Thépaut, L. Boumghar-Bourtchai, M. Boyer and C. Fourmestraux (2016). "Novel method based on chromogenic media for discrimination and selective enumeration of lactic acid bacteria in fermented milk products." Food Microbiology **55**: 86-94.

Gheyanchi, E., F. Heshmati, B. Shargh, J. Nowroozi and F. Movahedzadeh (2010). "Study on  $\beta$ -galactosidase enzyme produced by isolated lactobacilli from milk and cheese." African Journal of Microbiology Research **4**: 454-458.

Gkana, E., N. Chorianopoulos, A. Grounta, K. Koutsoumanis and G. E. Nychas (2017). "Effect of inoculum size, bacterial species, type of surfaces and contact time to the transfer of foodborne pathogens from inoculated to non-inoculated beef fillets via food processing surfaces." Food Microbiol **62**: 51-57.

Gouveia, A. and M. Nicoletti (2015). "Influence of the Sampling Technique on Microorganism Detection in the Monitoring of Flat Surfaces." LATIN AMERICAN JOURNAL OF PHARMACY **34**: 146-152.

Govaert, F., E. Temmerman and P. Kiekens (1999). "Development of voltammetric sensors for the determination of sodium dithionite and indanthrene/indigo dyes in alkaline solutions." Analytica Chimica Acta **385**(1): 307-314.

Grigoryan, K., G. Badalyan and D. Andreasyan (2010). "Prevalence of Staphylococcus aureus in fish processing factory." Potravinarstvo **4**(2): 25-28.

Gunda, N. S., R. Chavali and S. K. Mitra (2016). "A hydrogel based rapid test method for detection of Escherichia coli (E. coli) in contaminated water samples." Analyst **141**(10): 2920-2929.

Heery, B., C. Briciu-Burghina, D. Zhang, G. Duffy, D. Brabazon, N. O'Connor and F. Regan (2016). "ColiSense, today's sample today: A rapid on-site detection of beta-D-Glucuronidase activity in surface water as a surrogate for E. coli." Talanta **148**: 75-83.

Heinze, J. (1981). "Allen J. Bard and Larry F. Faulkner: Electrochemical Methods – Fundamentals and Applications. Wiley, New York 1980, 718 + XVIII S., Preis: £ 14.70." Berichte der Bunsengesellschaft für physikalische Chemie **85**(11): 1085-1086.

Hesari, N., A. Alum, M. Elzein and M. Abbaszadegan (2016). "A biosensor platform for rapid detection of E. coli in drinking water." Enzyme Microb Technol **83**: 22-28.

Hrbac, J., V. Halouzka, L. Trnkova and J. Vacek (2014). "eL-Chem Viewer: A Freeware Package for the Analysis of Electroanalytical Data and Their Post-Acquisition Processing." Sensors (Basel, Switzerland) **14**(8): 13943-13954.

Huss, H. H., L. Ababouch and L. Gram (2003). "Assessment and Management of Seafood Safety and Quality." (444): 227.

Ingham, S. C., J. C. Reyes, N. P. Schoeller and M. M. Lang (2000). "Potential use of presumptive enterococci and staphylococci as indicators of sanitary condition in plants making hard Italian-type cheese." J Food Prot **63**(12): 1697-1701.

ISO18593 (2004). Microbiology of food and animal feeding stuffs. Horizontal methods for sampling techniques from surfaces using contact plates and swabs. ISO/TC 34/SC 9 Microbiology. **18593:2004**.  
Ivnitski, D., I. Abdel-Hamid, P. Atanasov, E. Wilkins and S. Stricker (2000). "Application of Electrochemical Biosensors for Detection of Food Pathogenic Bacteria." Electroanalysis **12**(5): 317-325.

Jaiswal, N. and I. Tiwari (2017). "Recent build outs in electroanalytical biosensors based on carbon-nanomaterial modified screen printed electrode platforms." Analytical Methods **9**(26): 3895-3907.

Jay, J. M. (1995). Indicators of Food Microbial Quality and Safety. Modern Food Microbiology. J. M. Jay. Boston, MA, Springer US: 387-407.

Jay, J. M. (2005). Indicators of Food Microbial Quality and Safety. Modern Food Microbiology. J. M. Jay, M. J. Loessner and D. A. Golden. Boston, MA, Springer US: 473-495.

Jefferson, R. A., S. M. Burgess and D. Hirsh (1986). "beta-Glucuronidase from Escherichia coli as a gene-fusion marker." Proc Natl Acad Sci U S A **83**(22): 8447-8451.

Kalschne, D. L., R. Womer, A. Mattana, C. M. Sarmiento, L. M. Colla and E. Colla (2015). "Characterization of the spoilage lactic acid bacteria in "sliced vacuum-packed cooked ham". " Braz J Microbiol **46**(1): 173-181.

Keeratipibul, S., T. Laovittayanurak, O. Pornruangsarp, Y. Chaturongkasumrit, H. Takahashi and P. Techaruvichit (2017). "Effect of swabbing techniques on the efficiency of bacterial recovery from food contact surfaces." Food Control **77**: 139-144.

Kobayashi, S. D., N. Malachowa and F. R. DeLeo (2015). "Pathogenesis of Staphylococcus aureus abscesses." The American journal of pathology **185**(6): 1518-1527.

Komorsky-Lovrić, Š. (2000). "Square-wave voltammetry of an aqueous solution of indigo." Journal of Electroanalytical Chemistry **482**(2): 222-225.

Kuss, S., H. M. A. Amin and R. G. Compton (2018). "Electrochemical Detection of Pathogenic Bacteria-Recent Strategies, Advances and Challenges." **13**(19): 2758-2769.

Kusumaningrum, H. D., G. Riboldi, W. C. Hazeleger and R. R. Beumer (2003). "Survival of foodborne pathogens on stainless steel surfaces and cross-contamination to foods." Int J Food Microbiol **85**(3): 227-236.

Kvenberg, J. E. and D. J. Schwalm (2000). "Use of microbial data for hazard analysis and critical control point verification--Food and Drug Administration perspective." J Food Prot **63**(6): 810-814.

Laczka, O., C. García-Aljaro, F. J. del Campo, F. X. M. Pascual, J. Mas-Gordi and E. Baldrich (2010). "Amperometric detection of Enterobacteriaceae in

river water by measuring  $\beta$ -galactosidase activity at interdigitated microelectrode arrays." Analytica Chimica Acta **677**(2): 156-161.

Laghrib, F., N. Ajermoun, A. Hrioua, s. Lahrach, A. Farahi, A. Haimouti, M. Bakasse and M. Mhammedi (2018). "Investigation of voltammetric behavior of 4-nitroaniline based on electrodeposition of silver particles onto graphite electrode." Ionics.

Laghrib, F., W. Boumya, S. Lahrach, A. Farahi, A. El Haimouti and M. A. El Mhammedi (2017). "Electrochemical evaluation of catalytic effect of silver in reducing 4-nitroaniline: Analytical application." Journal of Electroanalytical Chemistry **807**: 82-87.

Lee, J.-S., Y.-M. Bae, S.-Y. Lee and S.-Y. Lee (2015). "Biofilm Formation of Staphylococcus aureus on Various Surfaces and Their Resistance to Chlorine Sanitizer." Journal of Food Science **80**(10): M2279-M2286.

Lemmen, S. W., H. Hafner, D. Zoldann, G. Amedick and R. Lutticken (2001). "Comparison of two sampling methods for the detection of gram-positive and gram-negative bacteria in the environment: moistened swabs versus Rodac plates." Int J Hyg Environ Health **203**(3): 245-248.

Li, G., Y. Zhao, L. Zhang, M. Gao, Y. Kong and Y. Yang (2016). "Preparation of graphene oxide/polyacrylamide composite hydrogel and its effect on Schwann cells attachment and proliferation." Colloids and Surfaces B: Biointerfaces **143**: 547-556.

Li, L., Y. Shi, L. J. Pan, Y. Shi and G. Yu (2015). "Additional Article Notification: Rational design and applications of conducting polymer hydrogels as electrochemical biosensors." J. Mater. Chem. B **3**.

Li, Z., W. Mi, H. Wang, Y. Su and C. He (2014). "Nano-hydroxyapatite/polyacrylamide composite hydrogels with high mechanical strengths and cell adhesion properties." Colloids and Surfaces B: Biointerfaces **123**: 959-964.

Lin, S., L. Yang, G. Chen, B. Li, D. Chen, L. Li and Z. Xu (2017). "Pathogenic features and characteristics of food borne pathogens biofilm: Biomass, viability and matrix." Microbial Pathogenesis **111**: 285-291.

Ma, Y., X.-L. Shen, Q. Zeng and L.-S. Wang (2017). "A glassy carbon electrode modified with graphene nanoplatelets, gold nanoparticles and chitosan, and coated with a molecularly imprinted polymer for highly sensitive determination of prostate specific antigen." Microchimica Acta **184**.

Manafi, M. (1996). "Fluorogenic and chromogenic enzyme substrates in culture media and identification tests." International Journal of Food Microbiology **31**(1): 45-58.

Manibalan, K., V. Mani, C. H. Huang, S. T. Huang and P. C. Chang (2015). "A new electrochemical substrate for rapid and sensitive in vivo monitoring of beta-galactosidase gene expressions." Analyst **140**(17): 6040-6046.

Manjunatha, J. G. G. (2018). "A novel poly (glycine) biosensor towards the detection of indigo carmine: A voltammetric study." Journal of Food and Drug Analysis **26**(1): 292-299.

Martin, N. H., A. Trmčić, T.-H. Hsieh, K. J. Boor and M. Wiedmann (2016). "The Evolving Role of Coliforms As Indicators of Unhygienic Processing Conditions in Dairy Foods." Frontiers in microbiology **7**: 1549-1549.

Mead, G. C. (2007). 4 - Faecal indicator organisms for red meat and poultry. Microbiological Analysis of Red Meat, Poultry and Eggs. G. C. Mead, Woodhead Publishing: 83-100.

Meighan, P. (2014). "Validation of the MicroSnap Coliform and E. coli Test System for Enumeration and Detection of Coliforms and E. coli in a Variety of Foods." Journal of AOAC International **97**(2): 453-478.

Mittelman, A. S., E. Z. Ron and J. Rishpon (2002). "Amperometric Quantification of Total Coliforms and Specific Detection of Escherichia coli." Analytical Chemistry **74**(4): 903-907.

Miyata, T., N. Asami and T. Uragami (1999). "A reversibly antigen-responsive hydrogel." Nature **399**(6738): 766-769.

Molina, F., E. López-Acedo, R. Tabla, I. Roa, A. Gómez and J. E. Rebollo (2015). "Improved detection of Escherichia coli and coliform bacteria by multiplex PCR." BMC Biotechnology **15**: 48.

Moore, G. and C. Griffith (2002). "A comparison of surface sampling methods for detecting coliforms on food contact surfaces." Food Microbiology **19**(1): 65-73.

Moore, G. and C. Griffith (2002). "A comparison of traditional and recently developed methods for monitoring surface hygiene within the food industry: an industry trial." Int J Environ Health Res **12**(4): 317-329.

Nataro, J. P. and J. B. Kaper (1998). "Diarrheagenic Escherichia coli." Clin Microbiol Rev **11**(1): 142-201.

Navarro-Garcia, F. (2014). "Escherichia coli O104:H4 Pathogenesis: an Enteroaggregative E. coli/Shiga Toxin-Producing E. coli Explosive Cocktail of High Virulence." Microbiol Spectr **2**(6).

Noh, S., Y. Choe, V. Tamilavan, M. H. Hyun, H. Y. Kang and H. Yang (2015). "Facile electrochemical detection of Escherichia coli using redox cycling of the product generated by the intracellular  $\beta$ -d-galactosidase." Sensors and Actuators B: Chemical **209**: 951-956.

Ntsendwana, B., B. B. Mamba, S. Sampath and O. Arotiba (2012). "Electrochemical Detection of Bisphenol A Using Graphene-Modified Glassy Carbon Electrode." International Journal of Electrochemical Science **7**: 3501-3512.

Odonkor, S. (2013). "E coli as an indicator of bacteriological quality of water: An overview." Microbiology research **4**.

Orenga, S., A. L. James, M. Manafi, J. D. Perry and D. H. Pincus (2009). "Enzymatic substrates in microbiology." J Microbiol Methods **79**(2): 139-155.

Ozkan, S. A., J.-M. Kauffmann and P. Zuman (2015). Electroanalytical Techniques Most Frequently Used in Drug Analysis. Electroanalysis in Biomedical and Pharmaceutical Sciences: Voltammetry, Amperometry,

Biosensors, Applications. S. A. Ozkan, J.-M. Kauffmann and P. Zuman. Berlin, Heidelberg, Springer Berlin Heidelberg: 45-81.

Pavitt, A. S., E. J. Bylaska and P. G. Tratnyek (2017). "Oxidation potentials of phenols and anilines: correlation analysis of electrochemical and theoretical values." **19**(3): 339-349.

Pérez-Ràfols, C., J. Bastos-Arrieta, N. Serrano, J. M. Díaz-Cruz, C. Ariño, J. de Pablo and M. Esteban (2017). "Ag Nanoparticles Drop-Casting Modification of Screen-Printed Electrodes for the Simultaneous Voltammetric Determination of Cu(II) and Pb(II)." Sensors (Basel, Switzerland) **17**(6): 1458.

Pingarron Carrazon, J. M., A. Gordon Vergara, A. J. Reviejo Garcia and L. M. Polo Diez (1989). "Determination of coumarins by voltammetric techniques in micellar and emulsified media." Analytica Chimica Acta **216**: 231-242.

Pinto, F., S. Hiom, S. Girdlestone and J. Y. Maillard (2009). "Evaluation of the effectiveness of commercially available contact plates for monitoring microbial environments." Lett Appl Microbiol **48**(3): 379-382.

Piriya V.S, A., P. Joseph, K. Daniel S.C.G, S. Lakshmanan, T. Kinoshita and S. Muthusamy (2017). "Colorimetric sensors for rapid detection of various analytes." Materials Science and Engineering: C **78**: 1231-1245.

Pleskov, Y. V. (2007). "V. S. Bagotzky. Fundamentals of electrochemistry (2nd edition). Wiley, 2006." Russian Journal of Electrochemistry - RUSSIAN J ELECTROCHEMISTRY **43**: 1326-1327.

Rachida, N. (2014). "Electrochemical Determination of 4-Nitroaniline at Natural Phosphate Modified Carbon Paste Electrode." Catalysis Reviews **4**: 78.

Rivera, D., V. Toledo, A. Reyes-Jara, P. Navarrete, M. Tamplin, B. Kimura, M. Wiedmann, P. Silva and A. I. Moreno Switt (2018). "Approaches to empower the implementation of new tools to detect and prevent foodborne pathogens in food processing." Food Microbiology **75**: 126-132.

Rochelet, M., S. Solanas, L. Betelli, B. Chantemesse, F. Vienney and A. Hartmann (2015). "Rapid amperometric detection of *Escherichia coli* in wastewater by measuring  $\beta$ -D glucuronidase activity with disposable carbon sensors." *Analytica Chimica Acta* **892**: 160-166.

Sadat Ebrahimi, M.-M., B. Steinhoff and H. Schönherr (2015). "Rapid remote detection of *Escherichia coli* via a reporter-hydrogel coated glass fiber tip." *European Polymer Journal* **72**: 180-189.

Sadat Ebrahimi, M. M., Y. Voss and H. Schonherr (2015). "Rapid Detection of *Escherichia coli* via Enzymatically Triggered Reactions in Self-Reporting Chitosan Hydrogels." *ACS Appl Mater Interfaces* **7**(36): 20190-20199.

Sakiç, T., B. Kleine and S. G. Gatermann (2007). "Biochemical characterization of the surface-associated lipase of *Staphylococcus saprophyticus*." *FEMS Microbiology Letters* **274**(2): 335-341.

Salo, S., A. Laine, T. Alanko, A.-M. Sjöberg, G. Wirtanen, B. Guobjörnsdóttir, B. Jessen, S. Langsrud, K. Lindquist, J. Lundén, M. Mäki, E. Nerbrink, Ó. Niclasen, P. Tuominen, H. Tuompo, E. Vatunen and A. Woivalin (2000). "Validation of the Microbiological Methods Hygicult Dipslide, Contact Plate, and Swabbing in Surface Hygiene Control: A Nordic Collaborative Study." *Journal of AOAC International* **83**: 1357-1365.

Sanagi, M. M., S. L. Ling, Z. Nasir, D. Hermawan, W. A. Ibrahim and A. Abu Naim (2009). "Comparison of signal-to-noise, blank determination, and linear regression methods for the estimation of detection and quantification limits for volatile organic compounds by gas chromatography." *J AOAC Int* **92**(6): 1833-1838.

Sangwan, V., S. K. Tomar, B. Ali, R. R. Singh and A. K. Singh (2015). "Production of beta-galactosidase from *Streptococcus thermophilus* for galactooligosaccharides synthesis." *J Food Sci Technol* **52**(7): 4206-4215.

Schardinger, F. (1892). Über das Vorkommen Gährerregender Spaltpilze im Trinkwasser und ihre Bedeutung für die hygienische Beurtheilung desselben. *Wien, Klin. Wochr* (5):403–405, 421–423.



- Schmiel, D. H. and V. L. Miller (1999). "Bacterial phospholipases and pathogenesis." Microbes Infect **1**(13): 1103-1112.
- Smith, T (1895). Notes on Bacillus coli commune and related forms, together with some suggestions concerning the bacteriological examination of drinking water. Am. J. Med. Sci 110:283–302.
- Shoaie, N., M. Forouzandeh and K. Omidfar (2018). "Voltammetric determination of the Escherichia coli DNA using a screen-printed carbon electrode modified with polyaniline and gold nanoparticles." Mikrochim Acta **185**(4): 217.
- Scholz, F. (2015). "Voltammetric techniques of analysis: the essentials." ChemTexts **1**(4): 17.
- Son, H., S. Park, L. R. Beuchat, H. Kim and J.-H. Ryu (2016). "Inhibition of Staphylococcus aureus by antimicrobial biofilms formed by competitive exclusion microorganisms on stainless steel." International Journal of Food Microbiology **238**: 165-171.
- Songer, J. G. (1997). "Bacterial phospholipases and their role in virulence." Trends Microbiol **5**(4): 156-161.
- Stradiotto, N. R., H. Yamanaka and M. V. B. Zanoni (2003). "Electrochemical sensors: a powerful tool in analytical chemistry." Journal of the Brazilian Chemical Society **14**: 159-173.
- Szczepanski, S. and A. Lipski (2014). "Essential oils show specific inhibiting effects on bacterial biofilm formation." Food Control **36**(1): 224-229.
- Taleat, Z., A. Khoshroo and M. Mazloum-Ardakani (2014). "Screen-printed electrodes for biosensing: a review (2008–2013)." Microchimica Acta **181**(9): 865-891.
- Taylor, A. R. (2013). "Methicillin-resistant Staphylococcus aureus infections." Prim Care **40**(3): 637-654.
- Titball, R. W. (1993). "Bacterial phospholipases C." Microbiological reviews **57**(2): 347-366.

Tomasevic, I., J. Kuzmanović, A. Anđelković, M. Saračević, M. M. Stojanović and I. Djekic (2016). "The effects of mandatory HACCP implementation on microbiological indicators of process hygiene in meat processing and retail establishments in Serbia." Meat Science **114**: 54-57.

Tomizawa, M., K. Tsumaki and M. Sone (2016). "Characterization of the activity of beta-galactosidase from Escherichia coli and Drosophila melanogaster in fixed and non-fixed Drosophila tissues." Biochim Open **3**: 1-7.

Tschirhart, T., X. Y. Zhou, H. Ueda, C.-Y. Tsao, E. Kim, G. F. Payne and W. E. Bentley (2016). "Electrochemical Measurement of the  $\beta$ -Galactosidase Reporter from Live Cells: A Comparison to the Miller Assay." ACS Synthetic Biology **5**(1): 28-35.

Tungkavet, T., N. Seetapan, D. Pattavarakorn and A. Sirivat (2015). "Graphene/gelatin hydrogel composites with high storage modulus sensitivity for using as electroactive actuator: Effects of surface area and electric field strength." Polymer **70**: 242-251.

Tuson, H. H., L. D. Renner and D. B. Weibel (2012). "Polyacrylamide Hydrogels as Substrates for Studying Bacteria." Chemical communications (Cambridge, England) **48**(10): 1595-1597.

Vazquez-Sanchez, D., J. A. Galvao and M. Oetterer (2018). "Contamination sources, biofilm-forming ability and biocide resistance of Staphylococcus aureus in tilapia-processing facilities." Food Sci Technol Int **24**(3): 209-222.

Wahyuni, W. T., E. Rohaeti and D. R. Sari (2018). "Graphene Modified Screen Printed Carbon Electrode for Voltammetric Detection of Glutathione as Oxidative Stress Biomarker." IOP Conference Series: Earth and Environmental Science **187**: 012078.

Wang, D. and J. Chen (2017). "Electrochemical Detection of Escherichia coli from Aqueous Samples Using Engineered Phages." **89**(3): 1650-1657.

Wang, L., Y. Li, G. Li, Z. Xie and B. Ye (2015). "Electrochemical characters of hymecromone at graphene modified electrode and its analytical application." Anal. Methods **7**.

Wang, L., Y. Li, G. Li, Z. Xie and B. Ye (2015). "Electrochemical characters of hymecromone at the graphene modified electrode and its analytical application." Analytical Methods **7**(7): 3000-3005.

Wang, P., J. Xiao, M. Guo, Y. Xia, Z. Li, X. Jiang and W. Huang (2015). "Voltammetric Determination of 4-Nitrophenol at Graphite Nanoflakes Modified Glassy Carbon Electrode." Journal of the Electrochemical Society **162**: H72-H78.

White, M. J., J. M. Boyd, A. R. Horswill and W. M. Nauseef (2014). "Phosphatidylinositol-Specific Phospholipase C Contributes to Survival of Staphylococcus aureus in Human Blood and Neutrophils." Infection and Immunity **82**(4): 1559.

Wu, Q. and H. D. Dewald (2001). "Voltammetry of Coumarins." Electroanalysis **13**(1): 45-48.

Yakoh, A., P. Rattanarat, W. Siangproh and O. Chailapakul (2018). "Simple and selective paper-based colorimetric sensor for determination of chloride ion in environmental samples using label-free silver nanoparticles." Talanta **178**: 134-140.

Yang, W., K. R. Ratinac, S. P. Ringer, P. Thordarson, J. J. Gooding and F. Braet (2010). "Carbon nanomaterials in biosensors: should you use nanotubes or graphene?" Angew Chem Int Ed Engl **49**(12): 2114-2138.

Yang, Y., L. Wei and J. Pei (2019). "Application of meta-analysis technique to assess effectiveness of HACCP-based FSM systems in Chinese SLDBs." Food Control **96**: 291-298.

Zhang, T., Y. Gu, C. Li, X. Yan, N. Lu, H. Liu, Z. Zhang and H. Zhang (2017). "Fabrication of Novel Electrochemical Biosensor Based on Graphene Nanohybrid to Detect H<sub>2</sub>O<sub>2</sub> Released from Living Cells with Ultrahigh Performance." ACS Applied Materials & Interfaces **9**(43): 37991-37999.

Zhang, Y., P. Y. Hong, M. W. LeChevallier and W. T. Liu (2015). "Phenotypic and Phylogenetic Identification of Coliform Bacteria Obtained Using 12 Coliform Methods Approved by the U.S. Environmental Protection Agency." Appl Environ Microbiol **81**(17): 6012-6023.

Zhao, F., L. Liu, F. Xiao, J. Li, R. Yan, S. Fan and B. Zeng (2007). "Sensitive Voltammetric Response of p-Nitroaniline on Single-Wall Carbon Nanotube-Ionic Liquid Gel Modified Glassy Carbon Electrodes." Electroanalysis **19**(13): 1387-1393.

Zou, J., L.-L. Huang, X.-Y. Jiang, F.-P. Jiao and J.-G. Yu (2018). "Electrochemical behaviors and determination of rifampicin on graphene nanoplatelets modified glassy carbon electrode in sulfuric acid solution." DESALINATION AND WATER TREATMENT **120**: 272-281.

## 9 Appendix

### Appendix 1 Growth of *E. coli* on commercial chromogenic media

(Experiments are described in section 4.4)

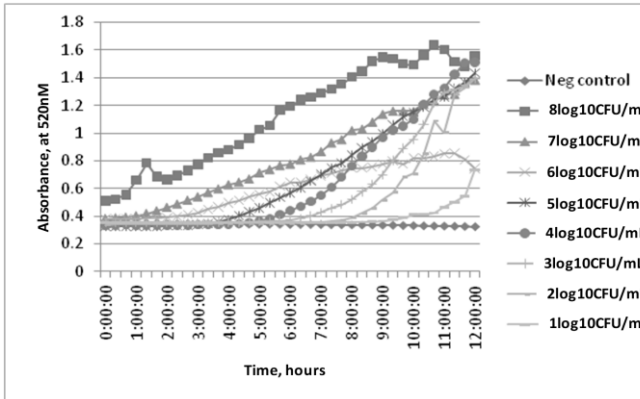


Figure 9-1 Growth of different concentrations of *E. coli* K12 (DSM498) on commercial chromogenic agar during 12h period

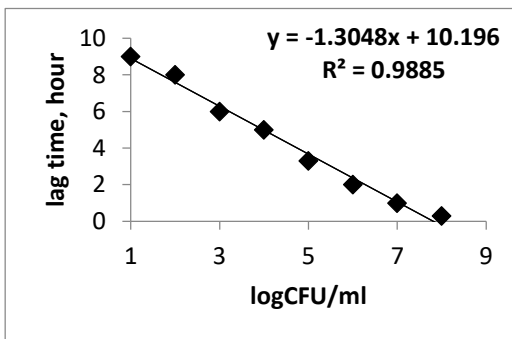


Figure 9-2 Correlation of lag times and concentrations of *E. coli* K12 (DSM498) on commercial chromogenic agar

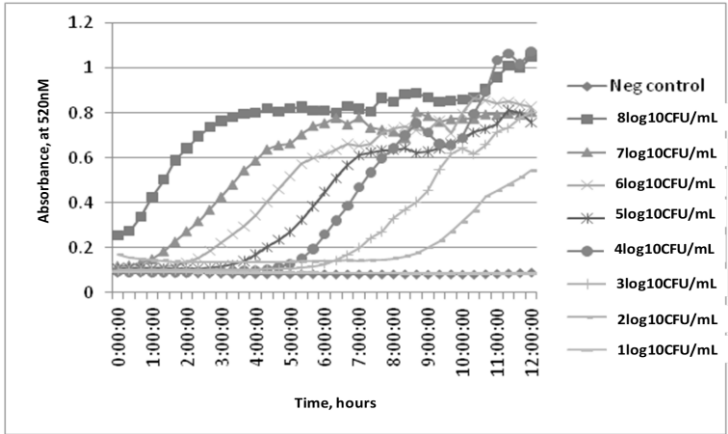


Figure 9-3 Growth of different concentrations of *E. coli* K-12 (DSM498) in commercial chromogenic broth during 12h period

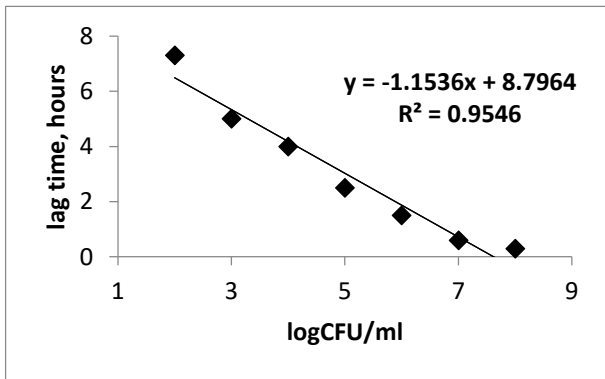


Figure 9-4 Correlation of lag times and concentrations of *E. coli* K-12 (DSM498) in commercial chromogenic broth

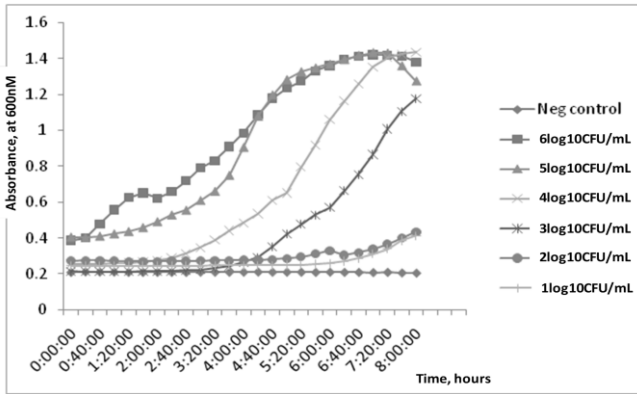


Figure 9-5 Growth of different concentrations of *E. coli* K12 in meat juice during 8h period

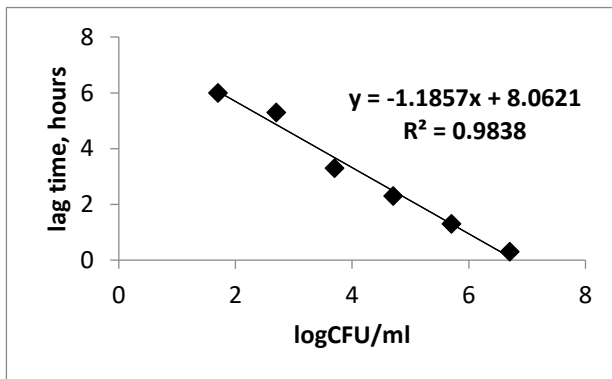


Figure 9-6 Correlation of lag times and concentrations of *E. coli* K12 meat juice

## Appendix 2 Calibration of plate count and Optical density (OD) values

(Experiments are described in section 4.4)

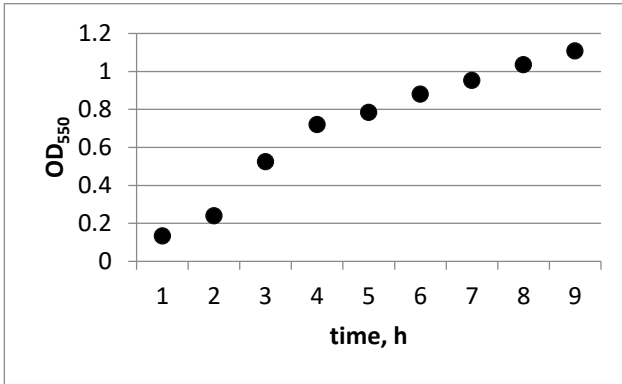


Figure 9-7 Plot of OD<sub>550</sub> vs. growth time of *E. coli* in TSB broth

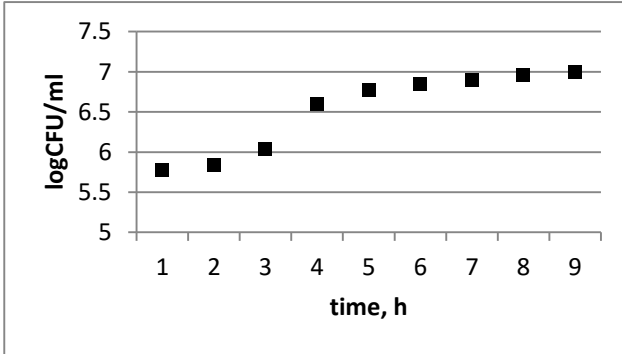
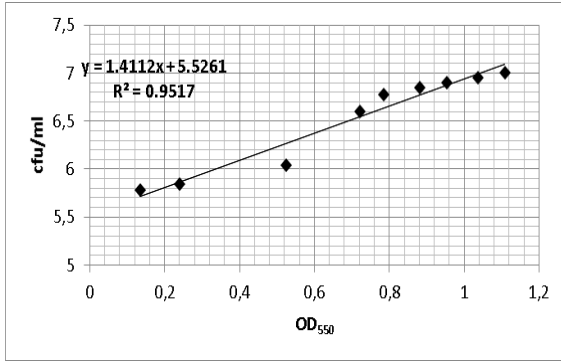
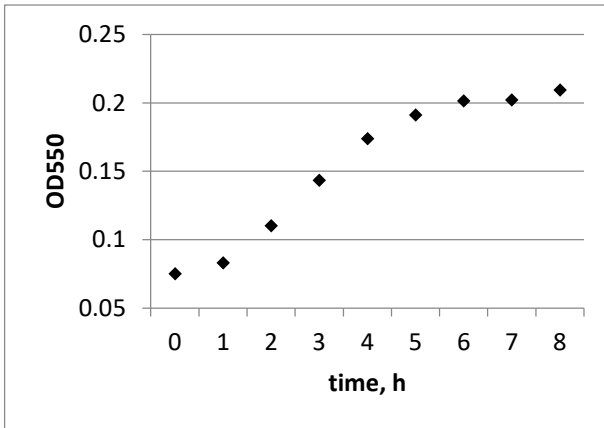


Figure 9-8 Plot of logCFUs vs. growth time of *E. coli* in TSB broth





**Figure 9-9 Correlation between optical density and colony forming units of *E. coli* in TSB broth**



**Figure 9-10 Plot of OD<sub>550</sub> vs. growth time of Coliforms in TSB broth**

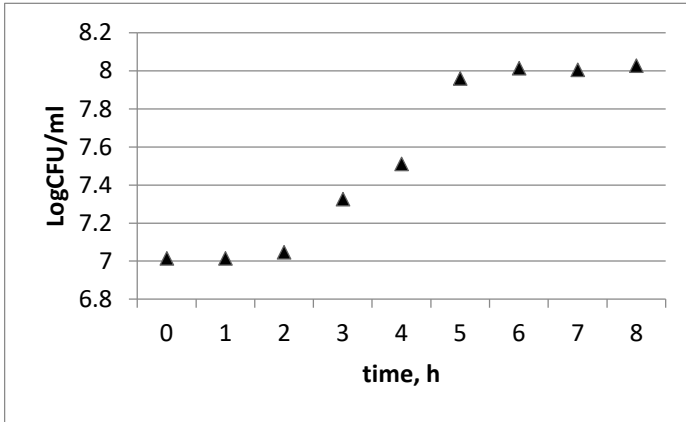


**Figure 9-11 Plot of logCFUs vs. growth time of Coliforms in TSB broth**

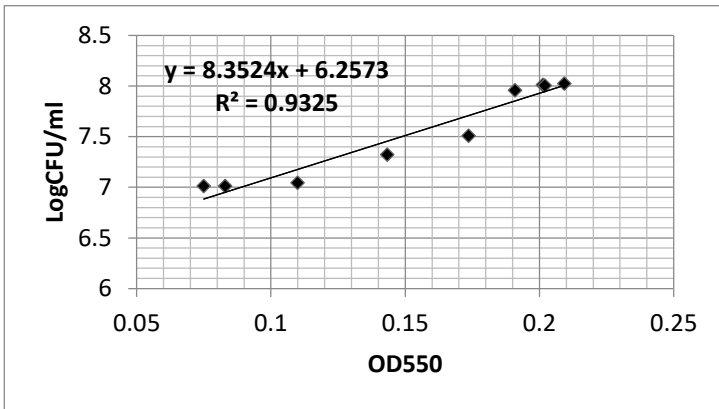


**Figure 9-12 Correlation between optical density and colony forming units of Coliforms in TSB broth**

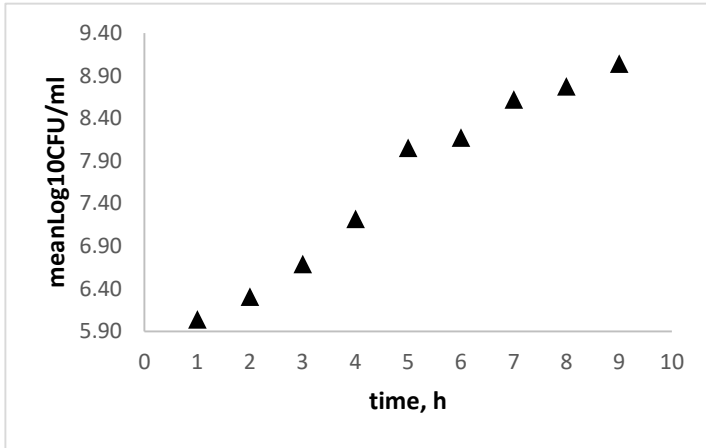


**Figure 9-13 Plot of  $OD_{550}$  vs. growth time of total count in TSB broth**

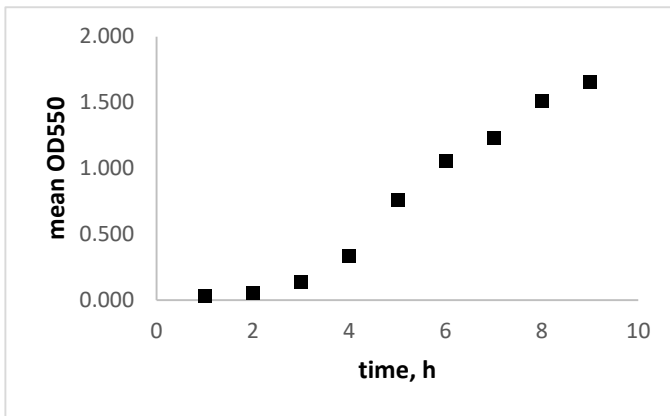


**Figure 9-14 Plot of logCFUs vs. growth time of total count in TSB broth**

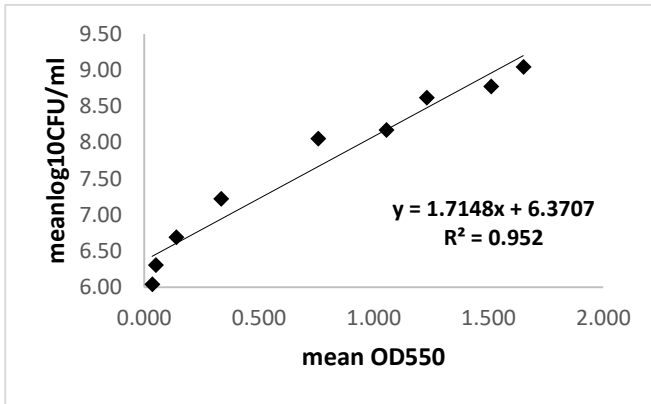


**Figure 9-15 Correlation between optical density and colony forming units of total count in TSB broth**

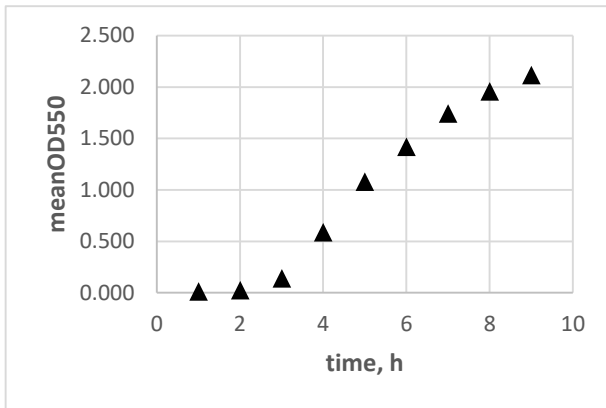


**Figure 9-16 Plot of OD<sub>550</sub> vs. growth time of *St. aureus* in TSB broth**

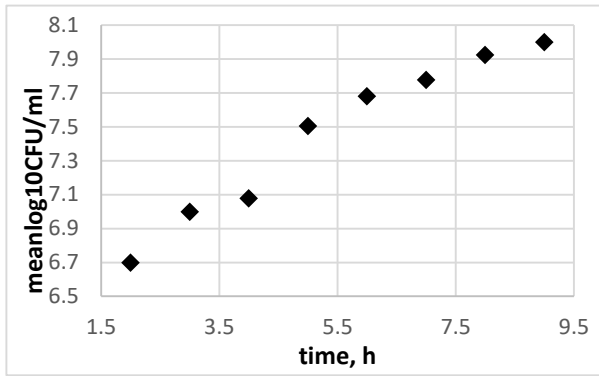


**Figure 9-17 Plot of logCFUs vs. growth time of *St. aureus* in TSB broth**

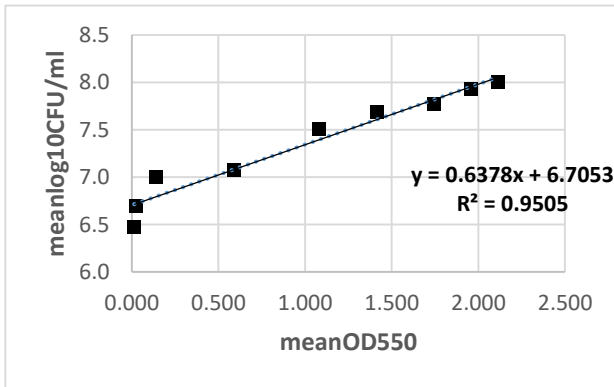


**Figure 9-18 Correlation between optical density and colony forming units of *St. aureus* in TSB broth**

### Appendix 3 Results on growth of *E. coli* on stainless steel surfaces

(Experiments are described in section 4.4)

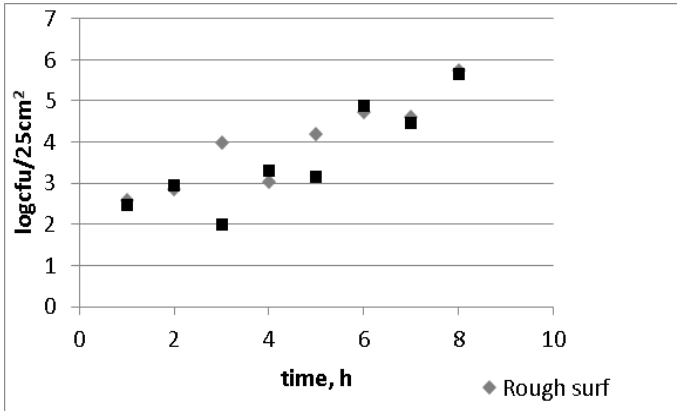


Figure 9-19 Growth of *E. coli* K12 on different type of surfaces during 8h period (meat juice)

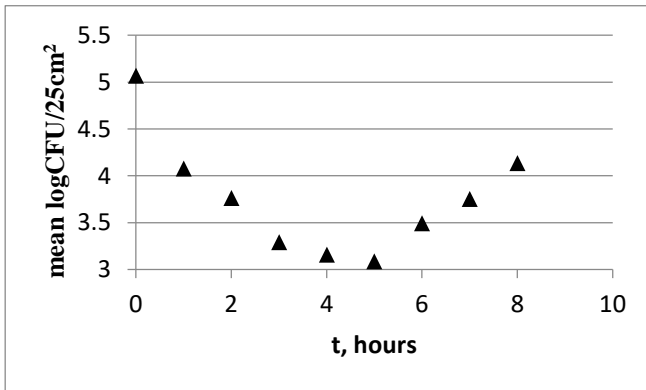
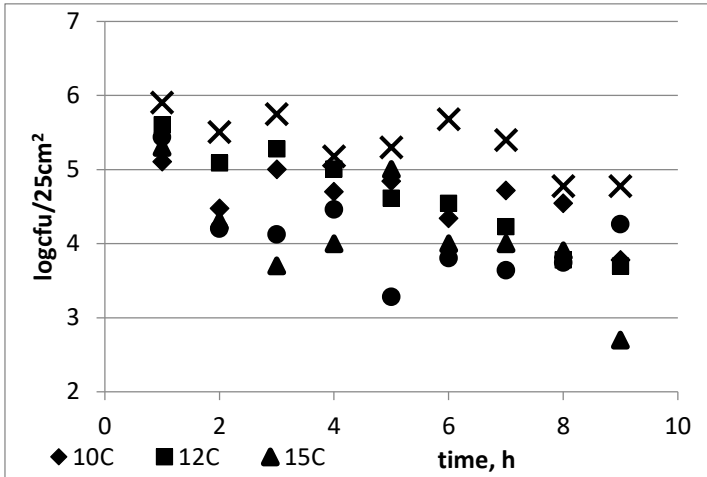
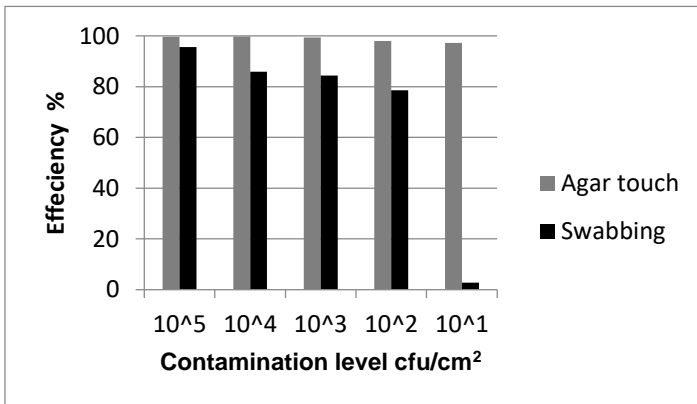


Figure 9-20 Survival of *E. coli* K12 on stainless steel surfaces during 8h of period (no meat juice)



**Figure 9-21 Survival of *E. coli* cells on stainless steel surface during 8h period at different temperatures**



**Figure 9-22 Efficiency of agar touching and swabbing methods**

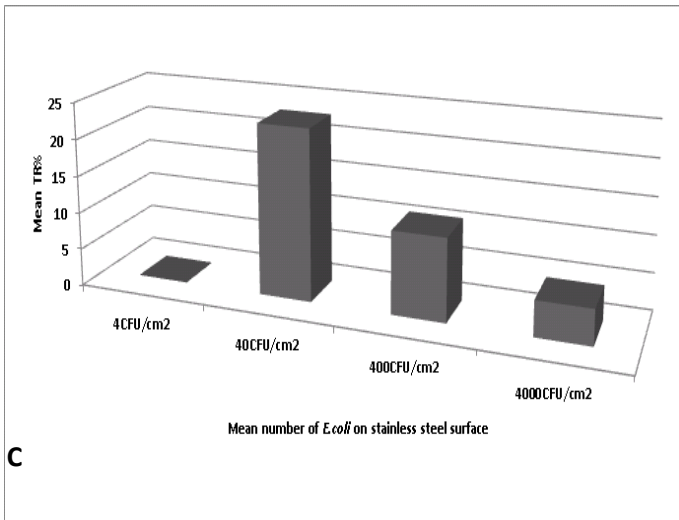
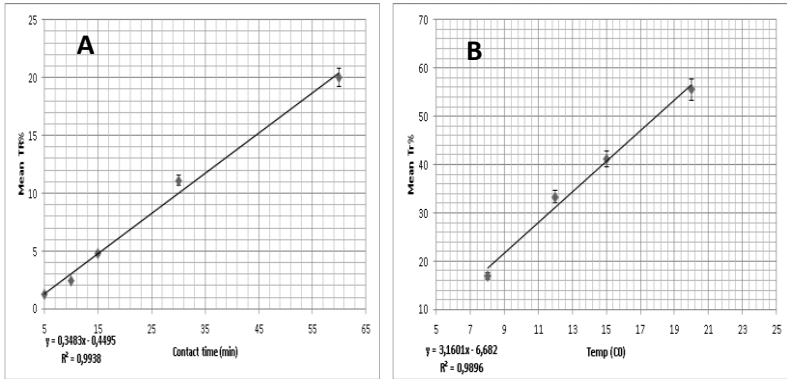


**Figure 9-23** Correlation between a) contact times, b) temperatures, c) inoculum levels and transfer ratios of *E. coli* to minced meat



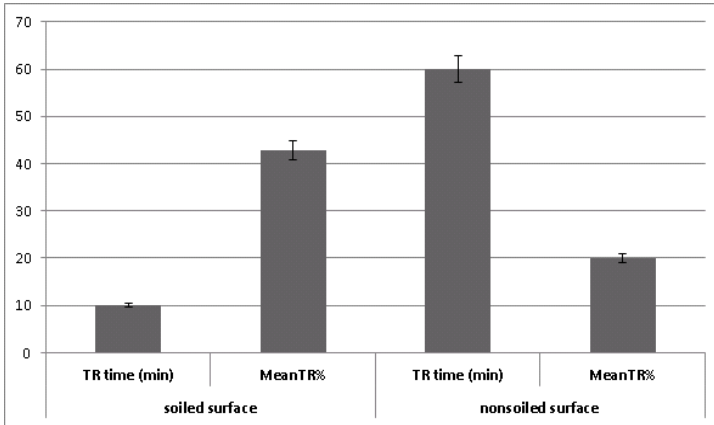


**Figure 9-24 Influence of soil on transfer ratios and transfer times of *E. coli* to minced meat**

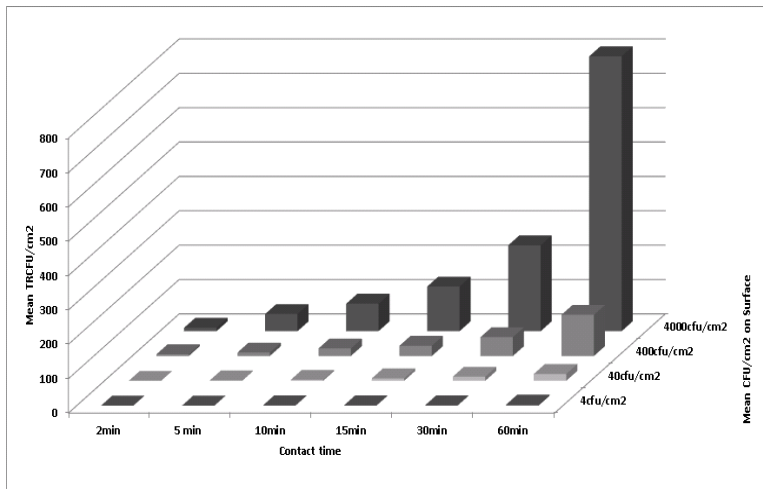


**Figure 9-25 Correlation between contact time, number of transferred *E. coli* and number of *E. coli* on stainless steel surfaces**